ANALYSIS OF RBM5 AND RBM10 EXPRESSION THROUGHOUT H9C2 SKELETAL AND CARDIAC MUSCLE CELL DIFFERENTIATION

by

Julie Jennifer Loiselle

A thesis submitted in partial fulfillment
of the requirements for the degree of
Master of Sciences (MSc) in Biology

School of Graduate Studies
Laurentian University
Sudbury, Ontario

THESIS DEFENCE COMMITTEE/COMITÉ DE SOUTENANCE DE THÈSE

Laurentian Université/Université Laurentienne
School of Graduate Studies/École des études supérieures

Title of Thesis Titre de la thèse	ANALYSIS OF RBM5 AND RBM10 EXPRESSION THROUGHOUT H9C2 SKELETAL AND CARDIAC MUSCLE CELL DIFFERENTIATION
Name of Candidate Nom du candidat	Loiselle, Julie Jennifer
Degree Diplôme	Master of Science
Department/Program Département/Programme	Biology
Date of Defence Date de la soutenance	July 15, 2013

APPROVED/APPROUVÉ

Thesis Examiners/Examinateurs de thèse:

Dr. Leslie Sutherland
(Supervisor/Directrice de thèse)

Dr. Céline Boudreau-Larivière
(Committee member/Membre du comité)

Dr. Éric Gauthier
(Committee member/Membre du comité)

Dr. Mazen Saleh
(Committee member/Membre du comité)

Dr. David A. Hood
(External Examiner/Examinateur externe)

Approved for the School of Graduate Studies
Approuvé pour l'École des études supérieures
Dr. David Lesbarrères
M. David Lesbarrères
Director, School of Graduate Studies
Directeur, École des études supérieures

ACCESSIBILITY CLAUSE AND PERMISSION TO USE

Abstract

RNA Binding Motif (RBM) domain proteins *RBM5* and *RBM10* have been shown to influence apoptosis, cell cycle arrest and splicing in transformed cells. In this study, *RBM5* and *RBM10* were examined in non-transformed cells in order to gain a wider range of knowledge regarding their function. Expression of Rbm5 and Rbm10, as well as select splice variants, was examined at the mRNA and protein level throughout H9c2 skeletal and cardiac myoblast differentiation. Results suggest that Rbm5 and Rbm10 may (a) be involved in regulating cell cycle arrest and apoptosis during skeletal myoblast differentiation and (b) undergo post-transcriptional or translational regulation throughout myoblast differentiation. All in all, the expression profiles obtained in the course of this study will help to suggest a role for Rbm5 and Rbm10 in differentiation, as well as possible differentiation-specific target genes with which they may interact.

Keywords

RNA Binding Motif domain proteins; RBM5; RBM10; H9c2; Myoblast Differentiation; Alternative Splicing

Acknowledgments

First and foremost, I would like to thank my Supervisor, Dr. Leslie Sutherland. Throughout my masters you have given me the opportunity to learn and to experience the ins and outs of research, from proposal writing to paper submission, and for this I will be forever grateful. The passion and dedication you have towards your students' learning and your research program are unmatched; I am very lucky to have been able to study and to grow under your guidance. Thank you also for your friendship and mentoring, which have helped me to successfully complete this research project and grow as a researcher.

I would also like to thank my thesis committee members, Dr. Éric Gauthier, Dr. Céline Boudreau-Larivière and Dr. Mazen Saleh, for all of their time and valuable input regarding my master's research project. I am fortunate to have had such a dedicated committee, and your perspectives on my work have undoubtedly made my project stronger.

I am very lucky and grateful for the funding I received from the Natural Sciences and Engineering Research Council of Canada (NSERC) and the Ontario government, which has allowed me to dedicate myself entirely to this project for the past two years.

Thank you to my lab mates Nina Rintala-Maki and Twinkle Masilamani for teaching me various molecular biology lab techniques and for helping me analyze and interpret my results. Thank you also to Sarah Tessier, who helped me optimize various experimental conditions. I am grateful to have been able to share the joys of successful experiments with all of you, and to have had your support and encouragement when those times were few and far between. In addition, thank you to all of the members of the

Advanced Medical Research Institute of Canada, particularly the other past and present members of the Sutherland lab research group, who have helped me laugh through the more difficult days and made the lab feel like a second home.

A special thank you to my wonderful husband, Mathieu Loiselle, for his unwavering support and faith in my abilities, I would not have been able to undertake this task without you by my side. Last but not least, thank you to my amazing family and friends who have encouraged me every step of the way and helped to keep me balanced and focused. The love and support I have received from of all of you means the world to me and has given me the strength to take on any new challenges.

List of Abbreviations

ATRA	All-Trans-Retinoic Ccid
CASP-2	Caspase 2
CDK	Cyclin Dependant Kinase
CDKI	Cyclin Dependant Kinase Inhibitor
D0 to D7	Day zero to day seven of differentiation
DM	Differentiation Medium
GM	Growth Medium
KD	Knockdown
LUST	LUCA-15-Specific Transcript
OE	Overexpression
PCR	Polymerase Chain Reaction
qPCR	Quantitative Polymerase Chain Reaction
Rb	Retinoblastoma
RBM	RNA Binding Motif
RT-PCR	Reverse Transcriptase-Polymerase Chain Reaction
TAE	Tri-Acetate-EDTA
TNF	Tumour Necrosis Factor

Table of contents

List of Figures

List of Tables

Appendix Index

Chapter 1. Introduction

RNA Binding Motif (RBM) domain proteins are so named due to the presence of one or more RNA-Recognition Motif (RRM) domains within their sequence, which allows them to interact with specific RNA sequences (Keene & Query, 1991; Sutherland et al., 2005). RRM domains are approximately 80 to 100 amino acids in length and can vary significantly in sequence, with the exception of two regions whose sequence are quite conserved: RNP-2, a hexapeptide, and RNP-1, an octapeptide located about 25 to 35 amino acids from the C-terminus of RNP-2 (Birney et al., 1993; Burd & Dreyfuss, 1994; Sutherland et al., 2005). The large variation in RRM domain sequences means that each RRM domain will have its own relatively unique structure and will recognize only specific mRNA sequences (Kenan et al., 1991; Sutherland et al., 2005). RBM-containing proteins can affect the metabolism of their corresponding RNA molecules in specific ways, enabling them to influence various cellular processes (Kim et al., 2009; Sutherland et al., 2005). For example, RBM proteins can bind pre-messenger mRNA molecules, forming heterogeneous nuclear ribonucleoproteins (hnRNP), which can influence a variety of processes such as RNA transcription, pre-mRNA processing and mRNA turnover (Dreyfuss et al., 1993; Krecic & Swanson, 1999). RBM proteins can also influence alternative splicing and are a component of small nuclear ribonucleoproteins, which are important, notably, in pre-mRNA splicing and 3'end processing (Lai et al., 2003; Zieve & Sauterer, 1990). RBM5 and RBM10 are two examples of such RBM proteins. The current study will focus on these two RBM proteins due to their important

roles in transformed cells, particularly in regards to modulation of apoptosis and cell cycle arrest.

1.1. RBM5

RBM5 is coded for on the short arm of chromosome 3, in the human lung cancer tumor suppressor region (Gazdar et al., 1994; Sutherland et al., 2005). It was first cloned as LUCA-15 by Wei at al. in 1996 while searching for genes encoded within this 370-kb segment of lung cancer tumor suppressor genes (TSG) located at 3p21.3. Since then, it has been cloned by several groups, leading to different names, including LUCA15 (Edamatsu et al., 2000), H37 (Oh et al., 1999), and RNA-Binding Motif protein 5 (RBM5) (Timmer et al., 1999).

1.1.1. Splice variants

The *RBM5* gene encodes a transcript of approximately 3000 bp, with an open reading frame encoding a sequence of 815 amino acids. Its translational product therefore has a predicted molecular weight of 92 kDa, but is detected at between 100 and 120 kDa by certain anti-RBM5 antibodies, suggesting that RBM5 protein undergoes post-translational modifications (Rintala-Maki & Sutherland, 2004; Shu et al., 2007; Sutherland et al., 2000; Timmer et al., 1999). Many *RBM5* splice variants have been identified to date, including *RBM5Δ6* in which exon 6 is deleted, *RBM5+6* in which intron 6 is retained, and *RBM5+5+6* in which both introns 5 and 6 are retained (Sutherland et al., 2005). Exclusion of exon 6 in *RBM5Δ6* causes a frameshift in the *RBM5* coding sequence and a premature stop sequence in exon 7 (Mourtada-Maarabouni et al., 2003). As for both intron-retaining transcripts, protein products of approximately

21.5 and 17 kDa, respectively, would be expected due to the presence of stop codons in the retained introns (in intron 6 for *RBM5+6* and in intron 5 for *RBM5+5+6*) (Sutherland et al., 2005). However, both intron-retaining transcripts and *RBM5Δ6* are candidates for nonsense-mediated decay, and hence result in no translational product (Maquat & Carmichael, 2001; Sutherland et al., 2000). A particularly important observation, however, is that there is also a truncated form of *RBM5+5+6* (*RBM5+5+6t* or *Clone 26*) which terminates in intron 6, upstream of the exon 7-8 junction; the transcript therefore no longer meets the criteria for nonsense- mediated decay and could yield a translational product (Rintala-Maki & Sutherland, 2009). This truncated variant has been previously identified in human spleen (Sutherland et al., 2000) and rat fibroblasts (Edamatsu et al., 2000).

A non-coding antisense RBM5 transcript has also been identified. This antisense transcript was first identified in bone marrow as a 326 bp cDNA fragment. This fragment was termed *Je2* and its sequence was antisense to that of *RBM5+6* (Sutherland et al., 2000). Later work by Rintala-Maki and Sutherland (2009) investigated whether this antisense sequence was part of a larger RBM5 antisense transcript. They did indeed identify a 1.4 kb RBM5 antisense transcript which began in intron 6, included intron 5 and terminated in intron 4 of *RBM5*, and thus included the *Je2* sequence. This longer antisense transcript was termed *LUST* for Luca-15-specific transcript (Rintala-Maki & Sutherland, 2009). The current study will focus on *RBM5*, as well as its splice variants *RBM5+5+6* and *LUST* (Figure 1), because the functions ascribed to these particular variants, including cell cycle arrest and apoptosis, are important to the model being used in the present work.

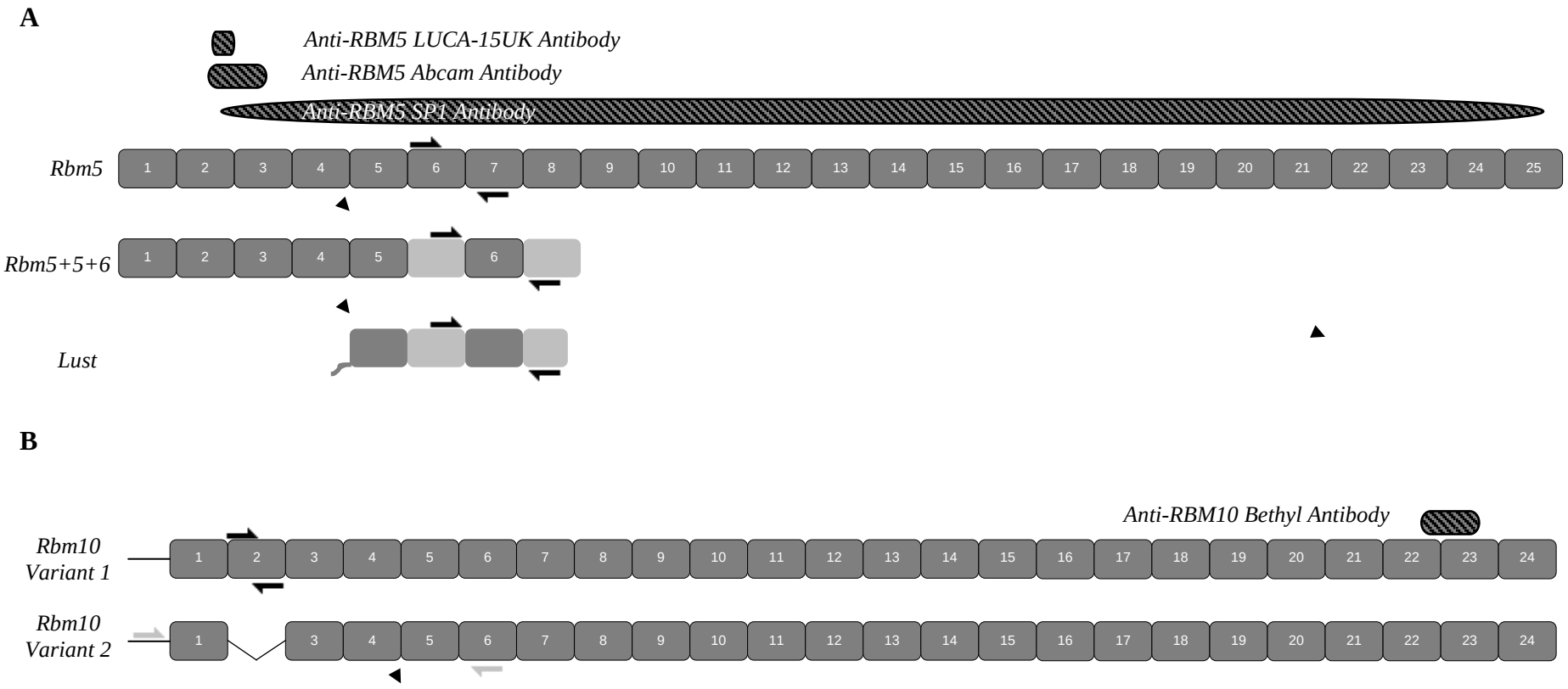

Figure 1. Rat *Rbm5* and *Rbm10* splice variants examined in this study. A. Rat full-length *Rbm5* transcript and select *Rbm5* splice variants illustrated based on reported human *RBM5* splice variant sequences. Lust is an antisense transcript. **B**. Rat *RBM10* splice variants. Exons are represented by correspondingly numbered dark grey blocks, and alternatively spliced introns are represented by light grey blocks. Block size does not correspond to exon or intron length. Approximate location of forward and reverse primers used for PCR and qPCR are indicated by right and left facing arrows, respectively, on the transcript in question. Size of arrow does not correspond to primer length in relation to exon or intron length, but gives the approximate position of the primer within the given exon or intron. Rat-specific sequences were used for primer design. Approximate antibody binding sites are indicated by black ovals with grey slanted lines, and the corresponding antibody's name is indicated.

1.1.2. Structure

RBM5 contains many different functional motifs, including two RMM domains (in exons 6 and 10), two bipartite nuclear localisation signals, two zinc finger motifs (Mourtada-Maarabouni et al., 2003; Sutherland et al., 2005) and a glycine rich sequence, or G-patch domain (Li & Bingham, 1991). In addition, RBM5 has an arginine-rich N-terminal region, which is believed to be involved in localizing RBM5 to subnuclear compartments containing many splicing factors (Aravind & Koonin, 1999). An *Oc*tomer *re*peat (OCRE) domain is also contained within the RBM5 sequence, and consists of a five-fold repeat of eight residues and a triplet of aromatic amino acids (Callebaut & Mornon, 2005). The OCRE domain has been shown to be involved with the regulation of splicing once RBM5 has been targeted to the RNA of interest (Bonnal et al., 2008). Taken together, these structural components suggest that RBM5 is located in the nucleus and affects RNA metabolism.

1.1.3. Expression

RBM5 and *RBM5+5+6* are widely expressed, with the highest expression of *RBM5*, as determined by Northern Blot, being found in the heart, skeletal muscle and pancreas (Drabkin et al., 1999; Sutherland et al., 2000; Timmer et al., 1999). Differences in *RBM5* expression levels been observed between foetal and adult states in the thymus and kidney: in adult thymus and fetal kidney *RBM5* levels were very high, however they were quite low in fetal thymus and adult kidney (Drabkin et al., 1999). Furthermore, older fibroblast cell lines and lymphocyte cultures were shown to have higher levels of *RBM5* expression compared to younger cells (Geigl et al., 2004). These results suggest that

RBM5 may be important for the development of certain tissues, or maintenance of a differentiated cellular state.

The expression of *RBM5* has been shown to be altered in certain transformed cells. For example, Oh et al. (2002) reported that in 82% of the primary non-small cell lung cancer samples considered, *RBM5* transcript levels were lower in the tumour samples compared to adjacent normal tissue. RBM5 protein levels were also lower in 73% of the primary non-small cell lung cancer samples considered, compared to adjacent normal bronchial cells (Oh et al., 2002). In addition, *RBM5* expression has been reported to be decreased in vestibular schwannomas (Welling et al., 2002), cancerous prostatic tissues (Zhao et al., 2012), biliary tract cancers (Miller et al., 2009), pancreatic cancers (Peng et al., 2013) and stage III serous ovarian carcinomas (Kim et al., 2010). On the other hand, in primary breast cancer specimens, expression of *RBM5* and *Her-2*, a proto-oncogene, were both high, and significantly positively correlated in non-Her-2 overexpressing tumours (Oh et al., 1999; Rintala-Maki et al., 2007). Furthermore, overexpression of *Her-2*, in the breast cancer cell line MCF-7 and in the ovarian cancer cell line CaOv-3, increased levels of *RBM5* mRNA (Oh et al., 1999). However, in another case, *RBM5* expression was seen to be decreased in breast cancer cells (Edamatsu et al., 2000). Therefore, *RBM5* expression in breast cancer samples may depend on an as-yet-unidentified variable.

Another important consideration with regards to *RBM5* expression is that *Je2* (a portion of the antisense transcript *LUST*) has been shown to negatively affect the levels of full-length *RBM5* (Mourtada-Maarabouni et al., 2002; Rintala-Maki & Sutherland, 2009). Inversely, overexpression of the full-length *LUST* was shown to increase *RBM5+5+6* levels and to lower *RBM5+5+6t* levels (the truncated form). A model in which the

transcription termination signal leading to the transcription of *RBM5+5+6t* is masked by *LUST*, thus increasing levels of *RBM5+5+6* and decreasing the levels of *RBM5+5+6t* upon *LUST* overexpression ,was proposed and gives an interesting perspective on how *RBM5* splice variants may regulate their own expression (Rintala-Maki & Sutherland, 2009).

1.1.4. Function

RBM5 is a putative tumour suppressor gene. In fact, *RBM5* was found to be one of nine genes down regulated in metastasis and part of the 17 common gene signatures associated with metastasis in various solid tumour types (Ramaswamy et al., 2003). In addition, a microarray analysis of 5603 genes showed that when *RBM5* was overexpressed in CEM-C7 cells, a human leukemic cell line, the expression of 35 genes involved in proliferation and apoptosis was changed (Mourtada-Maarabouni et al., 2006). Included in these differentially expressed genes were (a) Cyclin-dependent kinase 2 (*CDK2*), which is necessary for G1/S transition during cell cycle progression, (b) Signal transducer and activator of transcription 5B (*STAT5b*), which is important for many cellular processes including apoptosis, and (c) Bone morphogenic protein 5, which is notably important in organ development (Baśkiewicz-Masiuk & Machaliński, 2004; Golden et al., 1999; Mourtada-Maarabouni et al., 2006). Interestingly, overexpression of a portion of *Lust* decreased *RBM5* levels. It also caused opposite changes in the expression of six of the genes whose expression was initially found to be modulated by RBM5 overexpression in the microarray experiment (Mourtada-Maarabouni et al., 2006; Mourtada-Maarabouni & Williams, 2006). These findings support the previous statement

that *RBM5* antisense transcript works, at least in part, to downregulate the expression of the full-length *RBM5* variant.

The role of RBM5 in cell cycle arrest and apoptosis has been thoroughly investigated. In CEM-C7 cells, the overexpression of RBM5 was shown to suppress cell proliferation, and stable RBM5 transfectants were arrested in the G1 phase of the cell cycle (Mourtada-Maarabouni et al., 2003). RBM5 also induced apoptosis and cell cycle arrest at the G1 phase in A549 cells, a non-small cell lung cancer cell line (Oh et al., 2006). Growth inhibition and increased apoptosis levels following RBM5 overexpression was seen in PC-3 cells, a human prostate cancer cell line, as well (Zhao et al., 2012). In addition, RBM5 overexpression suppressed growth of human fibrosarcoma HT1080 cells (Edamatsu et al., 2000) and increased p53-mediated inhibition of cell growth of H1299 cells (non-small cell lung cancer cell line) (Kobayashi et al., 2011). When RBM5 was ectopically expressed in mouse fibroblast A9 cells, which were then injected into nude mice, tumour growth was even retarded (Oh et al., 2002). Furthermore, overexpression of full-length RBM5 in Jurkat human T lymphoblastoid cells enhanced apoptosis induced by various death receptor ligands including Fas, TNF-α, and TRAIL (Rintala-Maki & Sutherland, 2004; Sutherland et al., 2000). Similar results were observed upon investigation of RBM5 expression in clones of the breast cancer cell line MCF-7: loss of RBM5 and decreased susceptibility to death upon exposure to TNF-α were positively correlated (Rintala-Maki et al., 2004). Furthermore, overexpression of exogenous RBM5 in these cells increased their sensitivity to TNF-α mediated apoptosis (Rintala-Maki et al., 2004). These results therefore suggest that RBM5 is involved in inducing cell cycle arrest and modulating apoptosis. This can be accomplished through a number of different pathways and holds true in a variety of cell lines.

RBM5 splice variants have also been shown to influence the cell cycle and apoptosis. For instance, Jurkat cells stably transfected with *RBM5+5+6t* (*Clone 26*) showed a reduced growth rate and increased sensitivity to Fas-mediated apoptosis (Sutherland et al., 2000). In addition, decreased expression of *RBM5* and *Clone 26* was seen in Rat-1 cells, in which Ras, a small GTPase which is responsible for the activation of genes involved in cell growth and differentiation, was constitutively expressed (Edamatsu et al., 2000). These results suggest that *RBM5+5+6t*, like *RBM5*, functions to enhance cell cycle arrest and apoptosis.

With regards to antisense *RBM5* expression, however, the opposite effect to *RBM5* and *RBM5+5+6* expression in regards to modulation of the cell cycle and apoptosis is observed. For example, in CEM-C7 cells, stable expression of a portion of *LUST* inhibited Fas-mediated apoptosis (Mourtada-Maarabouni et al., 2001). Furthermore, in Jurkat cells *LUST* also inhibited Fas and TNF-α mediated apoptosis (Sutherland et al., 2001). It was also demonstrated that expression of the small antisense transcript and Bcl-x_L, an apoptotic inhibitor, were positively correlated (Mourtada-Maarabouni et al., 2006). Therefore, antisense *RBM5* expression seems to protect cells from certain types of apoptosis mediated by *RBM5* or *RBM5+5+6t*.

As previously mentioned, RBM5 can bind RNA molecules due to the specific domains contained in its sequence, and has been shown, to date, to specifically regulate the alternative splicing of six different genes. One such gene is caspase 2 (*CASP-2*). In this case, RBM5 has been shown to bind to a sequence within intron 9 of the *CASP-2* pre-mRNA, and by doing so excluded exon 9 from the mature transcript (Fushimi et al., 2008). This resulted in an increase in the levels of the proapoptotic CASP-2 variant. Conversely, when exon 9 is retained, the resulting full-length CASP-2 does not promote

apoptosis (Fushimi et al., 2008). RBM5 has also been shown to be involved in the regulation of Fas alternative splicing. More precisely, RBM5 promotes exclusion of exon 6 in the *Fas* mRNA, and consequently increases the levels of soluble Fas, the variant which does not promote apoptosis (in contrast to the retention of exon 6, which leads to the translation of a membrane bound, pro-apoptotic Fas receptor) (Bonnal et al., 2008). Furthermore, RBM5 has been shown to influence the alternative splicing of *c-FLIP* by promoting the exclusion of exon 7 (Bonnal et al., 2008). This leads to increased levels of c-FLIP(L) which can regulate apoptosis (Chang et al., 2002). These examples suggest that RBM5 may modulate apoptosis, at least in part, by influencing the alternative splicing of specific apoptosis-related factors. However, in these examples, its effects on apoptosis were contradictory: RBM5 promoted the exclusion of exon 9 in *CASP-2* (leading to translation of the pro-apoptotic variant) and promoted the exclusion of exon 6 and 7 in *Fas* and *c-FLIP*, respectively (leading to translation of the variant which does not promote apoptosis). In addition, RBM5 was shown to increase expression of a putative oncogenic isoform of Activation-induced cytidine deaminase (AID) by promoting exon 4 skipping in the *AID* pre-mRNA (Jin et al., 2012).

The two other genes whose alternative splicing has been shown to be regulated by RBM5 are Abscisic Acid Insensitive3 (*ABI3*) and Dystrophin. Firstly, in *Arabidopsis thaliana*, the suppressor of abi3-5 (SAU – an homologue of RBM5) was shown to decrease splicing of a cryptic intron in the *AIB3* pre-mRNA (Sugliani et al., 2010). Thus, RBM5 increased levels of the full length *ABI3* transcript (*ABI3*-α) which is important for seed maturation, and decreased levels of its splice variant (*ABI3*-β) (Nambara et al., 1995; Sugliani et al., 2010). In regards to dystrophin, RBM5 was shown to enhance the skipping of exons 40 and 72 (O'Leary et al., 2009). Dystrophin expression is important for muscle

health and a loss of dystrophin protein expression, as seen in patients with Duchenne Muscular Dystrophy (DMD), causes muscle wasting and usually death early in life (Koenig et al., 1987; Muntoni, 2003). In some cases of DMD however, dystrophin exon skipping was shown to restore an at least partially functional form of dystrophin, leading to a less serious phenotype (van Deutekom et al., 2007). The involvement of RBM5 in the alternative splicing of *ABI3* and dystrophin suggests a potential role for RBM5 as a developmental regulator.

Taken together, expression and functional data currently published regarding RBM5 point to its function as a regulator of apoptosis and of cell cycle arrest through its influence on alternative splicing. *RBM5+5+6t* has been shown to have similar effects on the cell as RBM5, whereas the antisense transcript generally affect the cell in an opposite manner.

1.2. RBM10

RBM10 is another RBM domain-containing protein and is located on the X chromosome at position p11.23 (Coleman et al., 1996; Thiselton et al., 2002). Through the process of X chromosome inactivation, one *RBM10* allele is inactivated, however, the remaining allele is highly expressed in human cell lines and mouse tissue (Coleman et al., 1996). RBM10 was first cloned from bone marrow in 1995 and has 49% amino acid sequence homology with RBM5 (Nagase et al., 1995; Sutherland et al., 2005).

1.2.1. Splice variants

Three *RBM10* variants have been identified in humans (Sutherland et al., 2005; Wang et al., 2012). The two main *RBM10* splice variants, which are also widely

expressed, are *RBM10 variant 1* (*RBM10v1*) and *RBM10 variant 2* (*RBM10v2*) (Sutherland et al., 2005) (Figure 1). The mRNA encoding *RBM10v1* is made up of 24 exons and codes for a protein product of approximately 930 amino acids (Johnston et al., 2010). The mRNA encoding *RBM10v2* lacks exon 4, resulting in a protein product of approximately 853 amino acids (Johnston et al., 2010). Protein products from both variants can be detected via Western Blot analysis, at approximately 103 and 94.7 kDa, respectively. The mRNA encoding *RBM10 variant 3* (Genbank accession number: AK024839) was identified in primary smooth muscle cells, has an alternate transcription start site and a deletion of 23 bp in exon 4 which causes a frameshift and consequently a premature stop codon within the modified exon (Wang et al., 2012). The current study will focus on RBM10v1 and RBM10v2, due to their wide expression and because the functional data reported for these two variants is also of relevance to the model used in this study.

1.2.2. Structure

Similar to RBM5, RBM10 contains two RRM domains, a G-patch sequence and two zinc finger motifs (Sutherland et al., 2005). Comparison of amino acid sequences between RBM5 and RBM10 reveals a 49% and 53% identity between RBM5 and the two RBM10 variants, respectively (Sutherland et al., 2005). However, three exons are particularly different between RBM5 and RBM10: (a) exon 4, which is completely different between RBM5 and RBM10v1, and absent in RBM10v2, and (b) exons 9 and 15, which are identical in both RBM10 variants, but hold only 14% homology to RBM5 (Sutherland et al., 2005). Due to their high level of homology, RBM5 and RBM10 may

be involved in similar cellular processes. However, since they do have exons with quite different sequences, they may also have different functions in the cell.

1.2.3. Expression

As mentioned previously, RBM10 is highly expressed in human cell lines and tissues, as well as in mouse tissues (Coleman et al., 1996). Of particular interest to this study, RBM10 expression has been detected consistently in heart and skeletal muscle, no matter the detection method used as graphed by GeneCards (www.genecards.org/cgi-bin/carddisp.pl?gene=RBM10&search=rbm10). Furthermore, expression of a non-mutated form of RBM10 is important since mutations in its sequence have been shown to be linked with TARP syndrome. The acronym of this syndrome describes some of its associated symptoms: *t*alipes equinovarus, *a*trial septal defect, *R*obin sequence (characterized by micrognathia, glossoptosis and cleft pallet) and *p*ersistence of the left superior vena cava (Johnston et al., 2010). This rare pleiotropic developmental abnormality syndrome has been reported to cause death before or soon after birth (Johnston et al., 2010). RBM10 has also been shown to be truncated in lung adenocarcinomas (Imielinski et al., 2012) and mutated in pancreatic intraductal papillary mucinous neoplasms (Furukawa et al., 2011). These findings confirm the importance of a non-mutated RBM10 gene in the cell, and even suggest a potential role for RBM10 in development.

1.2.4. Function

As reviewed by Sutherland et al. in 2005, at that point no functional studies regarding RBM10 had been undertaken. However, since then, some studies have begun to

examine the expression pattern of *RBM10* under specific conditions, and explore the effects of manipulating RBM10 expression on cellular processes. For example, in primary chondrocytes induced to hypertrophy, *RBM10* expression was shown to be elevated, which was accompanied by an increase in apoptosis and a decrease in proliferation (James et al., 2007). Also, in breast cancer samples, it was shown by RT-PCR that the expression of *RBM10* and caspase-3, a protein important in apoptosis, were positively correlated (Martín-Garabato et al., 2008). Furthermore, also in breast cancer samples, *RBM10v1* expression was correlated with the expression of proapoptotic *BAX* and tumour suppressor *p53* (Martínez-Arribas et al., 2006). This study also showed that *RBM10v1* and *RBM10v2* expression was correlated with that of vascular endothelial growth factor (VEGF), which stimulates the growth of new blood vessels. Together, these findings suggest that RBM10 may not only play a role in modulating apoptosis and cell cycle arrest, as shown for RBM5, but that RBM10 may also be important in controlling angiogenesis.

In addition, a recent paper by the Sutherland group showed a strong link between RBM10 expression and TNF-α mediated apoptosis: RBM10 knockdown decreased levels of both *TNF*-α mRNA and soluble TNF-α (sTNF- α) protein, as well as decreased the cells' sensitivity to TNF-α mediated apoptosis (Wang et al., 2012). The overexpression of RBM10 had the expected reverse effect, with increased levels of *TNF*-α mRNA and sTNF-α protein, as well as increased apoptosis. These investigators also showed that increased *TNF*-α mRNA expression upon RBM10 overexpression was associated with increased TNF-α transcription, and not simply stabilization of the corresponding mRNA. These results further support the possibility that RBM10 does in fact work as a modulator of apoptosis, and that its effects are mediated, at least in part, by TNF-α.

Potentially linked to its role in apoptosis and cell cycle modulation, RBM10 has also been shown to affect alternative splicing: RBM10 knock-down influenced the alternative splicing of many factors important in various cellular processes (unpublished data). RBM10 has also been purified from pre-spliceosomal complexes (Behzadnia et al., 2007; Deckert et al., 2006). Furthermore, as previously described, RBM5 expression was shown to favour exclusion of exon 6 in the *Fas* receptor (Bonnal et al., 2008); however, decreased RBM5 expression was not sufficient to change Fas receptor pre-mRNA splicing. Decreased RBM5, RBM10 and RBM6 levels were associated with preferential inclusion of exon 6 in Fas (Bonnal et al., 2008). These results suggest that RBM10, like RBM5, plays a role in alternative splicing.

Most of the work previously reported concerning RBM5 and RBM10 has been performed in transformed cells. Therefore, it is not yet known if these functions occur in non-transformed systems as well, or if they are a consequence of the transformed state of the cells. One particularly useful non-transformed model in which to study RBM5 and RBM10 is myoblast differentiation, since many of the events which have been associated to RBM5 and RBM10 in transformed cells also occur during differentiation (i.e., alternative splicing, apoptosis and cell cycle arrest). Furthermore, as described above, Rbm5 and RBM10 have been shown to be highly expressed in skeletal and heart muscle, and have a potential link to development (Drabkin et al., 1999; Johnston et al., 2010).

1.3. Muscle differentiation model

Differentiation involves the modulation of complex mechanisms. This leads to the transcription and translation of specific genes, whose downstream effects allow the differentiating cells to become specialized in a particular function (di Giacomo et al.,

2010). In terms of muscle cell differentiation, it is during early embryogenesis that cells from specific sections of the mesoderm become committed as skeletal and cardiac myoblasts, respectively, and then differentiate to form specialized myocytes (Yahi et al., 2006). During this differentiation from myoblast to myocyte, cells follow a highly ordered process involving cell cycle withdrawal and important metabolic and structural changes (Yahi et al., 2006; di Giacomo et al., 2010) (Figure 2). For example, during skeletal muscle differentiation, cells enter into the differentiation pathway, undergo irreversible cell cycle withdrawal, express specific contractile apparatus and metabolic factors, and finally fuse to form multinucleated myotubes (Andrés & Walsh, 1996). Three notable events that occur during differentiation from myoblast to myocyte are cell cycle arrest, apoptosis and alternative splicing. These three cellular events have also been shown to be modulated to a certain degree by RBM5 and RBM10 in transformed cells. Therefore it is specifically on these steps of differentiation, and their timing in the differentiation process, that this study will focus.

1.3.1. Cell cycle arrest in muscle differentiation

Cell cycle progression requires specific mitogenic signals to be expressed in a precisely regulated manner (Ahuja et al., 2007). In muscle differentiation, myoblasts must exit the cell cycle before expression of components of the contractile system can occur, which begins at around 48 hours after induction of differentiation (Andrés & Walsh, 1996; Yahi et al., 2006). Therefore, cell cycle arrest is one of the first events involved in muscle differentiation. For example, in skeletal muscle differentiation, within 24 hours after induction of differentiation, factors such as myogenin, a transcription factor

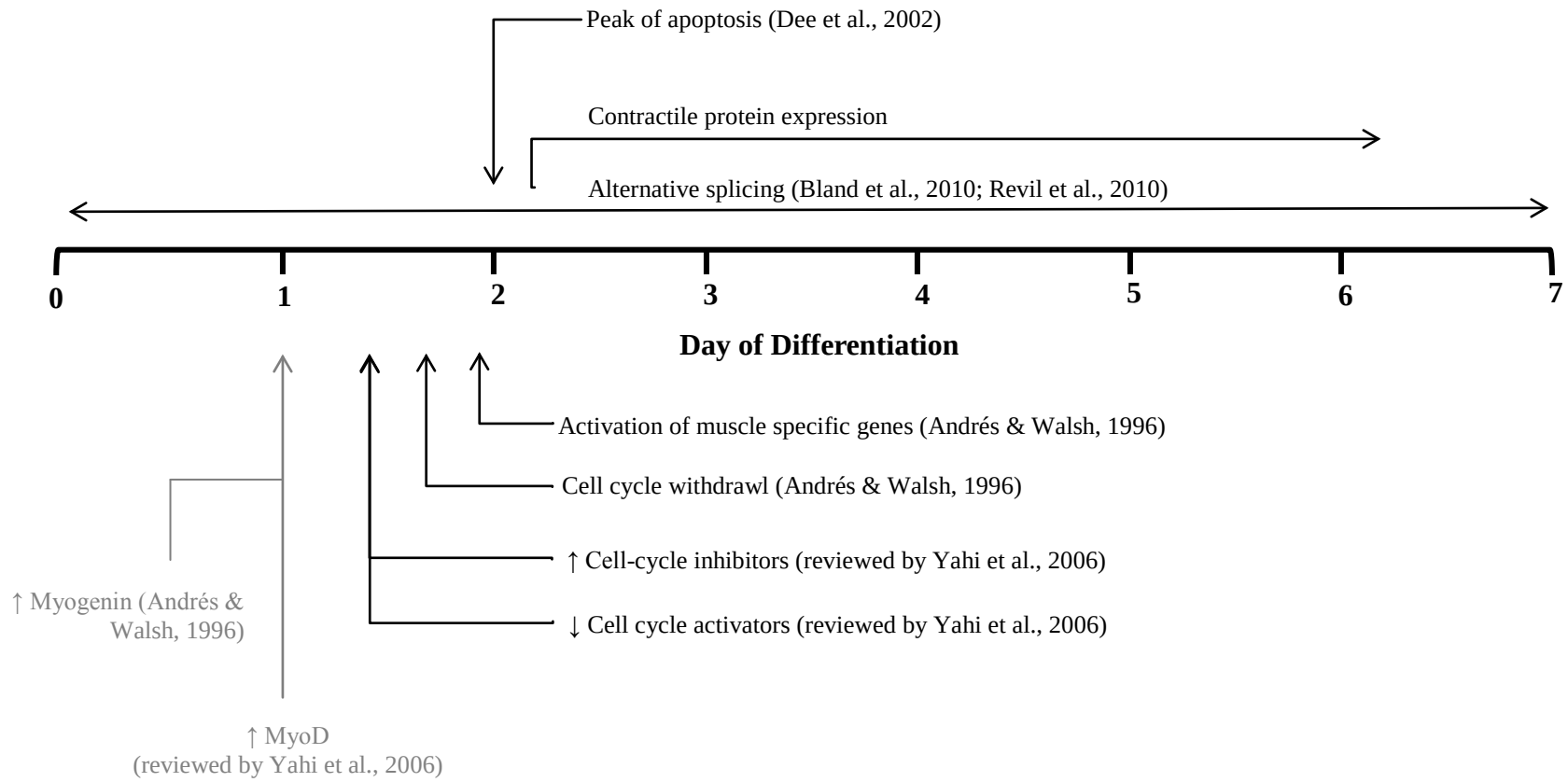

Figure 2. Timing of various cellular events throughout H9c2 skeletal and cardiac myoblast differentiation. Approximate timing of various events involved in H9c2 skeletal and cardiac myoblast differentiation. Timing of events based on information documented for H9c2 and other cell lines. Events indicated in gray are specific to skeletal muscle differentiation, while events indicated in black occur during both skeletal and cardiac muscle differentiation.

involved in regulating skeletal muscle differentiation, and cyclin dependent kinase inhibitor (CDKI) p21 are expressed and lead to downstream permanent cell cycle arrest in differentiating myoblasts (Andrés & Walsh, 1996; Walsh & Perlman, 1997). The expression of other cell cycle inhibitors, such as the CDKI p27 and p57, is also upregulated in the first days of skeletal muscle cell differentiation, while the expression of cell cycle activators, such as cyclin-dependent kinases (CDK) and cyclins, is downregulated (Martelli et al., 1994; Yahi et al., 2006). Expression of retinoblastoma protein (pRb) is also essential for cell cycle arrest during skeletal muscle differentiation: without its expression cell cycle arrest is not observed and apoptosis levels increase (Novitch et al., 1996; Zacksenhaus et al., 1996). Therefore, many factors are involved in the terminal cell cycle arrest observed within the first two to three days of skeletal muscle differentiation.

In cardiac differentiation, as in skeletal muscle differentiation, a key first step is cell cycle arrest. The cell cycle arrest involved in cardiac differentiation occurs in the G1 phase and involves regulation of similar factors, including upregulation of pRb, CDKI p21 and p27, as well as down regulation of several positive cell cycle regulators such as cyclin A (Ahuja et al., 2007; Koh et al., 1998; Poolman et al., 1998). However, in cardiac differentiation, cell cycle arrest is not permanent for fetal myoblasts: cardiac myocytes continue to proliferate in foetal life and terminal cell cycle arrest occurs only later, usually post-natality (Ahuja et al., 2007; Li et al., 1997). Therefore, in cardiac differentiation, although cells do not divide during differentiation from cardiac myoblast to myocyte in the foetus, once differentiated, they do retain a certain mitotic ability (Hayashi & Inoue, 2007; Li et al., 1997; Menard, 1999). This study will focus-on the differentiation of myoblasts to myocytes.

1.3.2. Apoptosis in muscle differentiation

Apoptosis is a type of programmed cell death which occurs in all tissues (Ellis et al., 1991). It is also a normal part of differentiation (Fidziańska & Goebel, 1991), and has been documented during differentiation of both primary myoblast cultures (Sandri et al., 1996), and established myoblast cell lines (Wang & Walsh, 1996). During muscle cell differentiation, the peak of apoptotic activity occurs at approximately 24 to 48 hours after the induction of differentiation, hence around the same time as cell cycle arrest (Wang & Walsh, 1996). It is thought that apoptosis is necessary in order to remove excess myoblasts (Miller & Stockdale, 1986), with the ability to escape apoptosis being linked to cell cycle exit: cells not differentiating and thus not undergoing subsequent cell cycle arrest would be targets for apoptosis (Fujio et al., 1999; Wang & Walsh, 1996). This is logical since myoblasts are susceptible to mitogen-deprivation induced apoptosis which occurs during differentiation, whereas terminally differentiated myocytes are not (Wang et al., 1997).

Many factors have been shown to be involved in the modulation of apoptosis during muscle differentiation. For example, cells with increased expression of CDK inhibitor p21 and dephosphorylated pRb have been shown to undergo cell cycle arrest and to adopt an apoptotic-resistant status (Walsh & Perlman, 1997; Wang et al., 1997; Wang & Walsh, 1996). This is logical since, as mentioned above, p21 and pRb are important for cell cycle arrest, therefore myoblasts expressing these factors would presumably be differentiating, hence not subjected to apoptosis.

1.3.3. Alternative splicing in muscle differentiation

Alternative splicing is a step in the pre-mRNA maturation process in which certain exons are preferentially retained or excluded, to produce many different mRNA transcripts from one gene (Black, 2003; Chen & Manley, 2009). This process therefore significantly increases the number of different mature transcripts that can be produced from a single gene, and even more so, from a genome: 98% of human multi-exonic pre-mRNAs are alternatively spliced (Pan et al., 2008; Wang et al., 2008). Proteins resulting from the alternative splicing of the same pre-mRNA can sometimes have different or even opposing functions. Therefore, alternative splicing, and not simply gene expression, can play a very important role in regulating a variety of cellular processes, including cell differentiation, migration, growth and apoptosis (Revil et al., 2010). Of particular interest for this study is a report which examined alternative splicing during mouse early embryonic development. This study showed that across developmental stages and tissues, alternative splicing and specific isoform expression occurs at high rates and is even comparable to changes in whole-transcript expression (Revil et al., 2010). This study also showed that the mRNA expression of known splicing factors significantly changed during early embryonic development. This suggests that a large part of the temporal and spatial regulation of isoform expression during differentiation is performed by specific splicing factors.

Alternative splicing is particularly important during muscle differentiation. For example, one study showed that 63 important alternative splicing events occurred in three distinct temporal patterns during mouse heart development (Kalsotra et al., 2008). They also showed that the levels of certain splicing factors changed during this differentiation process: for example, CUG-BP and ETR-3-like factor (CELF) protein was down-

regulated 10-fold, and muscleblind-like 1 (MBNL1) protein was up-regulated almost 4-fold. Furthermore, more than half of the observed alternative splicing events were also conserved in chicken heart development, suggesting their importance to developmental processes. Such results were also seen throughout mouse skeletal muscle differentiation (C2C12 cell line): significant splicing transitions were seen in 95 alternative splicing events, and more than half of these transitions were also conserved during avian myoblast differentiation (Bland et al., 2010). In summary, not only does muscle differentiation require exact spatial and temporal gene expression, but also necessitates precise regulation of the alternative splicing of these transcriptional products by specific splicing factors (Revil et al., 2010).

1.3.4. RBM proteins in muscle

Certain RBM proteins have already been shown to play a role in differentiation, or have emerged in various differentiation-related screens and arrays. For example, expression of RBM9 isoforms, also known as Fox-2, was found to change significantly during early embryogenesis (Revil et al., 2010). This may be associated with the reported role of RBM9 as a regulator of alternative splicing in neurons and muscle cells (Nakahata & Kawamoto, 2005). Many other RNA binding proteins have also been shown to vary in their expression throughout differentiation, such as Rbm13, Rbms3 and Rbm19 (Revil et al., 2010).

RBM4 and RBM20 are two RBM proteins which have been shown to play a role notably in muscle cell differentiation. First, RBM4 was shown to favor the inclusion of muscle-specific exons in tropomyosin, and thus increase the expression of the skeletal muscle-specific α-tropomyosin isoform during myogenic differentiation (Lin & Tarn,

2005). Overexpression of Rbm4 in C2C12 cells was also shown to promote the expression of muscle cell specific, or differentiation-induced, transcript isoforms of many genes including cardiac troponin T, insulin receptor, and ryanodine receptor (Lin & Tarn, 2011). In regards to RBM20, it was found to be involved in the regulation of splicing of over 30 genes, many of which are involved in cardiac physiology and disease, such as titin, in both rats and humans (Guo et al., 2012). Therefore, it is known that certain RBM proteins are particularly important to differentiation, and even muscle cell differentiation, with this role varying depending on the protein in question. However, the possible role of many other RBM proteins in this physiological process still remains to be evaluated, and many myoblast cell lines are available for such studies.

1.4. Models for muscle cell differentiation

Several muscle cell lines have been established which allow the *in vitro* study of muscle cell differentiation from myoblast to myocyte. The advantage of many of these cell lines is that they are secondary cell lines and thus are not transformed. This means that the division potential of these myoblasts has not been altered during the establishment of the cell line: the normal growth, differentiation and lifespan of these cells should be very close to that of myoblasts present in the organism of origin. Since the cells are not transformed, however, they will only divide a limited number of times and may eventually lose some of their characteristics. This is in contrast to (a) primary cells which are obtained directly from an organism and only grow in culture for a very short period of time (one or two divisions), and (b) immortalized cell lines, which have been transformed as such that the cells are able to divide indefinitely. These immortalized cell lines may be considered cancer cell lines, depending on certain characteristics such as

their ability to form colonies of cells in soft agar (a hallmark of cancer is anchorage independent growth) (Hanahan & Weinberg, 2000). Therefore, the advantage of secondary muscle cell lines is that they can be cultured in the lab and retain many of the characteristics of the cells from the tissue of which they originate. This can be very important when studying processes such as apoptosis and cell cycle arrest in myoblast differentiation, since these phenomena are generally altered in transformed cells.

Thus, these muscle differentiation models mimic quite accurately the *in vivo* processes which occur during differentiation, including cell cycle withdrawal, expression of muscle specific proteins, and even cellular morphological changes (Pownall et al., 2002; Sabourin & Rudnicki, 2000). Usually cell confluence and/or serum deprivation triggers myogenic differentiation in these cultures of myoblasts (Pownall et al., 2002). However, the timing of the resulting cascade of events will be different depending on if differentiation was induced by cell confluence or serum deprivation: differentiation occurs faster when cells are switched from normal growth medium to reduced serum medium (as opposed to prolonged culture in normal growth medium, which leads to cell confluence), the lag time being approximately 24 hours for C2C12 cells (Dee et al., 2002). The fact that both cell confluence and serum deprivation can trigger differentiation makes consistent and appropriate culture conditions essential in order to avoid the untimely differentiation of the myoblasts.

Examples of myoblast cell lines which can be used to study differentiation include the Rat L6 cell line which was derived from primary cultures of rat thigh muscle and can be induced to differentiate into skeletal myocytes upon growth medium serum reduction (Vandromme et al., 1992; Yaffe, 1968). The C2C12 cell line, which are murine myoblasts derived from C3H mice thigh muscle subjected to a crush injury, can also be induced to

differentiate into skeletal myocytes upon serum reduction (Blau et al., 1983; Burattini et al., 2004). A particularly interesting cell line is the H9c2 cell line, which was derived from embryonic BDIX rat heart tissue (Hescheler et al., 1991; Kimes & Brandt, 1976). Depending on their differentiation treatment, these myoblasts have the particular ability to differentiate into either skeletal or cardiac myocytes: upon only serum reduction skeletal muscle differentiation is induced however, when serum reduction is accompanied by treatments with a specific compound, like all-trans-retinoic acid (ATRA), cardiac differentiation is induced (Kimes & Brandt, 1976; Menard, 1999). Therefore, although H9c2 cells are derived from heart tissue, they have the ability to transdifferentiate and acquire a skeletal muscle cell phenotype (Brostrom et al., 2000; Menard, 1999). Therefore two muscle cell lineages can be studied within the same cell line and compared. This is a particularly useful characteristic, especially in expression studies, since it facilitates an evaluation of whether the expression of a certain gene is specific to a lineage, or how expression might change between lineages, providing additional information on the potential role of a gene of interest. For instance, if a gene's expression changes in a certain way during the establishment of only one of the lineages, based on documented differences between lineages, it is possible to narrow down potential functions for the gene.

Important differences between skeletal and cardiac muscle lineages exist. Firstly, embryonic cardiomyocytes can re-enter the cell cycle after undergoing their initial differentiation (Kageyama et al., 2002). Therefore cell cycle arrest is not permanent after cardiac differentiation in foetal life, unlike skeletal muscle differentiation in which cell cycle arrest is permanent (Kageyama et al., 2002). Secondly, different transcription factors are activated depending on the lineage, such as MyoD and myogenin, which are

specifically activated during skeletal muscle differentiation (Miner & Wold, 1990). It is important to take into account the differences between skeletal and cardiac muscle lineages when comparing expression results between these lineages.

1.4.1. Rbm5 and Rbm10 expression in rat

The H9c2 cell line used for this study was derived from rat tissue. As of yet, not all described *RBM5* and *RBM10* splice variants identified in humans have been reported in rat. Only full length *Rbm5* mRNA and protein have been identified in rat, and this, notably in the spleen (Accession numbers BC166477 and AAI66477, respectively) (Strausberg et al., 2002). In addition, *Rbm5* mRNA expression has been identified and studied in Rat-1 cells, a rat fibroblast 3T3 like cell line (Edamatsu et al., 2000). In that study, *Rbm5* mRNA was found to be downregulated by Ras, a protein involved in the activation of certain proto-oncogenes. This result is consistent with what has been reported in regards to *RBM5* in transformed cells, implicating *RBM5* in tumour growth suppression. However, there have been no reports, to our knowledge, on the expression of the *Rbm5* splice variants *Rbm5+5+6* and *Lust* in rat myoblasts. In regards to *Rbm10*, only one mRNA sequence, corresponding to *Rbm10v2*, is reported in the National Centre for Biotechnology Information (NCBI) nucleotide database and was derived from rat liver samples (Accession number NM_152861) (Inoue et al., 1996). However, both Rbm10v1 and Rbm10v2 translational products (with the accession numbers EDL97699 and NP_6090600, respectively) have been previously identified in rat tissue (Florea et al., 2005; Inoue et al., 1996).

1.5. Study Objective

RBM5 and RBM10 have been quite extensively studied in transformed systems. However, it is unknown if they play the same roles in non-transformed systems, or if these functions are a cause or a consequence of the transformed state. Therefore, we set out to first investigate the expression of RBM5 and RBM10 in a normal/non-transformed model. The system chosen for this work was the H9c2 differentiation model since RBM5 and RBM10 (a) are highly expressed in cardiac and skeletal muscle cells, and (b) have been associated with cell cycle arrest, apoptosis and alternative splicing in transformed cells, all processes also important to myoblast differentiation (Figure 2). The main objective of this study was to determine the mRNA and protein expression of Rbm5 and Rbm10 splice variants throughout the first seven days of H9c2 skeletal and cardiac myoblast differentiation, respectively. Subsequently, the expression results were to be compared within a lineage, and between both lineages. This was done as a first step in determining if Rbm5 and Rbm10 play a role in this non-transformed system, and what this role may involve, based on the temporal expression of the Rbm5 and Rbm10 genes (RNA and protein). We hypothesized that Rbm5 and Rbm10 have similar functions in transformed and non-transformed cells, and thus that they would be involved in cell cycle arrest, apoptosis and alternative splicing in differentiating cells. We therefore anticipated that increases in their expression levels would be seen at days when such cellular events occur in differentiating cells, i.e., at days two and three of differentiation, when cell cycle arrest and apoptosis occur at their maximum. We also expected that the mRNA and protein expression patterns of Rbm5 and Rbm10 splice variants would positively correlate during differentiation, if their regulation was at the transcriptional level.

Chapter 2. Materials and Methods

2.1. Cell culture and differentiation

H9c2 cells were purchased from ATCC (catalogue number: CRL-1446) and cultured in growth medium (GM) consisting of Dulbecco's Modified Eagle Medium (Life Technologies, Burlington, ON) supplemented with 10% foetal bovine serum (FBS) (Life Technologies) and 4 mM of L-Glutamine (Life Technologies). Cells were passed when they reached 75% confluency and GM was replaced every two days.

H9c2 cells were differentiated once they reached approximately 65% confluency, and within passage 16 to 20. Skeletal muscle differentiation was induced by reducing GM FBS concentration from 10% to 1% (Brostrom et al., 2000; Karagiannis et al., 2010). This reduced serum medium will be referred to as differentiation medium (DM). Cardiac differentiation was also induced by switching cells from GM to DM (Brostrom et al., 2000; Karagiannis et al., 2010), but this switch was accompanied by daily treatments of 10 nM ATRA (Sigma-Aldrich, Oakville, ON), as described by Ménard et al. (Menard, 1999). To verify successful differentiation into the desired lineage, the mRNA expression of skeletal muscle differentiation marker myogenin (*Myog*) (Edmondson & Olson, 1989; Kee et al., 2007) and cardiac differentiation marker myosin light chain 2 (*Myl2*) were evaluated (Bettiol et al., 2007). Differentiation day zero (D0) refers to the day at which the cells were first exposed to reduced serum medium (and ATRA in the case of cardiac differentiation). Cells were not passaged after being induced to differentiate, but DM was changed every two days.

Optimization of the ATRA concentration to be used in order to maximize the yield in cardiomyocytes was accomplished by administering daily ATRA concentrations of 0, 10, 20, 50 or 100 nM, respectively, to the differentiating cells. mRNA expression of cardiac differentiation markers *Myl2* and Troponin T type 2 (cardiac) (*Tnnt2*) were then examined by RT-qPCR at D5 differentiation (Bettiol et al., 2007; Ng et al., 2010).

2.2. RNA extraction

RNA extraction was performed using Tri-Reagent (Molecular Research Centre, Inc., USA), according to the manufacturer's instructions. Bromochloropropane (Sigma-Aldrich) was used for phase separation. RNA pellets were resuspended in special TE (10 mM of Tris-HCl, 0.1 mM EDTA, DEPC-treated water) supplemented with RNaseOUT (Life Technologies). RNA quantity was measured by spectrophotometry (Model Du530, Beckman Coulter, Mississauga, ON). To insure that there was no protein contamination in the RNA samples, their 260 nm/280 nm absorbance ratio was also evaluated, and only samples with ratios of 1.8 and above were used (Bustin & Nolan, 2004; Pfaffl, 2005). To verify RNA quality, 1 µg of each RNA sample was subjected to electrophoresis through a 1% Tris-Acetate-EDTA (TAE) agarose gel stained with SYBR Safe DNA gel stain (Life Technologies). Two crisp and clear bands, representing 28S and 18S rRNA, respectively, had to have been seen at approximately a 2.0 ratio on the stained gel, with low amounts of small fragments, for the RNA sample to be used in future experiments (Bustin & Nolan, 2004; Pfaffl, 2005).

Before the RNA samples were reverse-transcribed, genomic DNA contamination was evaluated by amplification of actin from the RNA samples via polymerase chain reaction (PCR) with 40 amplification cycles (Table 1). The experimental procedure for

the PCR reaction is explained below. Visualization of a product when the PCR reaction was separated by electrophoresis through a 2% TAE agarose gel indicated genomic contamination. If genomic contamination was found, the Turbo DNA-free kit (Ambion, USA) was used on all samples from that biological replicate, according to the manufacturer's instructions for rigorous DNase treatments. Following Turbo DNA-free treatment, a second actin amplification reaction was performed on the RNA samples to ensure the treatment was effective.

2.3. Reverse Transcription

Reverse transcription was performed using 1 µg of RNA, 1 µL of dNTP mix (10 mM) (Life Technologies), 1 µL of oligodT (500ng/µL) (AlphaDNA, Montreal, QC) and distilled water for a total volume of 12 µL. The mixture was heated to 65˚C for 5 minutes and quickly chilled on ice. Next, 2 µL of DTT (0.1M) (Life Technologies) and 4 µL of 5X First Strand Buffer (Life Technologies) were added. After a two minute incubation at 42˚C, 1 µL of Moloney Murine Leukemia Virus Reverse Transcriptase (MMLV-RT) (Life Technologies) was added. A 50 minute incubation at 42˚C followed, and the reaction was then inactivated by heating at 70˚C for 15 minutes. For examination of strand-specific *Rbm5* transcripts *Rbm5+5+6* and *Lust*, strand specific cDNAs were prepared. The steps involved in strand-specific cDNA synthesis were the same as described above, except (a) 1 µL of the gene-specific RT primer (10 µM) (Table 1) (AlphaDNA) was added instead of oligodT in the first step, and (b)

Table 1. Primers for RT-PCR and RT-qPCR

Gene name	Splice variant	Primers		Homology
Actb		Forward	5’ TGAGCGCAAGTACTCTGTGTGGAT 3’	R M
		Reverse	5’ TAGAAGCATTTGCGGTGCACGATG 3’	R
		Product size in rat	129 bp	
		Annealing Temperature	62˚C	
		Accession No.	Rat: NM_031144, Mouse: BC138611, Human: BC001301	
Tnnt2		Forward	5’ CTCCAAAACTCGTGGGAAGG 3’	R M
		Reverse	5’ TCTGCATCGGGTGCCTGGCA 3’	R
		Product size in rat	136 bp	
		Annealing Temperature	66.1˚C	
		Accession No.	Rat: BC161855, Mouse: L47599, Human: BC002653	
Myl2		Forward	5’ CCTGACGTCACCGGCAACC 3’	R
		Reverse	5’ CCTGGGGATGGAGAACAGGC 3’	R
		Product size in rat	122 bp	
		Annealing Temperature	60˚C	
		Accession No.	Rat: BC126064, Mouse: BC061144, Human: BC105821	
Myog		Forward	5’ CAACTGAGATTGTCTGCCAGGC 3’	R
		Reverse	5’ GTCTTATGTGAATGGACGGTGGG 3’	R
		Product size in rat	165 bp	
		Annealing Temperature	63˚C	
		Accession No.	Rat: M24393, Mouse: BC048683, Human: BC053899	
Gapdh		Forward	5’ ACCACAGTCCATGCCATCAC 3’	R M H
		Reverse	5’ TCCACCACCCTGTTGCTGTA 3’	R M H
		Product size in rat	452 bp	
		Annealing Temperature	58˚C	
		Forward	5’ ATGTTTGTGATGGGTGTGAA 3’	R M
		Reverse	5’ ATGCCAAAGTTGTCATGGAT 3’	R M
		Product size in rat	122 bp	
		Annealing Temperature	62.7˚C	
		Accession No.	Rat: BC059110, Mouse: BC082592, Human: BC004109	

Rps12		Forward	5’ TGAGCCCATGTATGTCAAGCTGGT 3’	R M
		Reverse	5’ ACTACAACGCAACTGCAACCAACC 3’	R
		Product size in rat	162 bp	
		Annealing Temperature	67˚C	
		Accession No.	Rat: M18547, Mouse: X15962, Human: BC017321	
Rbm5	*Rbm5*	Forward	5’ GTGTAAGCCGTGGTTTCGC 3’	R M H
		Reverse	5’ TTGCAATGTGCTTTCCTTGA 3’	R M H
		Product size	108 bp	
		Annealing Temperature	60˚C	
		Accession No.	Rat: BC166477, Mouse: BC023854, Human: AF091263	
	Rbm5+5+6	Reverse Transcription	5’ AAACTCTACTTGGTCCTTAACA 3’	R
		Forward	5’ TAACCTCTTCCCAACTGATTACATTC 3’	R
		Reverse	5’ CATCTGAGAAGTTATGCCTCTA 3’	R
		Product size in rat	176 bp	
		Annealing Temperature	63˚C	
		Accession No.	Rat: NC_005107, Mouse: NC_000075, Human: AB586690	
	Lust	Reverse Transcription	5’ TCTGACCTTTAAGATAAATGTA 3’	R
		Forward	5’ CATCTGAGAAGTTATGCCTCTA 3’	R
		Reverse	5’ TAACCTCTTCCCAACTGATTACATTC 3’	R
		Product Size in rat	176 bp	
		Annealing Temperature	63˚C	
		Accession No.	Rat: NC_005107, Mouse: NC_000075, Human: EF470865	
Rbm10	*Variant 1*	Forward	5’ CCCCAGAGACGGCGACTATC 3’	R M
		Reverse	5’ CCTGTGGCAGCATCCTCAGC 3’	R M H
		Product size in rat	128 bp	
		Annealing Temperature	60˚C	
		Accession No.	Rat: F1LWMO, Mouse: BC004674, Human: BC004181	
	Variant 2	Forward	5’ ATTGGCTCCCGTCGAACTAACAGT 3’	R
		Reverse	5’ ACTTCTCTCGGCGCTTGAAGTTCT 3’	R M
		Product size in rat	682 bp	
		Annealing Temperature	63˚C	
		Accession No.	Rat: NM_152861,Mouse: NM_001167776, Human: NM_152856	

H, R, M indicate homology to human, rat and mouse sequences, respectively

SuperScript II reverse transcriptase (Life Technologies) enzyme was used instead of MMLV-RT.

2.4. Polymerase chain reaction (PCR)

cDNA amplification by PCR was performed in BioRad iCycler thermocyclers (Mississauga, ON) using 1 µL of cDNA, 1 µL of the corresponding forward and reverse primers (10 µM) (Figure 1, Table 1), respectively, 1 µL of dNTP mix (10 µM), 2 µL of 10X Buffer (New England Biolabs, Whitby, ON), 1 µL of Taq DNA polymerase (500U/mL) (New England Biolabs) and sterile distilled water for a total volume of 15 µL per reaction. The number and duration of PCR cycles for actin, *Gapdh* and *Rbm10v2* were as follows: (1) one cycle of 95ºC for 5 minutes, (2) gene-specific cycle number of 95ºC for 30 seconds, primer-specific annealing temperature (Table 1) for 30 seconds, and 72ºC for 45 seconds, and (3) one final extension cycle of 72ºC for 10 minutes. PCR products were analyzed by TAE agarose gel electrophoresis, and gels were stained with SYBR Safe DNA Gel Stain. Densitometric analysis was performed using AlphaEase FC software (Alpha Innotec). It is important to note that the mRNA expression values obtained for each day of differentiation, for each biological replicate, were first expressed normalized to *Gapdh*, then expressed as fold-change from their respective D0 expression values. Following this, the average of the normalized fold-change in expression, for all three biological replicates, was determined for each day of differentiation and graphed.

2.5. Quantitative PCR (qPCR)

qPCR analysis was performed using the Applied Biosystems 7900HT Fast Real-Time PCR System. Sample reactions were prepared using 5 µL of cDNA sample diluted

as required, 12.5 µL of 2x Power SYBR Green PCR Master Mix (Applied Biosystems, Burlington, ON), 1 µL of the corresponding forward and reverse primers (10 µM) (AlphaDNA) (Figure 1, Table 1), respectively, and sterile distilled water for a total volume of 25 µL per reaction. The qPCR reaction program included (1) one cycle of 95ºC for 10 minutes, (2) 40 cycles of 95ºC for 30 seconds, primer-specific annealing temperature (Table 1) for 30 seconds and 72ºC for 15 seconds, and (3) one dissociation curve cycle of 95ºC for 15 seconds, primer-specific annealing temperature for 15 seconds, and 95ºC for 15 seconds. Standard curves were prepared using serial dilutions of pooled cDNA from samples of the respective biological replicate. The efficiency of each primer pair was determined as previously described based on the slope of their corresponding standard curve (Schmittgen & Livak, 2008). Potential reference genes *Rps12* and *Gapdh* were screened as previously described (Schmittgen & Zakrajsek, 2000).

2.5.1. Comparative Ct qPCR result quantification method

The $2^{-\Delta\Delta Ct}$ equation was used to determine the normalized mRNA expression value for *Rbm5* and *Rbm10* splice variants, relative to D0 differentiation, for each day of differentiation, in each biological replicate. Ct refers to the cycle threshold (Ct) of a sample and thus indicates the number of PCR cycles required for the number of amplicon copies to reach the set threshold value. Hence, a gene's Ct is inversely proportional to its expression in the sample of interest. The equation used for comparative Ct qPCR quantification was described in Applied Biosystems User Bulletin No. 2 (P/N 4303859). In this case, $\Delta\Delta Ct$ = [Ct, target (day of differentiation) – Ct, reference (day of differentiation)] – [Ct, target, D0 of differentiation) – Ct, reference (D0 of differentiation)]. The normalized relative expression value was determined for each day

of differentiation within a biological replicate, and then averaged between all biological replicates and graphed. This ensured that observed changes in gene expression were only the result of the differentiation conditions administered to the cells, and not due to any previous cell culture conditions. This also ensured consistency throughout biological replicates. Also, with this quantification method, changes in expression between 2 and 0.5 fold were not considered for statistical significance since it is the sensitivity limit for this type of qPCR quantification analysis: variations between 2 and 0.5 fold can be expected, but larger variations may be significant (Karlen et al., 2007).

2.5.2. Relative standard curve qPCR result quantification method

The relative expression level of differentiation markers in specific samples was calculated using the ABI software (SDS 2.4) and uses the formula log 10^((Ct(sample)-y intercept)/(-slope)) to calculate concentrations. Based on the standard curve of the gene of interest, its relative expression level in the samples was determined. To normalize these values, the relative expression of the gene of interest in each biological replicate was divided by the geometric mean of the expression of the reference genes in the corresponding sample. These normalized gene expression values were then divided by the normalized D0 expression value for that biological replicate, to get the fold-change in expression from D0 differentiation. These fold-change values were then averaged for the various biological replicates and plotted. Again, this ensured that observed changes in expression were only due to differentiation conditions administered to cells, and not previous culture conditions of that biological replicate.

2.6. Transfections

The plasmids used for the transient overexpression of RBM5, RBM10v1 and RBM10v2, respectively, were pcDNA3.RBM5, pcDNA3.RBM10v1 and pcDNA3.RBM10v2, with pcDNA3 as the negative control. Note, *RBM5*, *RBM10v1* and *RBM10v2* sequences were human.

Cells in GM were passaged such that a confluency of 35% would be obtained on the day of the experiment. At that point, 12 µg of the respective pcDNA3 plasmid and 18 µL of Lipofectamine 2000 Transfection Reagent (Life Technologies) were each mixed separately with 1.5 ml of Opti-MEM reduced serum medium with GlutaMAX (Life Technologies). After a 5 minute incubation at room temperature, the DNA+Opti-MEM and Lipofectamine 2000+Opti-MEM mixtures were mixed together, and incubated at room temperature for 20 minutes. Following this, the transfection mixture was added to the cells. The medium was not changed after addition of the transfection mixture, and cell pellets were collected at 48 and/or 72 hours post-transfection.

2.7. Protein extraction and quantification

Cell pellets were resuspended in cell lysis buffer (50 mM Tris-HCl pH 8.0, 150 mM NaCl, 0.5% NP-40, 100 mM NaF, 1 mM EDTA pH 8.0, 1 mM EGTA pH 7.5, 10 µL/mL of 100X protease inhibitor cocktail [Sigma-Aldrich]), and centrifuged at 14,000 x g for 10 minutes. Protein quantification was performed using the BioRad DC Protein Assay Kit and a SpectraMax 340PC384 absorbance microplate reader (Molecular Devices, Downingtown, PA, USA).

2.8. Western blot analysis

Protein samples were prepared as previously described (Sutherland et al., 2000). Prior to loading, protein samples were diluted 1:2 in Western sample buffer (0.06 M Tris-HCl pH 6.8, 25% glycerol, 2% SDS, 0.01% bromophenol blue [BioRad], 5% 2-mercaptoethanol [ThermoFisher Scientific, Ottawa, ON]) and heated to 95ºC for at least four minutes. Twenty-five microliters of Precision Plus protein ladder (BioRad) or 50 µg of the appropriate protein sample was loaded, per lane, onto polyacrylamide gels. Seven percent resolving gels (0.37 M Tris pH 8.8, 0.1% SDS, 7% acrylamide [BioRad], 0.1% APS, 0.1% TEMED [BioRad]) and four percent stacking gels (0.1 M Tris pH 6.8, 0.1% SDS, 4% acrylamide, 0.05% APS, 0.1% TEMED) were used. Gels were run in running buffer (0.025M Tris, 0.19M glycine, 0.1% SDS) at 100V until samples ran through the stacking gel (approximately 1.5 hours), and then at 200V until the dye front ran off the bottom of the resolving gel (approximately 4 hours). Following gel electrophoresis, the proteins were transferred to a PVDF membrane (0.45 µm pore size) (GE Health Care, Mississauga, ON) using a wet transfer apparatus for 90 minutes at 350 mA in transfer buffer (25 nM Tris, 192 mM glycine, 20% methanol). Transfer efficiency was verified by staining with Ponceau S (Sigma-Aldrich). Following transfer, membranes were washed in three times in TBS-T (20 mM Tris, 0.5 M NaCl, 0.1% Tween-20) (one 15 minute wash, followed by two 5 minute washes). Membranes were then blocked for 1 hour, at room temperature, in TBS-T supplemented with 5% non-fat dry milk (BioRad). Next, the membranes were washed three times with TBS-T (one 15 minutes wash, followed by two 5 minute washes), and incubated overnight, at 4˚C, with a primary antibody diluted in TBS-T supplemented with 3% non-fat dry milk. The primary antibodies used were mouse anti-rat-α-tubulin (1:10,000, sc-8035, Santa Cruz Biotechnologies Inc., Santa Cruz, CA),

rabbit anti-rat-RBM10 (1:1000, A301-006A, Bethyl Laboratories Inc/Cedarlane, Burlington, Canada), rabbit anti-rat-RBM5 (1:2500, ab85504, Abcam, Toronto, ON), rabbit anti-rat-RBM5 LUCA-15UK (1:2000, non-commercially available [Sutherland et al., 2000]) and rabbit anti-rat-RBM5 SP1 (1:1000, non-commercially available [Bonnal et al., 2008]).

Following the incubation with the primary antibody, the membranes were washed three times with TBS-T (one 15 minute wash, followed by two 5 minutes washes), and incubated 1 hour, at room temperature, with their corresponding secondary antibody diluted in TBS-T supplemented with 3% non-fat dry milk. A goat anti-mouse HRP-conjugated secondary antibody (1:20,000, sc-2005, Santa Cruz Biotechnologies Inc.) and a goat anti-rabbit HRP-conjugated secondary antibody (1:10,000, sc-2004, Santa Cruz Biotechnologies Inc.) were employed. The presence of antibodies on the membrane was detected using Amersham ECL Western Blotting Detection Reagents (GE Healthcare) and Amersham Hyperfilm ECL (GE Healthcare).

The membranes were stripped between probing with different primary antibodies by being washed twice for 10 minutes in mild stripping buffer (1.5% glycine, 0.1 % SDS, 0.1% Tween 20, pH 2.2), twice for 10 minutes in phosphate-buffered saline (1x PBS, pH 7.4, Life Technologies), and finally twice for 5 minutes with TBS-T. Since all anti-RBM5 antibodies used were raised in rabbit, blots were covered with ECL and exposed for 30 minutes after each strip, to ensure stripping efficiency. Quantification of the signal was performed using the AlphaEase FC software (Alpha Innotech) and the values were normalized to α-tubulin. It is important to note that, just as with the determination of *Rbm5* and *Rbm10* mRNA expression, protein expression values obtained for each day of differentiation for a specific biological replicate were first normalized to α-tubulin, then

expressed as fold-change from their respective D0 expression values. Following this, the average of the normalized fold-change in expression values, for all three biological replicates, was determined. This ensured that any observed expression changes were not due to any previous cultures conditions, and only to the differentiation procedures administered.

Chapter 3. Results - Model Optimization

Since Rbm5 and Rbm10 have not yet been studied in rat muscle cells, many optimization steps were required prior to examining their splice variant mRNA and protein expression throughout rat skeletal and cardiac myoblast differentiation. The three main factors requiring optimization, which will be described in this chapter, were (a) RNA quantification techniques, (b) cell culture and differentiation procedures, and (c) protein expression analysis. First, in order to correctly determine and analyze *Rbm5* and *Rbm10* mRNA expression throughout differentiation, optimal qPCR primers and amplification conditions had to be determined for all genes of interest, including differentiation markers and reference genes. Furthermore, as described, not all *Rbm5* and *Rbm10* variants being analyzed have previously been documented in H9c2 cells, therefore it was necessary to verify that our primer sets would allow the detection of specific alternative splicing products if they are expressed in the cells. Appropriate housekeeping genes also had to be found for our model of study, and gene quantification methods for qPCR data analysis had to be validated.

In regards to cell culture and differentiation, differentiation conditions had to be tested and the optimal ATRA concentration for differentiation into cardiomyocytes had to be determined. Differentiation into the desired cell lineage was confirmed by examining the expression of specific cardiac and skeletal muscle differentiation markers myosin light chain 2 regulatory subunit and myogenin, respectively. This was important since it ensured that the desired muscle lineage was in fact achieved in the various samples.

Finally, protein overexpression experiments were performed using various antibodies in order to determine which bands on a Western blot did in fact correspond to

the various Rbm5 and Rbm10 splice variants studied. This was a necessary step since many bands were being detected around the expected molecular mass of our proteins of interest. Therefore, identification of the appropriate protein band was necessary before attempting the quantification of protein levels during myocyte differentiation.

3.1. RNA

First, the efficiency of the qPCR primers had to be verified to ensure the expression of their corresponding gene was in fact correctly represented in the subsequent qPCR result (Pfaffl, 2006; Souazé et al.,1996). Also, the method used for qPCR gene expression quantification, comparative Ct or relative standard curve analysis, had to be validated for the genes of interest. This is an important step since each method has particular criteria which need to be met before it can be used to quantify the expression of a gene based on qPCR data. Finally, the expression of specific housekeeping genes had to be examined throughout the differentiation processes to ensure that their expression did not change, and they were therefore good reference genes to use in our models. Without proper verification, the expression of our genes of interest could be misinterpreted (Schmittgen & Zakrajsek, 2000). All of these factors had to be addressed before *Rbm5* and *Rbm10* mRNA expression analysis could take place.

3.1.1. qPCR primer efficiency evaluation

qPCR primer efficiencies had to be verified and be above 1.6 to be considered for future use in qPCR experiments. This would ensure correct representation of the expression of their corresponding gene in qPCR results (Pfaffl, 2006; Souazé et al., 1996). The efficiency of each qPCR primer pair was determined (Figure 3) based on the

slope of their standard curve. Since all primer sets had efficiencies above 1.6, they could all be used to determine the expression of their corresponding gene in qPCR experiments (Pfaffl, 2006; Souazé et al., 1996).

3.1.2. Validation of comparative Ct quantification method for Rbm5 and Rbm10 splice variant qPCR results

The advantage of the comparative Ct quantification method is that data can be presented as fold-change from a control sample, or in this case, from D0 differentiation. This is particularly useful when evaluating *Rbm5* and *Rbm10* expression throughout differentiation, since we are looking for rapid and significant changes in expression from our reference sample (D0) and between two consecutive days of differentiation in a particular lineage. However, specific criteria must be met since this quantification method uses only a sample's Ct value for the calculation of gene expression (unlike the relative standard curve quantification method , a standard curve for the primer pair in question is not necessary). Notably, the efficiencies of the target and reference genes must be between approximately 1.8 and 2.2, and within approximately 10% of each other (Applied Biosystems, 2008; Livak & Schmittgen, 2001). This ensures that the expression of each gene is correctly represented. To determine if the efficiencies of the primer pairs are sufficiently close, the Ct of the gene of interest and potential reference genes are obtained using dilutions of pooled sample cDNA. The difference between Ct_{Target} and $Ct_{Reference}$ vs. log of input cDNA quantity is then graphed, and the slope of the trendline must be less than 0.1 in order for the comparative Ct quantification method to be used for the genes in question (Applied Biosystems, 2008). First, we determined that the *Gapdh*,

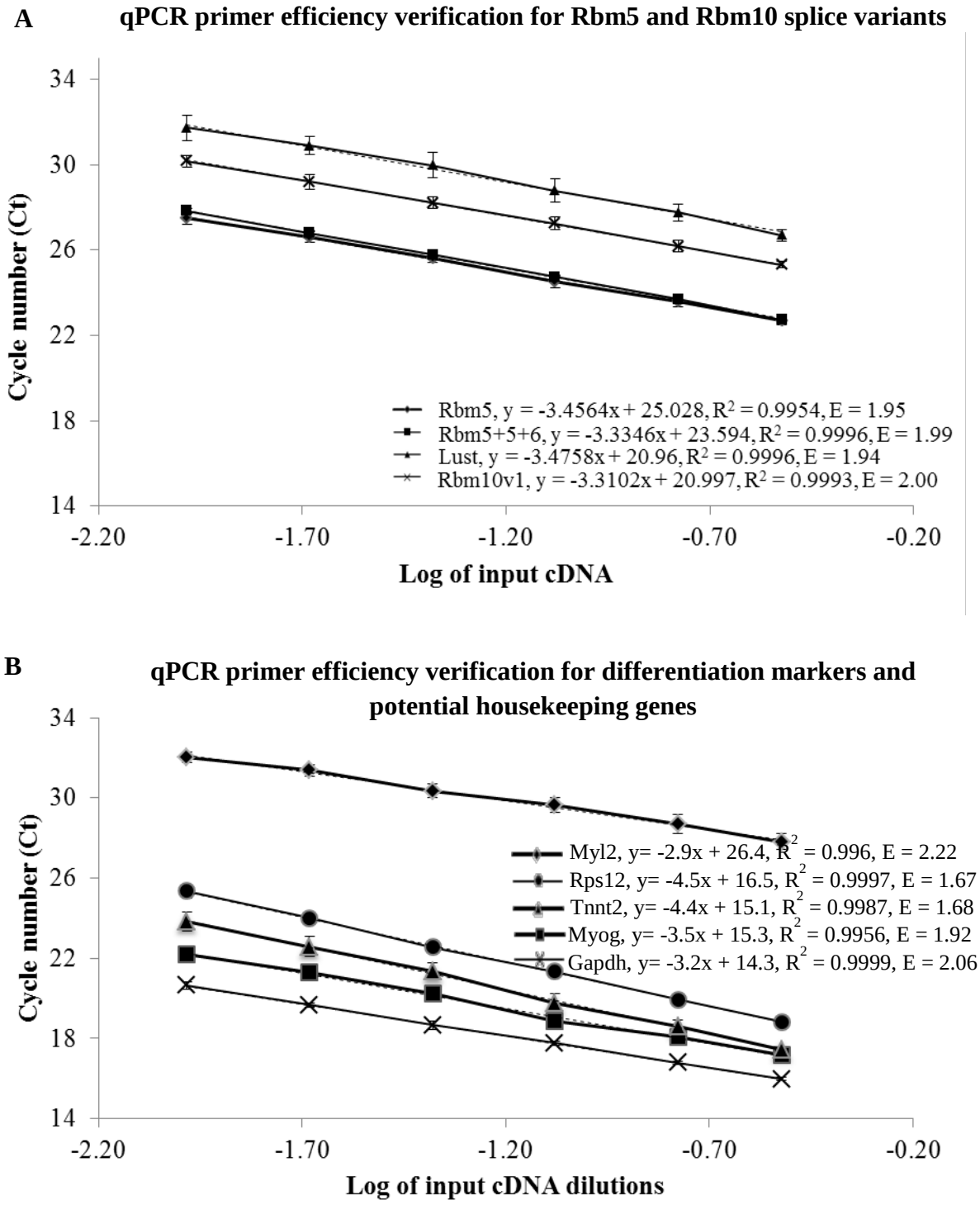

Figure 3. Primer pair efficiency verification. Standard curves of various primer pairs used for the amplification of the corresponding genes (Table 1). **A**. Standard curves for Rbm5 and Rbm10 splice variants studied. **B**. Standard curves for differentiation markers Myl2, MyoG, and Tnnt2, and potential reference genes Gapdh and Rps12. Standard curves constructed from RT-qPCR results of the corresponding primer pair and pooled dilutions of sample cDNA. Corresponding equation of the best-fit linear trendline is indicated. R^2 represents the correlation coefficient of the trendline, and E represents the efficiency of the corresponding primer pair. Data shown for biological triplicates, done in technical duplicate. Error bars represent standard error.

Rbm5 and *Rbm10* primer pairs had efficiencies within the required range (Figure 3). Also, the slope of the (Ct_{Target} - $Ct_{Reference}$) vs. log of input cDNA graph trendline was less than 0.1 for all four *Rbm5* and *Rbm10* splice variant primer pairs tested, when normalized to Gapdh (Figure 4). Therefore, the efficiencies of the target and reference genes were sufficiently close and the comparative Ct quantification method could be used to quantify the mRNA expression of *Rbm5* and *Rbm10* splice variants in our differentiation samples. It is important to note that the efficiency of *Rps12* (1.67) was not within the necessary range (1.8-2.2) for this type of quantification method, therefore it was not considered as a candidate for gene expression normalization.

3.1.3. Validation of the relative standard curve quantification method

The relative standard curve quantification analysis method is particularly useful when determining the relative expression of a gene in a sample when there is no control sample from which we can express their expression as fold-change. Therefore, this method was useful for determining the expression of differentiation markers: we could use it, for example, to compare the expression of markers only at D5 differentiation between lineages and replicates. This quantification method uses the standard curve obtained for a primer pair to determine the expression of the corresponding gene in a sample, as described in Chapter 2. Since it uses the slope and y-intercept of a primer pair's standard curve to extrapolate a sample's relative expression of the gene of interest, the difference in efficiencies between the target and reference gene's primers can be greater than that permitted with the comparative Ct quantification method, but all must be above 1.6 (Pfaffl, 2006; Schmittgen & Livak, 2008; Souazé et al., 1996). Since the efficiencies of all differentiation markers and both potential reference gene efficiencies

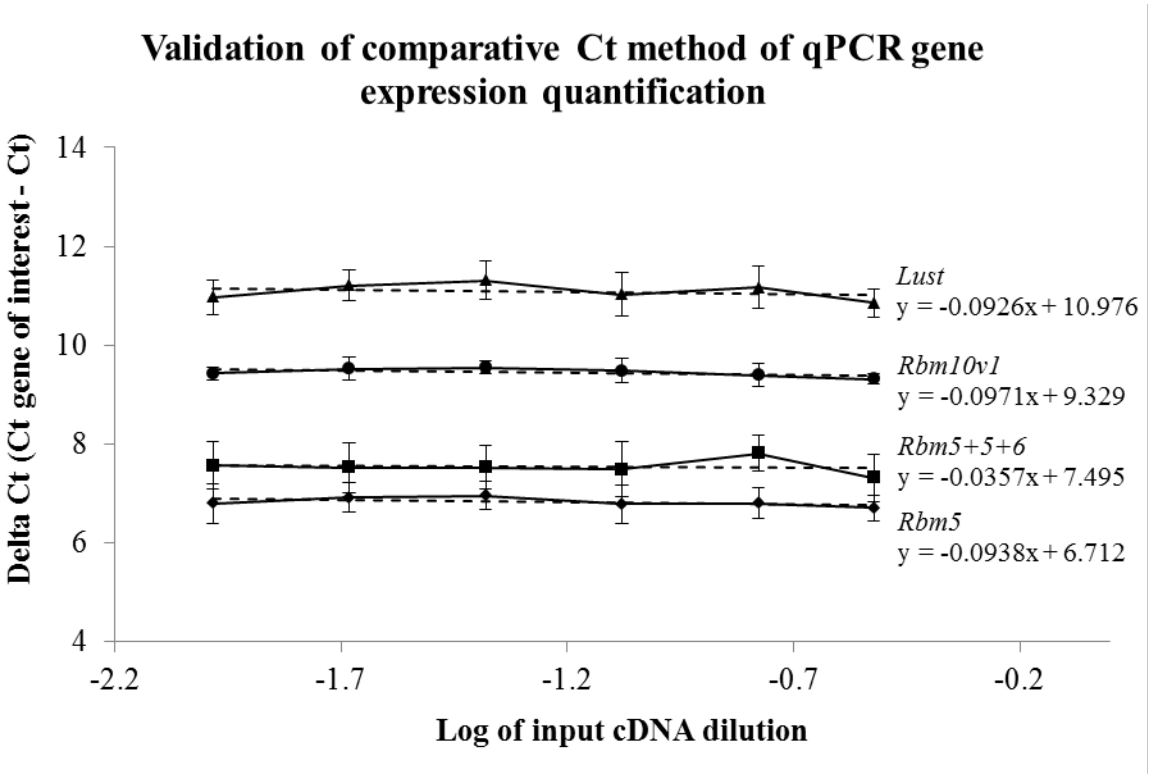

Figure 4. Validation of comparative Ct qPCR quantification method for *Rbm5* and *Rbm10* splice variant expression. RT-qPCR data for the expression of various *Rbm5* splice variants, *Rbm10v1* and *Gapdh* in dilutions of pooled cDNA. Expression is graphed as change in Ct of gene of interest from *Gapdh*, which is used to normalize. Equation of the best-fit trendline is indicated on the graph. Data shown is from three biological replicates, performed in technical quadruplicate.

were within this range (Figure 3B), this qPCR quantification could be and was used to quantify the mRNA expression of all differentiation markers used in this study.

3.1.4. Reference gene validation for H9c2 skeletal and cardiac myoblast differentiation models

Reference genes must be validated before studying gene expression in a system which does not already have specific and well established reference genes. One such method includes determining the Ct value of the potential reference gene, by qPCR, throughout the experimental conditions. The Ct values are then expressed as a fold-change from the reference sample (D0 differentiation in this case), and a one-way ANOVA is performed: if there is a statistically significant change in the expression of the reference gene throughout the experimental condition, it is not a suitable reference gene for the system (Schmittgen & Zakrajsek, 2000). This method of reference gene validation was performed in this study to evaluate whether *Gapdh* and *Rps12* were appropriate reference genes for the H9c2 skeletal and cardiac myoblast differentiation models. Since $p > 0.05$ for the one-way ANOVA on *Gapdh* and *Rps12* expression throughout skeletal and cardiac myoblast differentiation (Figure 5), *Gapdh* and *Rps12* expression did not change significantly during the establishment of either lineage. Therefore, both *Gapdh* and *Rps12* were suitable genes for the normalization of gene expression throughout both lineages.

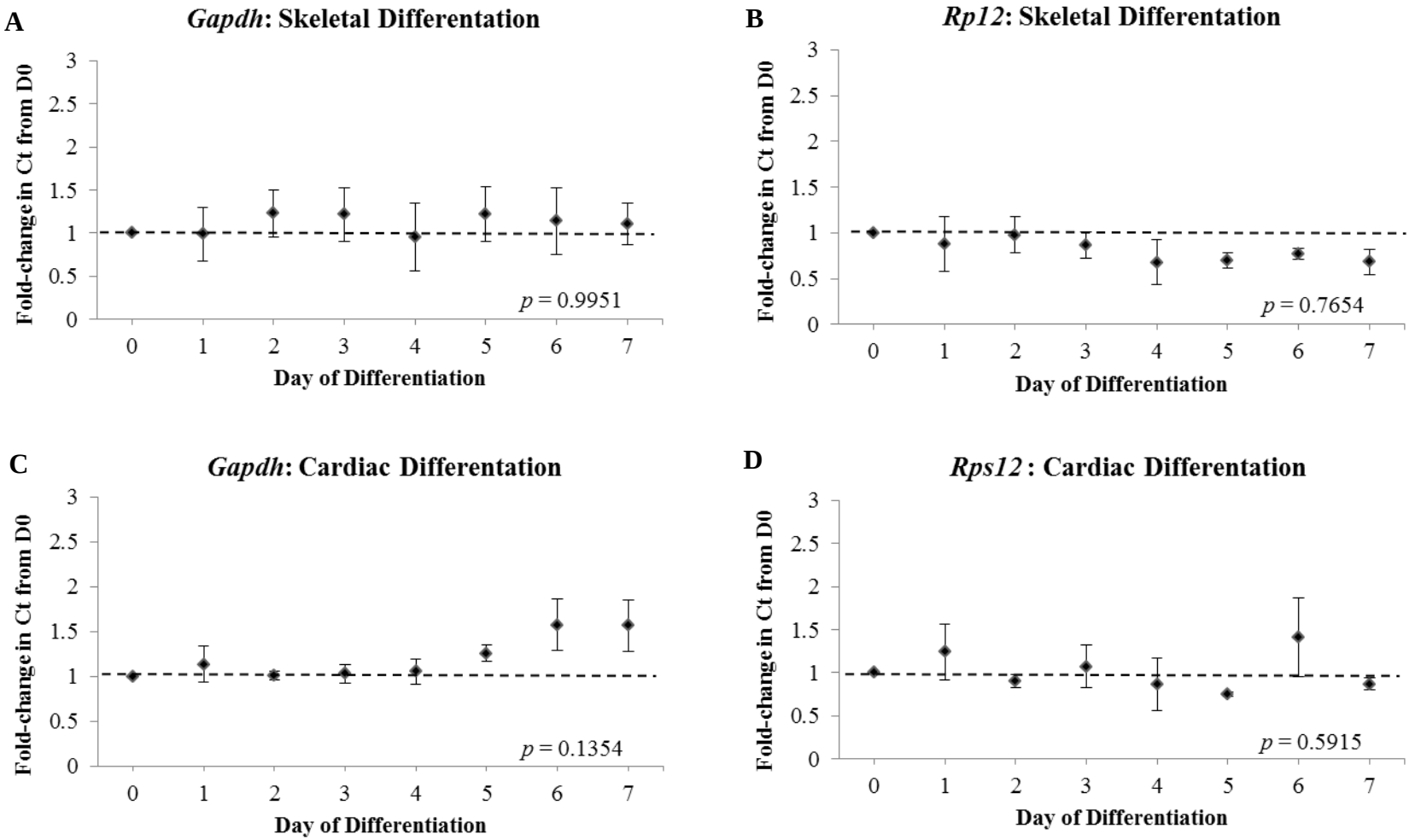

Figure 5. Reference gene verification. Expression of two potential reference genes, *Gapdh* (**A**, **C**) and *Rps12* (**B**, **D**), was examined throughout both experimental conditions: H9c2 skeletal (**A**, **B**) and cardiac (**C**, **D**) myoblast differentiation. RT-qPCR results of the fold-change in Ct values from D0 differentiation are graphed for D1 through D7 of differentiation. Data shown are from three biological replicates, performed in technical quadruplicate. Indicated *p*-value is from a one-way ANOVA performed on graphed data. Changes in expression throughout a differentiation lineage were considered statistically significant if $p < 0.05$.

3.2. Cell Differentiation

H9c2 myoblast differentiation into skeletal and cardiac myocytes has been extensively studied (Brostrom et al., 2000; Karagiannis et al., 2010; L'Ecuyer et al., 2001; Menard, 1999). However, to ensure maximum cardiomyocyte yield, we optimized the concentration of ATRA administered to the cells. Since it is the ATRA that prevents H9c2 cells from transdifferentiating to skeletal myocytes upon serum reduction, higher ATRA concentrations should decrease the number of cells transdifferentiating to skeletal myocytes, and maximize cardiomyocyte yield. However, too high a concentration of ATRA could be toxic due to its pleiotropic effects (Germain et al., 2006). The mRNA expression of the cardiac markers *Myl2* and *Tnnt2* was used to quantify cardiac differentiation in a cell population (Bettiol et al., 2007; Karagiannis et al., 2010; Ng et al., 2010; Pereira et al., 2011). In addition, cells were observed by phase-contrast microscopy to determine if the administered ATRA concentration had a visible effect on cell morphology.

The proportion of skeletal versus cardiac muscle cells in each biological replicate was determined once differentiation procedures were optimized. To this end, cells were observed by phase contrast microscopy and the expression of skeletal muscle differentiation marker *Myog* and cardiac differentiation marker *Myl2* were determined. Measuring the expression of differentiation markers also allowed quantification of the degree of skeletal and cardiac muscle differentiation in each replicate. Again, lineage had to be confirmed to ensure that treatment of cells successfully produced skeletal or cardiac myocytes, respectively.

3.2.1. ATRA Titration

In order to maximize the yield in cardiomyocytes, various doses of ATRA were administered daily to the differentiating cells. As mentioned, cardiac differentiation levels were evaluated by examining the expression of cardiac differentiation markers *Myl2* and *Tnnt2* at D5 under each ATRA treatment condition. *Myl2* encodes a protein that wraps around the extension of the myosin heavy chains in the cell's contractile system, and is necessary for contraction and thick filament stabilization (Moss & Fitzsimons, 2006; Rottbauer et al., 2006). *Tnnt2* also encodes a protein which is an important part of the contractile system of cardiomyocytes, allowing myosin to bind the actin filament upon stimulation (Pereira et al., 2011). It is important to note that *Tnnt2* can also be expressed in certain early stages of skeletal myoblast differentiation (Swiderski & Solursh, 1990). At D5 of H9c2 differentiation, the expression profile of *Myl2* and *Tnnt2* indicated that there was no statistically significant difference in cardiomyocyte yield with ATRA treatments of 10 nm and above (Figure 6). Daily administration of doses higher than 10 nM, therefore, did not increase cardiomyocyte yield.

Phase contrast microscopy showed that, when cells were only exposed to DM (no ATRA), by D5 most cells looked very elongated and many had fused together: indicating H9c2 skeletal muscle differentiation (Figure 7) (Comelli et al., 2011; Menard, 1999). This was expected since simple serum reduction should cause cells to transdifferentiate and adopt a skeletal muscle cell phenotype. With daily treatments of 10 nM or higher of ATRA, however, cells also looked elongated, but the majority had not fused together. Furthermore, most had round and easily visible nuclei, all characteristics of H9c2 cardiac differentiation (Brostrom et al., 2000; Menard, 1999). This suggested that cardiac differentiation had successfully been induced. However, at ATRA concentrations above

A

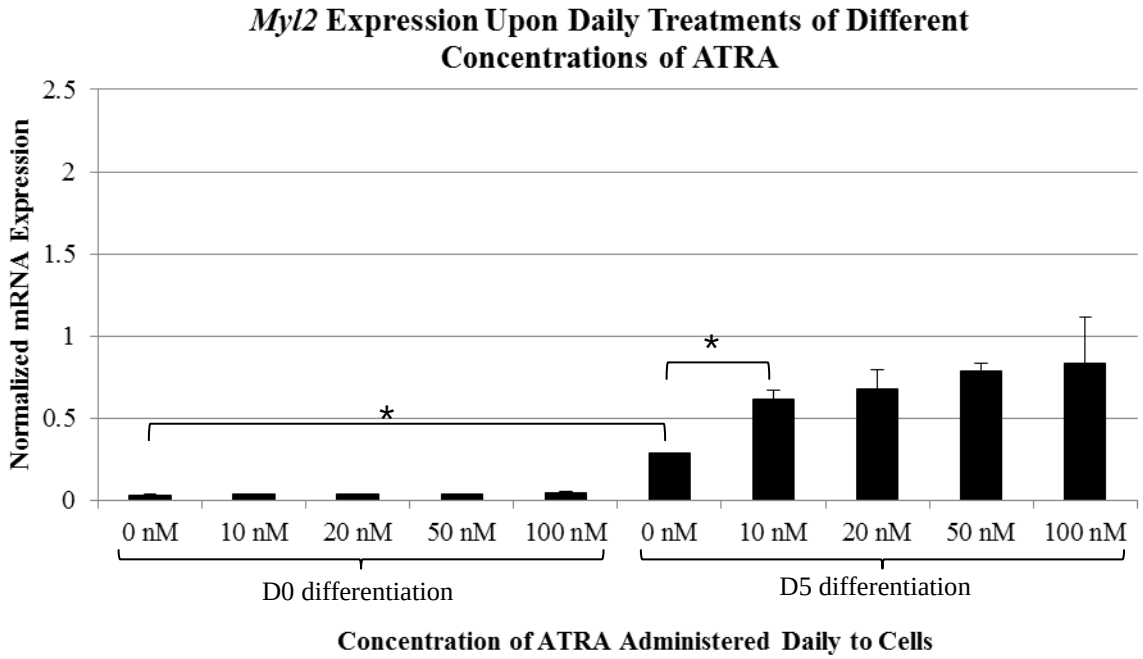

B

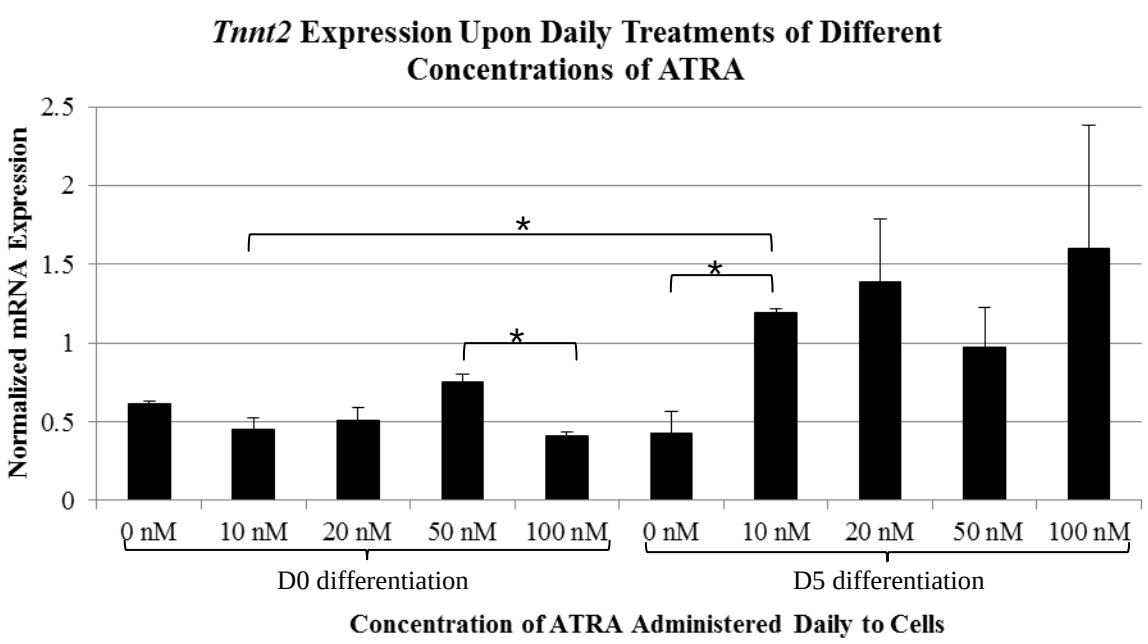

Figure 6. Cardiac differentiation marker expression following various doses of ATRA. RT-qPCR results showing the expression of cardiac differentiation markers Myosin light chain 2 (**A**) and Troponin T type 2 (cardiac) (**B**) in differentiating H9c2 cells treated daily with different concentrations of ATRA. Data shown are from one biological replicate, done in technical quadruplicate. Error bars represent standard error of the mean. Expression determined by the relative standard curve qPCR quantification method and normalized to *Gapdh* and *Rsp12*. Statistically significant differences determined by unpaired Student's *t*-test (GraphPad Prism 6 Software). * indicates $p < 0.05$.

A. D0 Differentiation

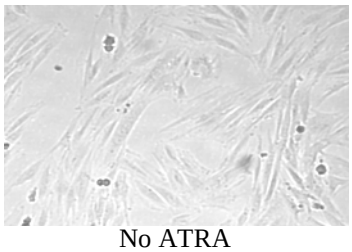

No ATRA

B. D5 Differentiation

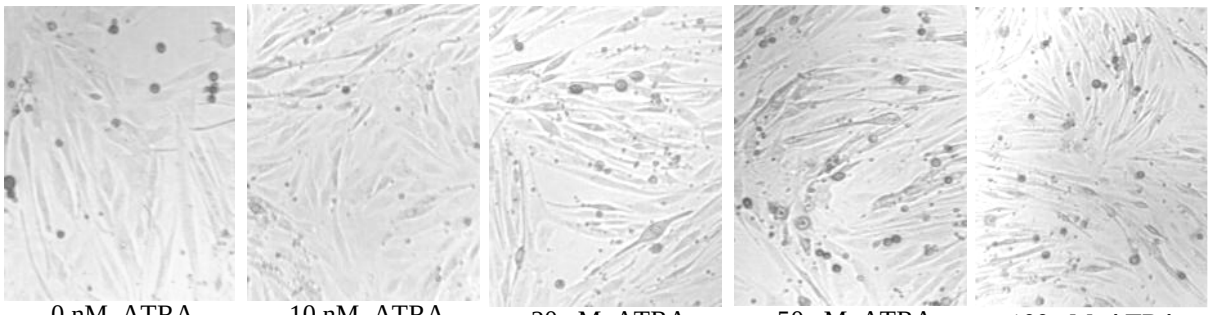

0 nM ATRA | 10 nM ATRA | 20 nM ATRA | 50 nM ATRA | 100 nM ATRA

Figure 7. Morphology of differentiating H9c2 cells treated daily with different concentrations of ATRA. Phase-contrast microscopy of H9c2 cells at (**A**) day zero (D0) differentiation, and (**B**) day five (D5) differentiation, after daily treatments of varying concentrations of ATRA. Images taken at 100X magnification.

20 nM, by D5 fewer cells were adhering to the cell culture plate, suggesting that higher concentrations of ATRA were toxic. Therefore, 10 nM ATRA accompanied by serum reduction was used in this study to induce cardiac differentiation in H9c2 cells since it gave maximum cardiomyocyte yield with minimal toxicity. This treatment regime is consistent with the vast majority of current literature on H9c2 cells.

3.2.2. Confirmation of lineage

The progress of myocyte differentiation over time was examined next by phase contrast microscopy (Figure 8). As determined above, with only serum reduction (for skeletal muscle differentiation), cells became progressively longer and fused together, resulting in long, multinucleated myotubes (Brostrom et al., 2000; Comelli et al., 2011; Menard, 1999). When serum reduction was accompanied by daily treatments of 10 nM ATRA, cells also became more elongated, but did not fuse together. Furthermore, their nuclei became rounder and more evident with phase-contrast microscopy (Brostrom et al., 2000; Comelli et al., 2011; Menard, 1999). Therefore, microscopy results suggested the desired lineages had in fact been achieved in our time courses with the treatments described.

The proportion of skeletal vs. cardiac muscle differentiation in a lineage was further evaluated by examining the mRNA expression of skeletal muscle differentiation marker *Myog* and cardiac differentiation marker *Myl2*, at day 6 (D6) of differentiation (Figure 9). *Myog*, a marker of skeletal muscle differentiation, is a transcription factor and one of four myogenic regulatory factors that are involved in the activation of skeletal myoblast differentiation (Edmondson & Olson, 1989; Kee et al., 2007; Sabourin & Rudnicki, 2001). The expression of these differentiation markers under both

A. Skeletal Muscle Differentiation (1% FBS)

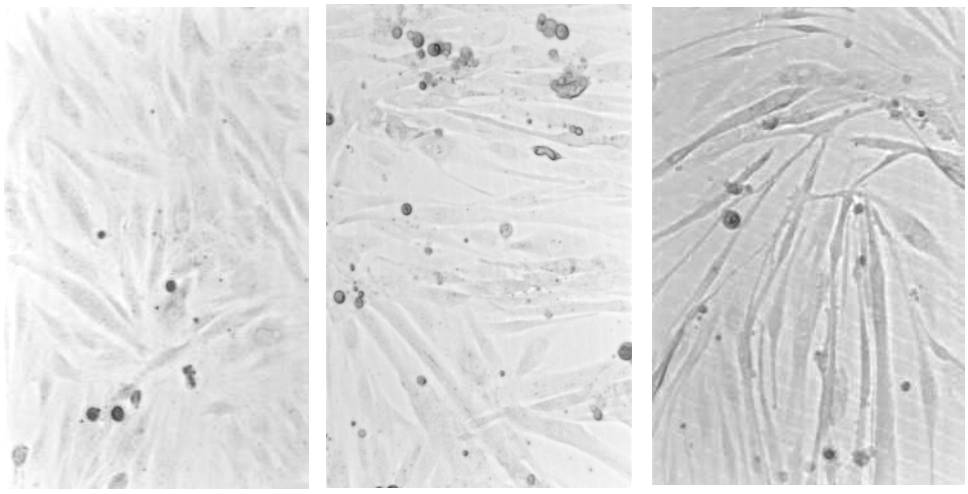

DO D4 D7

B. Cardiac Differentiation (1% FBS and daily treatments of 10 nm ATRA)

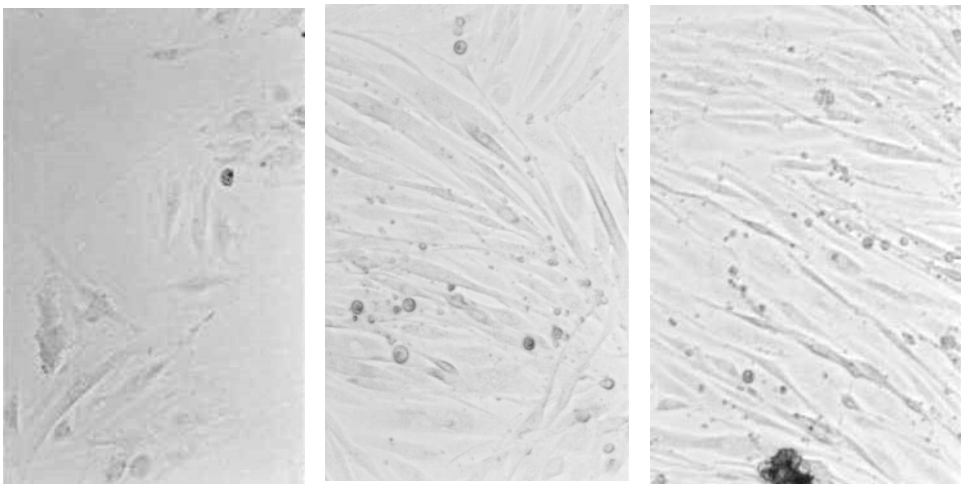

D0 D4 D7

Figure 8. Verfication of lineage - Morphology of differentiating H9c2 cells. Morphology of H9c2 at D0, D4 and D7 of exposure to (**A**) serum reduced medium or, (**B**) serum reduced medium and daily treatments of 10 nM of ATRA. Images taken with phase-contrast microscopy at 100X magnification.

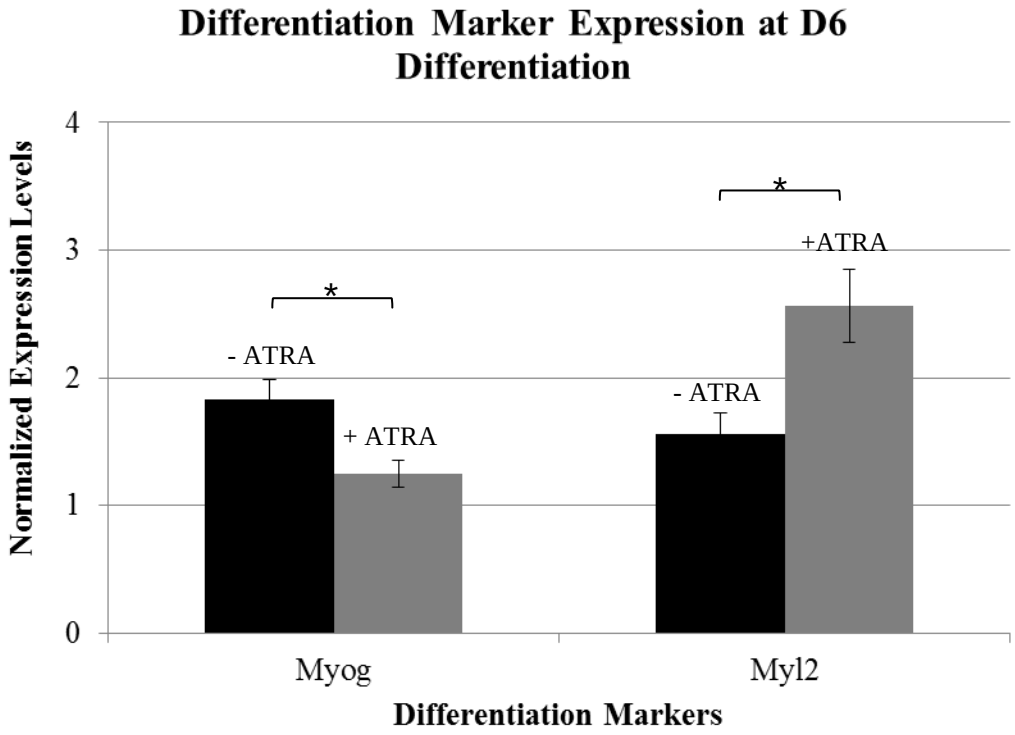

Figure 9. Verification of lineage - mRNA expression of differentiation markers. Lineage confirmation by examining the expression of skeletal muscle differentiation marker Myogenin (*Myog*), and cardiac differentiation marker myosin light chain 2 regulatory subunit (*Myl2*), at D6 differentiation. (-)ATRA indicates that these cells were only exposed to reduced serum medium, in an effort to induce skeletal muscle differentiation. (+)ATRA indicates that serum reduction was also accompanied by daily treatments of 10 nM ATRA in an effort to induce cardiac differentiation. Data represents RT-qPCR results from three biological replicates, done in technical quadruplicate. Results were analyzed by the relative standard curve quantification method and normalized to *Gapdh* and *Rsp12*. Error bars represent standard error of the mean. Statistically significant differences determined by unpaired Student's *t*-test (GraphPad Prism 6 Software) with $p < 0.05$.

differentiation regimes showed that cells treated with ATRA and serum reduction had a statistically significant higher level of the cardiac differentiation marker *Myl2* by D6 differentiation. This confirmed that significantly higher levels of cardiac differentiation were achieved with ATRA treatments. Furthermore, cells subjected to serum withdrawal (but not treated with ATRA) had a statistically significant higher level of the skeletal muscle differentiation marker *Myog* at D6 differentiation. This in turn confirmed that skeletal muscle differentiation was successful, at least for a significant portion of this serum-deprived population. All in all, these results-confirmed that we were successful in inducing myoblast differentiation into skeletal and cardiac muscle lineages. Therefore, mRNA and protein expression data for various genes could be confidently collected throughout differentiation and compared between lineages.

3.3. Protein expression analysis

Before analyzing the protein expression pattern of Rbm5 and Rbm10 during myoblast differentiation, it was essential to ensure that the correct bands being detected by Western blot analysis were used for protein expression quantification. Therefore transient overexpression experiments were performed in H9c2 cells during normal growth. RBM10v1, RBM10v2 and RBM5 were separately overexpressed and the resulting protein samples analyzed via Western Blot. We expected that when a specific Rbm protein's cDNA was overexpressed, the corresponding band would increase in intensity compared to the control cells.

3.3.1. Rbm10 band identification

For the detection of Rbm10, blots were probed with a commercially available rabbit anti-RBM10 (A301-006A) antibody from Bethyl Laboratories raised to residues 880-930 (C-terminal region) of human RBM10 (100% homology with rat (accession number: P70501)) (Figure 1) (Amanchy et al., 2008; Wang et al., 2012). Both Rbm10v1 and Rbm10v2 were expected to react with this antibody since they both only vary in the sequence of their N-terminal region. Western blots of protein extracts from cells overexpressing Rbm10v1 and Rbm10v2 enabled us to identify which band corresponded to each variant (Figure 10A): the approximately 135 kDa band corresponding to Rbm10v1, and the approximately 107 kDa band corresponding to Rbm10v2.

3.3.2. Rbm5 band identification

Western Blots of protein extracts from cells overexpressing RBM5 were first probed with a non-commercially available anti-RBM5 antibody, LUCA-15UK, which was raised to the first 15 N-terminal amino acids of the human RBM5 sequence (100% homology with rat [accession number: AAI66477]) (Figure 1). This antibody was used since it was well characterized and optimized (Fushimi et al., 2008; Mourtada-Maarabouni et al., 2002; Rintala-Maki & Sutherland, 2004; Sutherland et al., 2000). LUCA-15UK detected two bands, only one of which, at approximately 113 kDa, increased in intensity when RBM5 was transiently overexpressed (Figure 10B). This indicated that the 113 kDa band corresponded to the full-length 25 exon Rbm5 transcript. Since this was the first time that this non-commercially available antibody had been used on rat protein sample, it was necessary to verify that these results were reproducible with another anti-RBM5 antibody. Therefore, a commercially available rabbit anti-RBM5

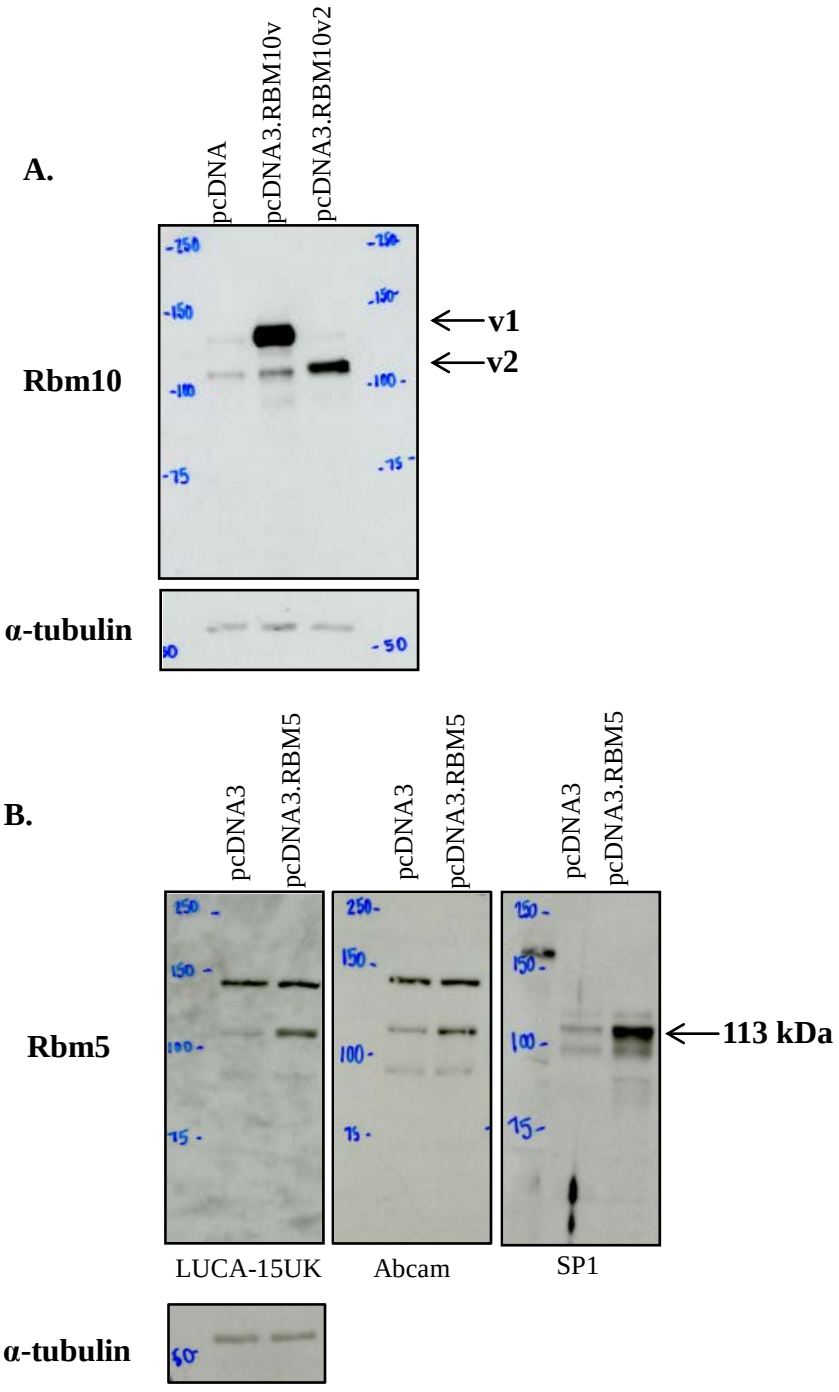

Figure 10. Rbm5 and Rbm10 Western blot band identification. A. Western blot results of protein from H9c2 cells transiently transfected with pcDNA3, pcDNA3.RBM10v1 or pcDNA3.RBM10v2 at 72 hours post-transfection. Blot probed with anti-Rbm10 antibody from Bethyl Laboratories, then stripped and probed for α-tubulin. **B**. Western blot results of protein from H9c2 cells transiently transfected with pcDNA3 or pcDNA3.RBM5 at 48 hours post-transfection. Blot probed for Rbm5 with non-commercially available LUCA-15UK antibody, then stripped and probed for α-tubulin. Following this, blot was probed for Rbm5 with Abcam antibody, stripped, and probed again for Rbm5 with SP1 antibody. Indicated ladder is in kDa.

antibody from Abcam (ab85504) was tested next. This second anti-RBM5 antibody was raised to the first 50 N-terminal amino acids of the human RBM5 sequence (100% homology with rat [accession number: AAI66477]) (Figure 1). Results with this Abcam antibody showed three distinct bands at approximately 92 kDa, 113 kDa and 140 kDa, respectively (Figure 10B). However, only the 113 kDa band increased in intensity when RBM5 was transiently overexpressed, which was consistent with the LUCA-15UK antibody results. This suggested that the upper and lower-most bands detected by the Abcam anti-RBM5 antibody were the result of non-specific interactions. Yet, the molecular mass of Rbm5 calculated from its amino acid content should be approximately 92 kDa, the size of the lowest band detected by the anti-RBM5 Abcam antibody. Therefore, we used a third anti-RBM5 antibody raised to the whole RBM5 sequence in order to ensure that it was indeed the 113 kDa band that corresponded to Rbm5 (Figure 1). This last anti-RBM5 antibody was a non-commercially available antibody, termed SP1, and was in fact raised to the recombinant purified full-length human RBM5 protein (Bonnal et al., 2008). The only band detected with the SP1 anti-RBM5 antibody, that was also consistent with those picked up by either the Abcam or LUCA-15UK anti-RBM5, was once again the 113 kDa band (Figure 10C). Furthermore, this was again the only band whose intensity increased when RBM5 was overexpressed. In summary, these results strongly suggested that the approximately 113 kDa band identified by all three anti-RBM5 antibodies corresponded to full-length Rbm5. For the following Western blots, only the Abcam anti-RBM5 antibody was used since it was commercially available. This antibody was also previously used in other Rbm5 studies (Li et al., 2012; Liang et al., 2012; Shao et al., 2012).

Using the optimal parameters determined in this chapter for gene expression quantification, cell culture and differentiation, and protein expression, the expression of Rbm5 and Rbm10 throughout H9c2 skeletal and cardiac myoblast differentiation could accurately be assessed.

Chapter 4. Results – Rbm5 and Rbm10 Splice Variant Expression Throughout Rat Skeletal and Cardiac Myoblast Differentiation

The results described in the previous chapter confirmed that we could commit myoblast cells to a specific lineage, and that mRNA and protein expression analysis techniques were optimized. Therefore, *Rbm5* and *Rbm10* splice variant mRNA and protein expression was examined throughout H9c2 skeletal and cardiac myoblast differentiation. It is important to note that we were particularly interested in significant changes in Rbm5 and Rbm10 expression that occurred within the first three days of differentiation, because this is when apoptosis and cell cycle arrest occur in differentiating cells. However, statistically significant changes in expression were evaluated throughout differentiation. At the mRNA level, differences of at least (+)2- or (-)0.5-fold were considered for statistical significance. In addition, we compared temporal expression of individual variants and isoforms between lineages (e.g., Rbm5 expression at D4 of skeletal and cardiac muscle differentiation). We also compared the expression levels of *Rbm5* to *Rbm10v1* in rat myoblasts to determine if their relative expression levels were the same as in transformed cells.

4.1. *Rbm5* splice variant expression analysis

The mRNA expression of three *Rbm5* splice variants was investigated: *Rbm5*, *Rbm5+5+6* and *Lust* (Figure 1). Sequences used for variant-specific primer design were based on known human *RBM5* splice variant sequences since only full-length *Rbm5* mRNA had been reported in rat at that point. To date, the only *Rbm5* transcript documented in rat remains full-length *Rbm5*.

At the protein level, only full-length Rbm5 expression was investigated in this study since, even in human samples, a translational product has rarely been identified for RBM5+5+6 (Maquat & Carmichael, 2001; Sutherland et al., 2000) and not previously identified for Lust (Rintala-Maki & Sutherland, 2009).

4.1.1. mRNA and protein expression of full-length Rbm5 did not correlate during myoblast differentiation

First, RT-qPCR and Western blot analysis results showed that full-length *Rbm5* was expressed at the mRNA and protein levels in rat myoblasts and throughout their differentiation into skeletal and cardiac myocytes, respectively (Figure 11A, B and Figure 12A-D). Surprisingly, during skeletal muscle differentiation, there were no statistically significant changes in *Rbm5* mRNA expression between any two days of differentiation (Figure 11A). In fact, *Rbm5* expression was very steady throughout the establishment of the skeletal muscle lineage, with expression values for each day of differentiation being very close to that at D0. These results, however, were not mirrored at the protein level (Figure 12E), which showed a gradual decline in Rbm5 from D2 to D7 of skeletal muscle differentiation.

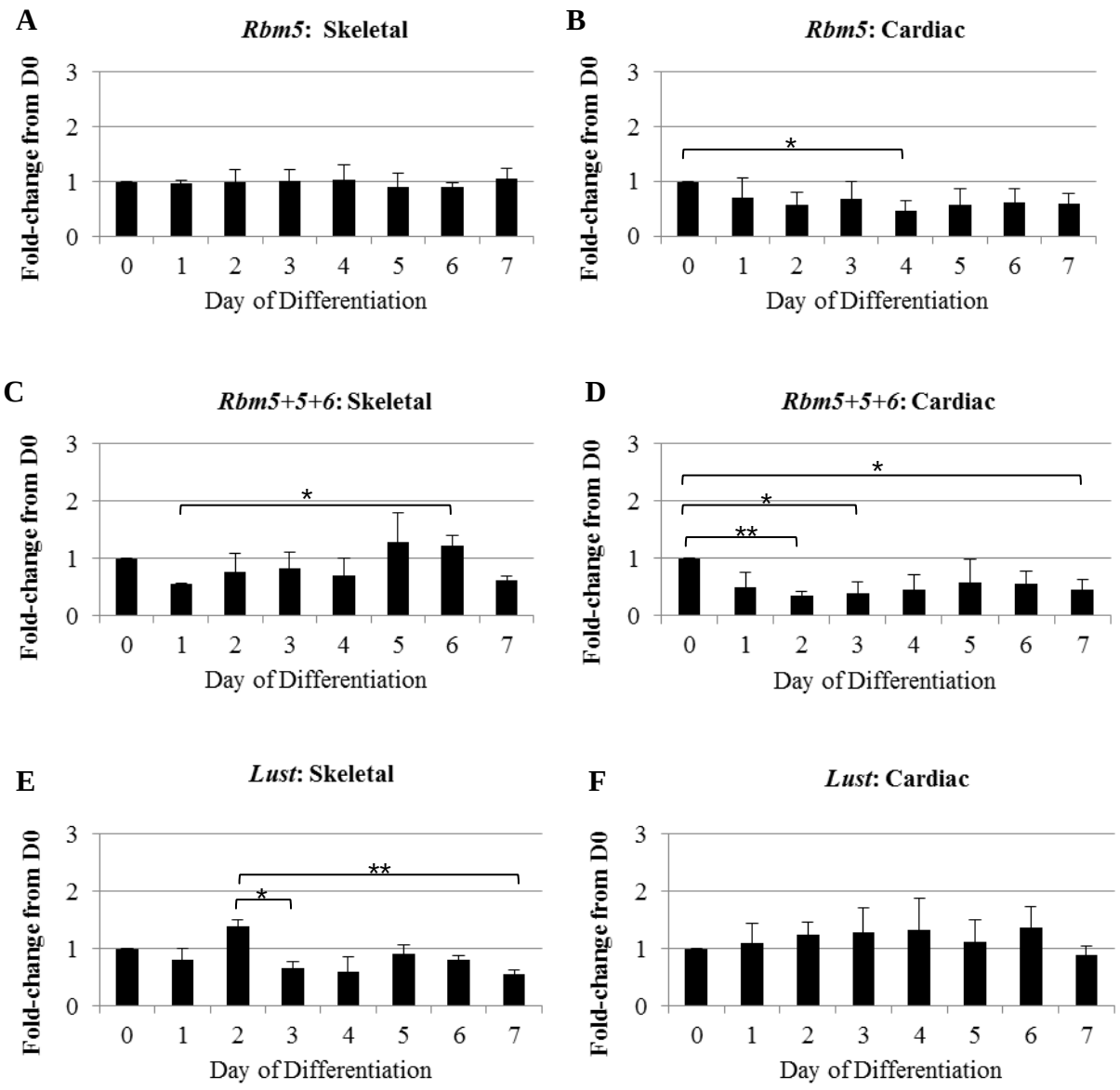

Figure 11. *Rbm5* mRNA splice variant expression throughout H9c2 skeletal and cardiac myoblast differentiation. RT-qPCR results for fold-change in expression of various *Rbm5* splice variants from D0 through D7 of H9c2 skeletal and cardiac myoblast differentiation. Figures **A**, **C** and **E** show the various *Rbm5* splice variants' expression throughout skeletal myoblast differentiation, whereas **B**, **D** and **F** show their expression throughout cardiac differentiation. mRNA expression analyzed by the comparative Ct qPCR quantification method and expressed as fold-change in expression from D0 differentiation. Values normalized to *Gapdh*. Statistically significant differences were evaluated between two days of differentiation with fold-changes at least greater than 2 or less than 0.5 with a Student's unpaired *t*-test (* indicates $p < 0.05$, ** indicates $p < 0.01$). Data represent results from biological triplicates, performed in technical quadruplicate. Error bars represent standard error.

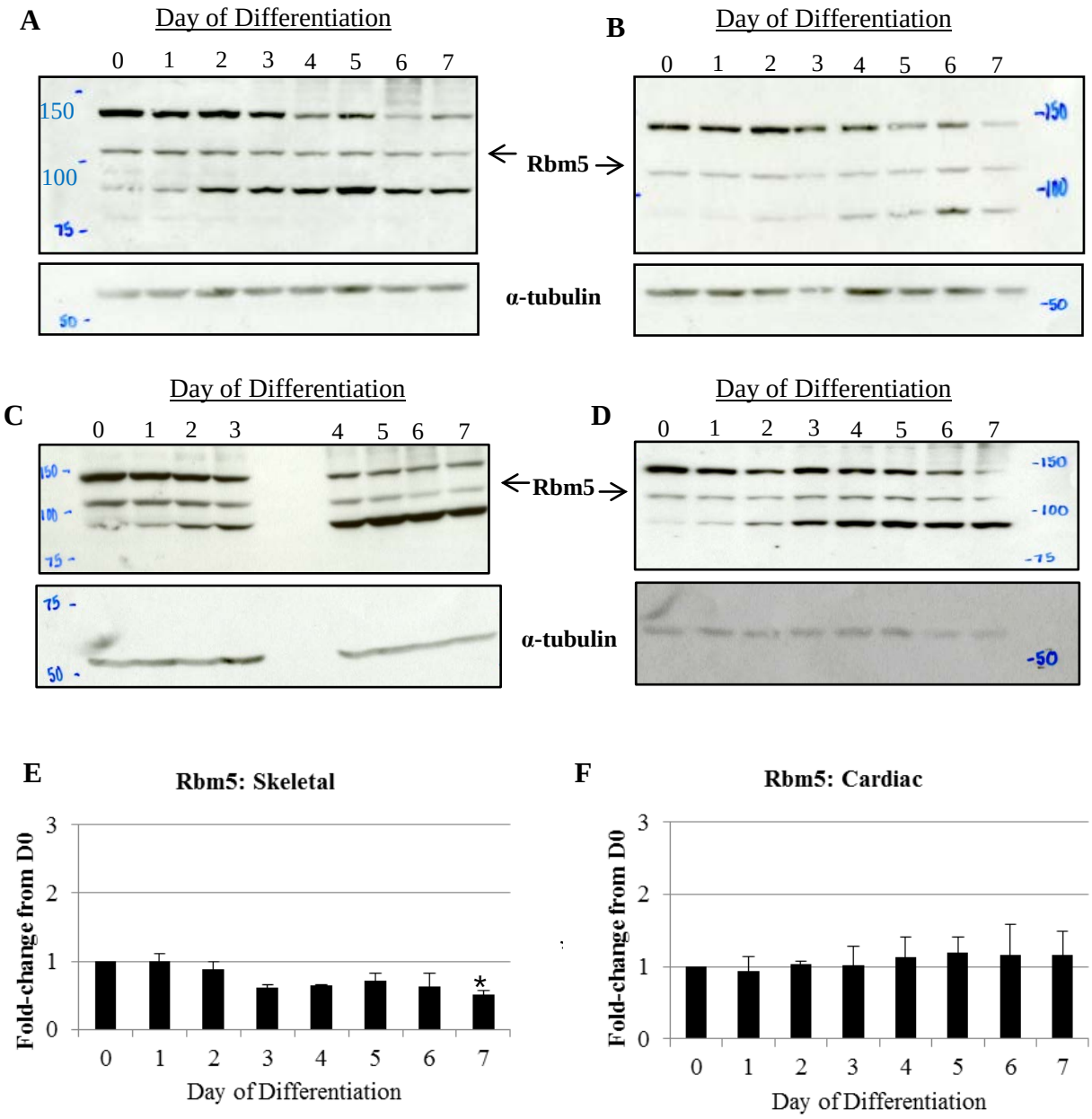

Figure 12. **Rbm5 protein expression throughout H9c2 skeletal and cardiac myoblast differentiation.** **A - D.** Western blots of H9c2 skeletal (**A**, **C**) and cardiac myoblast differentiation (**B**, **D**) protein samples, from D0 to D7 of differentiation, probed with anti-Rbm5 Abcam antibody. Following Rbm5 exposure, blots were stripped and probed for α-tubulin (used to normalize results). Blots are results from biological duplicates, and represent results for technical duplicates performed for each biological replicate. **E** and **F**. Quantification of Western blot results for Rbm5 expression throughout H9c2 skeletal and cardiac myoblast differentiation, respectively. Blots were probed with anti-Rbm5 antibody from Abcam, then stripped and probed for α-tubulin, which was used to normalize. Densitometry was carried out to quantify expression. Results are shown as fold-change in expression from D0 differentiation, and represent data from biological duplicates, performed in technical duplicates. Error bars represent standard error. Statistically significant differences were only evaluated between two days of differentiation with fold-changes at least greater than 2 or less than 0.5 with a Student's unpaired *t*-test (* indicate $p < 0.05$). Indicator of statistical significance placed directly above a bar refers to a statistically significant difference with the D0 value.

Throughout cardiac differentiation, *Rbm5* mRNA expression only changed significantly at D4 differentiation, when it decreased compared to D0 (Figure 11B). Overall, the trend of *Rbm5* mRNA expression during cardiac differentiation revealed a non-statistically significant drop in *Rbm5* expression soon after induction of differentiation, and quite low expression levels sustained throughout the establishment of the lineage. However, again in opposition to the mRNA data, protein levels of Rbm5 were very stable throughout cardiac differentiation, and always close to that at D0 (Figure 12F).

Comparison of full-length Rbm5 expression patterns between skeletal and cardiac myoblast differentiation showed similar results in the sense that in both lineages, only Rbm5 mRNA *or* protein expression changed. During skeletal muscle differentiation, it was Rbm5 protein expression that gradually decreased, with mRNA levels remaining steady. In opposition, during cardiac differentiation, it was *Rbm5* mRNA expression that decreased, while its protein expression remained constant. Therefore, during the establishment of both lineages only Rbm5 mRNA *or* protein expression decreased, while Rbm5 expression at the other level stayed constant.

4.1.2. Rbm5+5+6 mRNA expression varied significantly throughout both skeletal and cardiac myoblast differentiation

The second *Rbm5* splice variant studied from D0 to D7 of rat skeletal and cardiac myoblast differentiation was *Rbm5+5+6*. First, RT-qPCR results showed that *Rbm5+5+6* was expressed in rat myoblasts and throughout their differentiation into both skeletal and cardiac myocytes, respectively (Figure 11C, D). Within the skeletal muscle lineage, *Rbm5+5+6* expression showed a statistically significant difference only between D1 and

D6 of differentiation (D1<D6) (Figure 11C). Nonetheless, *Rbm5+5+6* expression did vary throughout skeletal muscle differentiation, with expression decreasing slightly during the first few days of differentiation, increasing around D5, and decreasing again by D7.

During cardiac differentiation, however, this peak in expression at D5 of differentiation was not seen, at least not to the degree at which it occurred during skeletal muscle differentiation. Rather, throughout cardiac differentiation *Rbm5+5+6* expression was decreased immediately following induction of differentiation and stayed quite low until D7 (statistically significant decreases in expression occurred at D2, D3 and D7 of differentiation, compared to D0) (Figure 11D). Therefore, overall *Rbm5+5+6* expression was higher during skeletal muscle differentiation, compared to cardiac. Thus, *Rbm5+5+6* mRNA expression varied more and was generally higher during skeletal muscle differentiation, than during cardiac differentiation.

4.1.3. Lust expression only varied significantly during skeletal muscle differentiation

The last *Rbm5* splice variant which was analyzed in this study was *Lust*. RT-qPCR results showed that *Lust* was also expressed in rat myoblasts and throughout rat skeletal and cardiac myoblast differentiation (Figure 11E, F). Throughout the establishment of the skeletal muscle lineage, significant changes in *Lust* expression were observed at D3 and D7 of differentiation, when *Lust* expression significantly dropped compared to D2 (Figure 11E). The general trend of *Lust* expression throughout skeletal muscle differentiation showed that it varied, with slightly higher expression levels being seen around D2 and D5, and lower levels detected on the days in between. Different results were obtained when *Lust* expression was examined during cardiac differentiation: *Lust* mRNA levels

remained close to that at D0 and did not change significantly between any two days of differentiation (Figure 11F).

4.1.4. Lust mRNA expression was lower than that of full-length Rbm5 and Rbm5+5+6 in rat myoblasts

Raw qPCR results (Ct values) from D0 of differentiation for all *Rbm5* splice variants studied were compared in order to determine their relative expression in rat myoblasts. The Ct values of *Rbm5* and *Rbm5+5+6* were quite similar; however those for *Lust* were approximately 2.5 cycles higher (Table 2). This indicated that *Lust* mRNA expression was lower than that of full-length *Rbm5* and *Rbm5+5+6* in rat myoblasts (Ct values and expression levels are inversely correlated). It is important to note that although different primer pairs were used to quantify the expression of the various *Rbm5* splice variants, primer pair efficiencies were quite similar and all above 1.9 . Therefore, the variation in primer efficiencies should not account for the large difference in Ct values seen between *Lust* and the other *Rbm5* splice variants studied.

4.1.5. Rbm5 splice variants had different expression patterns throughout differentiation

Comparison of *Rbm5* splice variant mRNA expression profiles first showed that the expression of *Rbm5+5+6* and *Lust* changed throughout skeletal muscle differentiation and that their corresponding expression patterns were very similar (Figure 11C, E). However, full-length *Rbm5* mRNA expression was stable throughout skeletal muscle differentiation (Figure 11A). On the other hand, throughout cardiac differentiation, it was the expression of full-length *Rbm5* and *Rbm5+5+6* that changed and which showed similar expression patterns (Figure 11B, D). Therefore, only *Rbm5+5+6* mRNA

***Rbm5* splice variants**				
	Splice variant primer efficiency	**Average splice variant Ct**	**Average Gapdh Ct**	**Average delta Ct ($Ct_{splice\ variant} - Ct_{Gapdh}$)**
Rbm5	1.95	24.494 ± 0.454	17.768 ± 0.526	6.726 ± 0.553
Rbm5+5+6	1.99	24.926 ± 0.432	18.069 ± 0.440	6.858 ± 0.638
Lust	1.94	27.628 ± 0.763	18.065 ± 0.440	9.563 ± 0.701
***Rbm10* splice variants**				
	Splice variant primer efficiency	**Average splice variant Ct**	**Average Gapdh Ct**	**Average delta Ct ($Ct_{Rbm10v1} - Ct_{Gapdh}$)**
Rbm10v1	2.00	27.393 ± 0.451	17.768 ± 0.526	9.625 ± 0.560

Table 2. Raw qPCR data for *Rbm5* and *Rbm10* splice variant expression at D0 differentiation.
Values represent the average Ct value for the variant in question from D0 skeletal and cardiac myoblast differentiation mRNA samples performed in biological triplicate and technical duplicate for each lineage. Values are shown as ± standard error. Gapdh was used to normalize. Splice variant primer efficiency calculated as shown in Figure 3.

expression changed significantly throughout both skeletal and cardiac muscle differentiation, whereas *Rbm5* mRNA expression changed only during cardiac differentiation and *Lust* during skeletal muscle differentiation.

4.2. Rbm10 splice variant expression analysis

Expression of the two most highly expressed *Rbm10* variants, *Rbm10v1* and *Rbm10v2*, was examined. Sequences used for variant-specific primer design were from documented rat *Rbm10* splice variant sequence data available at the time of primer design, as described in Chapter 1. It is important to note that since we designed these primers, the exon numbering for rat *Rbm10* has been changed to match the human *RBM10* mRNA (exon numbering was previously offset by two between rat and human Rbm10). *Rbm10v1* mRNA expression levels were measured using RT-qPCR. End point (RT-PCR) was used to evaluate *Rbm10v2* mRNA expression, since primers that spanned the spliced exon would not specifically amplify *Rbm10v2*.

4.2.1. Rbm10v1 expression varied only during skeletal muscle differentiation, and only at the protein level

RT-qPCR and Western blot results for Rbm10v1 expression first showed that this Rbm10 variant was in fact expressed in rat myoblasts and throughout rat skeletal and cardiac myoblast differentiation (Figure 13C, D and Figure 14A-D). At the mRNA level, *Rbm10v1* expression did not change significantly between any two days of skeletal muscle differentiation, and did not significantly vary throughout the establishment of the lineage (Figure 13C). At the protein level, however, Rbm10v1 expression slowly

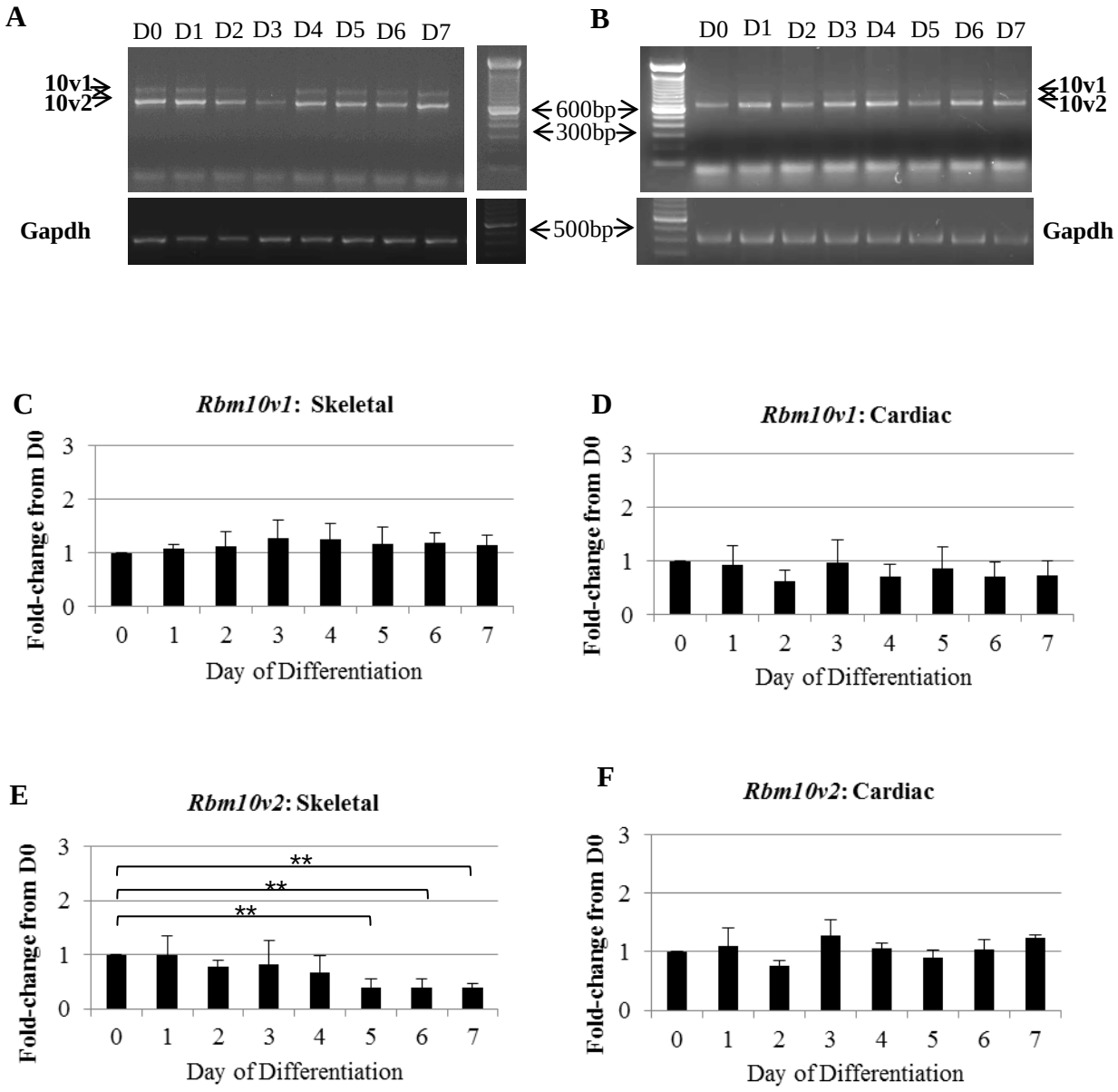

Figure 13. *Rbm10* splice variant expression throughout H9c2 skeletal and cardiac myoblast differentiation. A and **B**. Raw RT-PCR data for *Rbm10v1* and *Rbm10v2* expression throughout rat skeletal (**A**) and cardiac myoblast differentiation (**B**), respectively. Results are representative of results from biological triplicates, performed in technical duplicate. *Gapdh* was used as reference gene and the ladder is a 100bp ladder. **C** and **D**. RT-qPCR results for expression of *Rbm10v1* from D0 to D7 of H9c2 skeletal (**C**) and cardiac (**D**) myoblast differentiation. mRNA expression was analysed by the comparative Ct qPCR quantification method. **E** and **F**. RT-PCR results for *Rbm10v2* expression from D0 to D7 of H9c2 skeletal (**E**) and cardiac (**F**) myoblast differentiation. mRNA expression was determined by electrophoresing PCR products on a 2% TAE Agarose Gel, and densitometry was carried out. All expression values were graphed as fold-change in expression from D0 differentiation. Values were normalized to *Gapdh*. Statistically significant differences were evaluated between two days of differentiation with fold-changes at least greater than 2 or less than 0.5 with a Student's unpaired *t*-test (** indicates $p < 0.01$). Data represent results from biological triplicates, performed in technical duplicates. Error bars represent standard error.

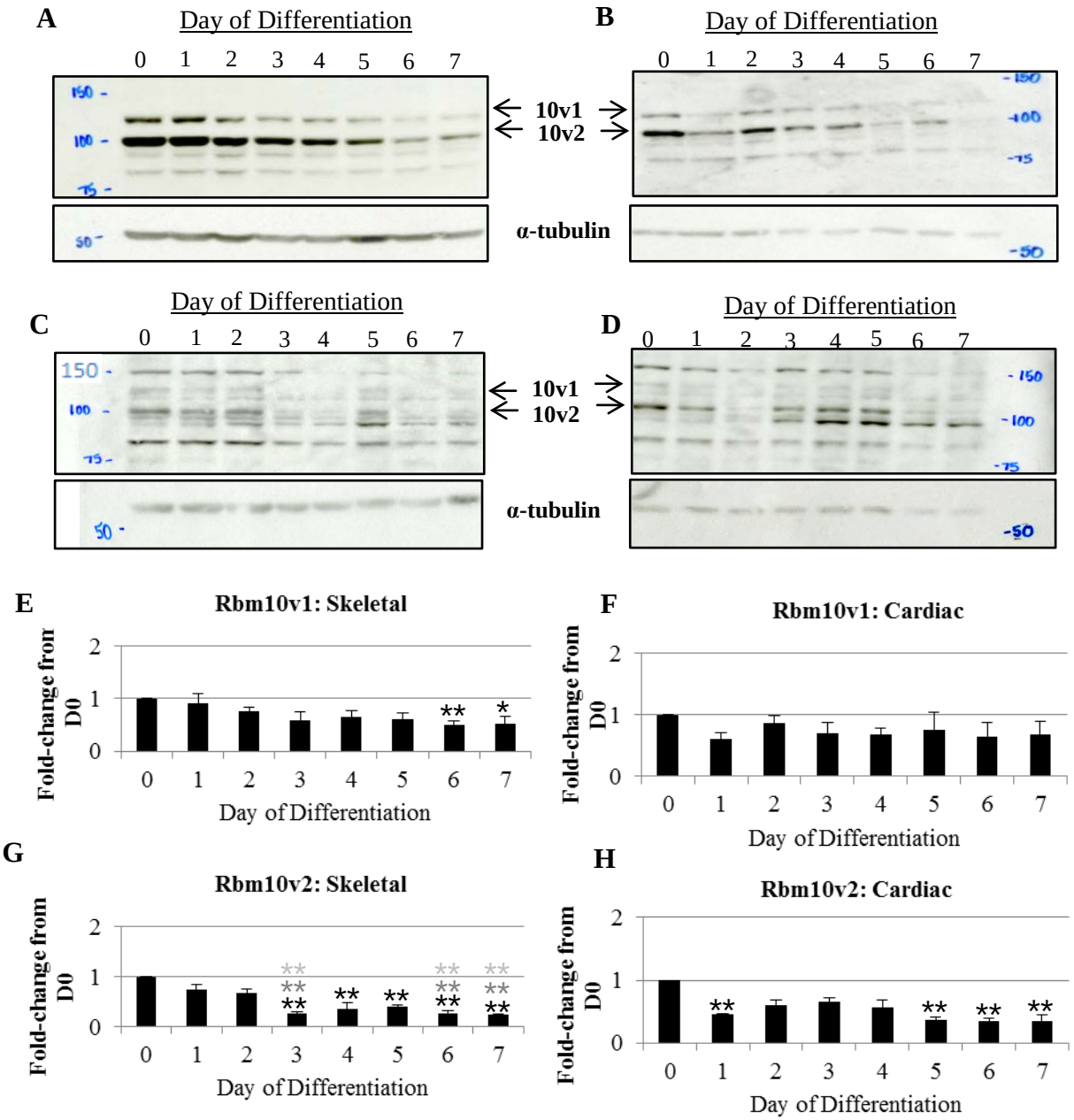

Figure 14. Rbm10v1 and Rbm10v2 protein expression throughout H9c2 skeletal and cardiac myoblast differentiation. A - D. Western blots of H9c2 skeletal (**A**, **C**) and cardiac (**B**, **D**) myoblast differentiation protein samples, from D0 to D7 of differentiation, probed with anti-Rbm10 Bethyl antibody. Following, blots were stripped and probed for α-tubulin (used to normalize results). Blots are from biological duplicates, and representative of technical duplicates performed for each biological replicate. **E - H**. Quantification of Western blot results for Rbm10 expression throughout H9c2 skeletal and cardiac myoblast differentiation, respectively (normalized to α-tubulin). Densitometry was carried out to quantify expression. Results are shown as fold-change in expression from D0 differentiation, and represent data from biological duplicates, performed in technical duplicates. Error bars represent standard error. Statistically significant differences were only evaluated between two days of differentiation with fold-changes at least greater than two or less than 0.5 with a Student's unpaired *t*-test (* indicates $p < 0.05$, and ** indicates $p < 0.01$). Indicator of statistical significance placed directly above a bar refers to a statistically significant different with the D0 value (black indicator), D1 value (grey indicator), or D2 (light grey indicator).

decreased, with significantly lower levels being seen at D6 and D7 of skeletal muscle differentiation, compared to D0 (Figure 13E).

During cardiac differentiation, *Rbm10v1* mRNA expression also showed no statistically significant change (Figure 13D). Rbm10v1 protein expression during cardiac differentiation was consistent with these mRNA results (Figure 14F). In sum, only during skeletal muscle differentiation, and at the protein level, did Rbm10v1 expression change significantly.

4.2.2. Rbm10v2 expression varied most significantly at the protein level throughout both skeletal and cardiac myoblast differentiation

RT-PCR and Western blot results showed that Rbm10v2 is expressed in rat myoblasts and throughout their differentiation into skeletal and cardiac myocytes, respectively (Figure 13A, B and Figure 14G, H). At the mRNA level, *Rbm10v2* expression gradually decreased throughout skeletal muscle differentiation, with a statistically significant drop in expression achieved by D5, compared to D0 (Figure 13E). At the protein level, a decrease in *Rbm10v2* expression was also seen throughout skeletal muscle differentiation. However, a statistically significant drop was seen much earlier than at the mRNA level: Rbm10v2 protein expression was statistically significantly decreased as soon as D3 of differentiation, while mRNA expression was only significantly decreased by D5 (Figure 14G).

In regards to *Rbm10v2* expression during cardiac differentiation, no statistically significant changes in expression were seen at the mRNA level. At the protein level though, a significant decrease was seen at D1, D5, D6 and D7, compared to D0 (Figure 14H). Therefore, during skeletal muscle differentiation both *Rbm10v2* mRNA and protein

expression were significantly decreased near the end of differentiation, with particularly significant decreases occurring as of D3 at the protein level. During cardiac differentiation, however, only Rbm10v2 protein expression changed significantly, and only by D5.

4.2.3. Rbm10v2 was more highly expressed than Rbm10v1 in myoblasts, and throughout differentiation

Raw RT-PCR results for *Rbm10* expression showed that *Rbm10v2* was much more highly expressed than *Rbm10v1* in rat myoblasts, and throughout their differentiation into skeletal and cardiac myocytes (Figure 13A, B). This was also true at the protein level, with the difference being even more pronounced during skeletal muscle differentiation, compared to cardiac (Figure 14A-D). In fact, Rbm10v2 protein expression was almost always twice that of Rbm10v1 throughout a large part of skeletal muscle differentiation (Figure 15A).

It is important to note that the same RT-PCR primer pair was used to evaluate *Rbm10v1* and *Rbm10v2* mRNA expression in this part of the analysis (the primer pair corresponded to sequences within the exons on each side of the spliced exon, and thus both variants were detected in the same PCR reaction). Therefore, the difference in expression observed between *Rbm10v1* and *Rbm10v2* could not be simply due to a difference in primer pair efficiencies. Furthermore, at the protein level, Rbm10 expression was evaluated using the Bethyl anti-Rbm10 antibody described in Chapter 2, which was raised to the C'-terminus of Rbm10. Since the exon which differentiates Rbm10v1 and Rbm10v2 is in the N'-terminal region of the protein, both variants contained the entire sequence to which the antibody was raised. Therefore, Rbm10v1 and Rbm10v2 should be

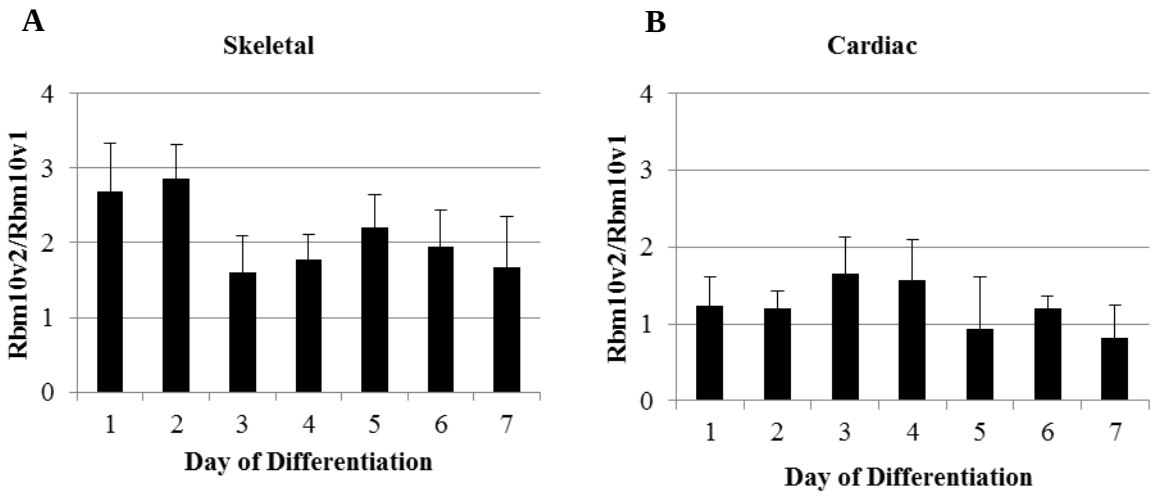

Figure 15. Ratio of Rbm10v2/Rbm10v1 protein expression throughout H9c2 skeletal and cardiac myoblast differentiation. A, **B**. Ratio of Rbm10v2/Rbm10v1 protein expression resulting from quantification of Western blot results for Rbm10 expression throughout H9c2 skeletal and cardiac myoblast differentiation, respectively. Blots were probed with Bethyl anti-Rbm10 antibody, and densitometry was carried out. Results represent data from biological duplicates, performed in technical duplicates. Error bars represent standard error.

detected by the antibody with approximately the same affinity. In sum, Rbm10v2 mRNA and protein expression was greater than that of Rbm10v1 in rat myoblasts and throughout their differentiation into both skeletal and cardiac myocytes. Also, during skeletal muscle differentiation, these differences in expression were more pronounced.

4.2.4. Rbm10v1 mRNA expression was lower than that of Rbm5 in myoblasts

Comparison of Ct values for *Rbm10v1* and the various *Rbm5* splice variants studied revealed that *Rbm10v1* expression levels in rat myoblasts were lower than that of *Rbm5* and *Rbm5+5+6*, and close to that of *Lust* (Ct values and expression levels are inversely proportional) (Table 2). It is important to note that different primer pairs were used to amplify *Rbm10v1* and the various *Rbm5* splice variants. Therefore, some of the observed variations in expression could be due to differences in primer efficiencies. However, in this case, all primer efficiencies were very close (all within 0.06 of each other), and the expression differences were quite large. Hence, differences in primer pair efficiencies alone are not likely to be the cause of the important expression differences seen between *Rbm10v1* and *Rbm5* in rat myoblasts. Due to the lack of specificity of qPCR primers for *Rbm10v2*, it was not possible to directly compare the expression of *Rbm10v2* to that of *Rbm5* and *Rbm5+5+6* in rat myoblasts. However, based on RT-PCR and Western blot results, we had determined that *Rbm10v2* expression was at least higher than that of *Rbm10v1* in rat myoblasts, and thus closer to that of *Rbm5* and *Rbm5+5+6*.

Chapter 5. Discussion

RNA-binding proteins can influence various cellular processes due to the important role they play in many co- and post-transcriptional events. Two such RNA binding proteins, RBM5 and RBM10, have been studied quite heavily in transformed cells. However, much remains to be elucidated concerning their exact mechanism of action, and whether their associated roles in transformed cells are the same as in non-transformed systems. As a first step in determining if these RNA binding proteins play a role in non-transformed cells, and to gain a hint as to what this role may be, Rbm5 and Rbm10 expression was examined throughout rat skeletal and cardiac myoblast differentiation. The myoblast differentiation model is a particularly useful model in which to study Rbm5 and Rbm10 since, as described in Chapter one, Rbm5 and Rbm10 are both highly expressed in mature human skeletal and cardiac muscle cells (Figure 2). Furthermore, cellular processes in which Rbm5 and Rbm10 have been associated in transformed cells are also important to myoblast differentiation, particularly cell cycle arrest, apoptosis and alternative splicing. These three cellular events occur at specific times during myoblast differentiation. For instance, cell cycle arrest occurs approximately two days following induction of myogenic differentiation (Andrés & Walsh, 1996; Novitch et al., 1999; Walsh & Perlman, 1997), similar to what is seen during cardiac differentiation (Ahuja et al., 2007; Poolman et al., 1998). Apoptosis levels in differentiating cells also reach a maximum after approximately two days in DM (Dee et al., 2002; Sandri et al., 1996). Finally, alternative splicing occurs throughout differentiation, with various factors being alternatively spliced at specific times throughout this process (Bland et al., 2010; Revil et al., 2010). Therefore, if Rbm5 and

Rbm10 are involved in the same cellular processes in transformed and non-transformed systems, we would expect their expression to change when these events occur in differentiating cells.

5.1. *Rbm5* and *Rbm10* splice variants are expressed in rat myoblasts

First, we found that all examined *Rbm5* and *Rbm10* splice variants were in fact expressed in rat myoblasts, as revealed by PCR or qPCR amplification of the mRNA encoding the specific splice variants, or the detection of specific protein isoforms by Western blot. This is the first report of *Rbm5+5+6* and *Lust* mRNA expression in rat tissue, in myoblasts, and throughout skeletal and cardiac myoblast differentiation. Also, this is the first report of *Rbm5*, *Rbm10v1* and *Rbm10v2* mRNA and protein expression in rat muscle cells, and throughout rat skeletal and cardiac myoblast differentiation. Thus, this study not only gives a first idea as to whether Rbm5 and Rbm10 splice variants play a role in non-transformed systems, but is the first to describe their expression in rat muscle cells.

5.2. *Rbm5* and *Rbm10* splice variants are not expressed at the same level in rat myoblasts

5.2.1. In myoblasts, as in transformed cells, Lust expression is lower than that of Rbm5

Based on Ct values for *Rbm5*, *Rbm5+5+6* and *Lust* at D0 of differentiation, it was possible to conclude that the expression of *Lust* was much lower than that of the other two *Rbm5* variants in rat myoblasts (Table 2). Lower levels of *Lust*, compared to *Rbm5*, have also been previously reported in human heart and skeletal muscle tissues, as well as in a

wide range of other lymphoid and non-lymphoid tissues, including the brain and pancreas (Sutherland et al., 2000). This has also been reported in transformed systems, including Hela (cervical cancer cells), A549 (adenocarcinomic alveolar basal epithelial cells) and SW480 (colon adenocarcinoma cells) cell lines (Sutherland et al., 2000). The consistency in the relative expression levels of *Lust* and *Rbm5* throughout these various transformed and non-transformed systems is another hint that these *Rbm5* variants may play a similar role in all of these cell types.

5.2.2. Unlike in transformed cells, Rbm10v2 expression is higher than that of Rbm10v1 in rat myoblasts and throughout myoblast differentiation

In rat myoblasts, and throughout their differentiation into skeletal and cardiac myocytes, respectively, Rbm10v2 expression was shown to be consistently higher than that of Rbm10v1. These results were observed at both the mRNA and protein levels (Figure 13A-D and Figure 15). However, previous reports investigating RBM10 expression in transformed cells have shown Rbm10v1 expression to be higher than that of Rbm10v2. For instance, in Jurkat cells, RT-PCR results showed much higher expression levels for *Rbm10v1* compared to *Rbm10v2* (Wang et al., 2012). These opposing results suggest that Rbm10v2 may have a particularly important role in myoblasts, and perhaps throughout differentiation, thus explaining its increased expression compared to Rbm10v1. Alternatively, these results could also suggest that Rbm10v1 is necessarily down-regulated or less highly expressed in these non-transformed cells (assuming Rbm10v1 does indeed influence such functions in myoblast, like it has been shown to do in transformed cells).

5.3. Possible functions of Rbm5 and Rbm10 splice variants in myoblast differentiation

Based on the temporal expression of Rbm5 and Rbm10 throughout differentiation, and comparison of their expression patterns between lineages, it was possible to determine possible functions with which Rbm5 and Rbm10 splice variants may be associated during differentiation.

5.3.1. Rbm5 may be involved in apoptosis and cell cycle arrest

The analysis of the protein expression profiles showed that during skeletal muscle differentiation, the expression of Rbm5 began decreasing at D3 of differentiation, and continued to drop for the remainder of the differentiation period studied (Figure 12E). The timing of this drop in expression suggests that Rbm5 may be involved in cellular events which occur during the first two days of differentiation, before this decrease in expression is observed. Such events could include apoptosis and cell cycle arrest (Figure 2). As described in Chapter one, Rbm5 has indeed been shown to modulate apoptosis and cell cycle arrest in transformed cells; therefore Rbm5 could also play such a role in non-transformed system. It is important to note that no such drop in Rbm5 protein expression was observed during cardiac differentiation (Figure 12F). Hence, Rbm5 may be involved in skeletal muscle differentiation-specific apoptosis and cell cycle arrest events. For example, Rbm5 may be involved in the terminal cell cycle arrest which occurs at approximately D2 of only skeletal muscle differentiation (cell cycle withdrawal is not permanent during cardiac myoblast differentiation). This potential role for Rbm5 in skeletal muscle differentiation could be further investigated by determining how/if the

expression of cell cycle regulatory factors vary when Rbm5 expression levels are altered in differentiating skeletal myoblasts.

5.3.2. Rbm5+5+6 and Lust may regulate similar cellular events, or each other, throughout skeletal myoblast differentiation

Rbm5+5+6 and *Lust* mRNA expression profiles were very similar throughout skeletal myoblast differentiation. Notably, both showed an increase in expression at D2 and D5 of differentiation (Figure 11C, D). This coordinated expression during skeletal muscle differentiation may hint at the role of *Rbm5+5+6* and *Lust* in this process. For instance, the increase in expression at D2 could indicate their involvement in cell cycle arrest and/or apoptosis, since it is around this time that these events occur in differentiating cells (Figure 2). This possibility could be tested by overexpressing *Rbm5+5+6* and/or *Lust* in myoblasts and during the first days of skeletal muscle differentiation, and examining the effect on the expression of cell cycle arrest and apoptosis markers, such as p21 and poly(ADP ribose) polymerase (Parp), respectively.

An increase in *Rbm5+5+6* and *Lust* expression was also observed at D5, which could indicate their involvement in the alternative splicing of metabolic or structural proteins important to skeletal muscle differentiation, since the expression of such factors begins at approximately this point in differentiation. To further investigate this potential role, levels of *Rbm5+5+6* and *Lust* could once again be modified in myoblasts, and changes in the alternative splicing of important metabolic and structural proteins evaluated via RT-qPCR.

In transformed cells *Rbm5+5+6* and *Lust* have been shown to have opposing effects in regards to their role in cell cycle arrest and apoptosis. For instance,

overexpression of *RBM5+5+6t* cDNA (a truncated form of *RBM5+5+6*) in transformed cells inhibited proliferation and sensitized cells to apoptosis mediated by cell surface receptor CD95 (Sutherland et al., 2000). On the other hand, overexpression of *Je2* (a partial *LUST* sequence) has been shown to suppress various types of apoptosis, including CD95-mediated apoptosis (Mourtada-Maarabouni et al., 2002; Sutherland et al., 2000). Therefore, another possible explanation for the correlation between *Rbm5+5+6* and *Lust* expression throughout skeletal muscle differentiation could be that they are regulating each other's expression. For example, *Lust* expression may mirror that of *Rbm5+5+6* in order to prevent excessive cell cycle arrest or apoptosis in differentiating cells. Or, *Rbm5+5+6* expression may mirror that of *Lust* in order to ensure that differentiating cells do undergo cell cycle arrest at the right time following induction of skeletal muscle differentiation. This assumes that *Rbm5+5+6* and *Lust* play similar roles in both transformed and non-transformed systems, and thus that these roles are antagonistic. In order to evaluate this possibility, future experiments could involve examining the expression of skeletal muscle differentiation-specific cell cycle arrest markers upon *Rbm5+5+6* and *Lust* overexpression, respectively, in rat myoblasts: if both Rbm5+5+6 and Lust alter the expression of these markers in different ways, it could further suggest that Rbm5+5+6 and Lust's roles in differentiation are antagonistic. In sum, *Rbm5+5+6* and *Lust* may both play a similar role in the events of early skeletal myoblast differentiation, including apoptosis and/or cell cycle arrest. Alternatively, their roles in differentiation may be opposite, as in transformed cells, thus, *Rbm5+5+6* and *Lust* may regulate each other's expression during skeletal muscle differentiation in order to ensure that the establishment of the skeletal muscle cell lineage is successful.

5.3.3. Lust expression, and/or a decrease in Rbm5+5+6 expression may be important to the establishment of the cardiac lineage

In contrast to what was observed throughout skeletal muscle differentiation, the expression patterns for *Rbm5+5+6* and *Lust* did not correlate during cardiac differentiation: *Rbm5+5+6* mRNA expression decreased and remained low as of D1 differentiation (Figure 11D), while *Lust* mRNA levels remained constant (Figure 11F). It is important to note that, in transformed cells, *Lust* has been shown to influence *Rbm5+5+6* expression. In fact, *Lust* has been shown to upregulate *Rbm5+5+6* expression, and down regulate *Rbm5+5+6t* (Rintala-Maki & Sutherland, 2009). Therefore, the observed *Rbm5+5+6* and *Lust* expression profiles during cardiac differentiation could suggest that (a) *Lust* expression is consistent during cardiac differentiation since down-regulation of *Rbm5+5+6(t)* is necessary for the establishment of the cardiac lineage, and/or (b) *Lust* expression itself is important for establishing the cardiac lineage. In the first possibility, *Rbm5+5+6* may necessarily be down-regulated in cardiac myoblast differentiation in order to ensure that differentiating cells are not targets for apoptosis, even though they do not undergo irreversible cell cycle. This hypothesis assumes that *Rbm5+5+6* can sensitize non-transformed cells to apoptosis, as it has been shown to do in transformed cells. This possibility could be further evaluated by overexpressing *Rbm5+5+6* in myoblasts and determining its effect on apoptosis (by examining the expression of apoptosis markers such as Parp), and cell number and viability (using a CASY counter for example). The second possibility is that *Lust* expression is important to cardiac differentiation. This could be the case if *Lust* plays a general role in regulating the expression and/or alternative splicing of cardiac-specific differentiation factors. To test this alternate hypothesis, *Lust* could be overexpressed in

myoblasts, and the expression and/or alternative splicing of cardiac-specific differentiation factors, such as Tnnt2, evaluated by RT-qPCR and/or Western Blot (may be hard to knockdown only the *Lust Rbm5* transcript, therefore overexpression experiments would be a good starting point). Thus, *Rbm5+5+6* and *Lust* also seem to play an important, and potentially antagonistic, role in cardiac differentiation.

5.3.4. Rbm10v1 and Rbm10v2 may also be involved in apoptosis and cell cycle arrest events which are specific to skeletal muscle differentiation

Like Rbm5, Rbm10v1 and Rbm10v2 protein expression varied significantly during skeletal muscle differentiation, dropping around D2, and remaining low until D7 (Figure 14E, G). Since cell cycle arrest and apoptosis occur at their maximum during the first few days of differentiation (Figure 2), when Rbm10v1 and Rbm10v2 expression is high, it suggests that both variants may play a role in these cellular processes. This would be consistent with what has been previously documented regarding the role of Rbm10v1 and Rbm10v2 in transformed cells, and could be evaluated by altering levels of Rbm10v1 and Rbm10v2 in rat myoblasts and throughout differentiation, and evaluating the consequent changes in expression of cell cycle arrest and apoptosis markers (i.e. p21 and Parp). During cardiac differentiation, however, similar variations in Rbm10v1 and Rbm10v2 protein expression were not observed. This suggests that the role of these Rbm10 variants in apoptosis, cell cycle arrest and/or other cellular processes may be specific to skeletal muscle differentiation. Thus, for instance, they may be involved in the terminal cell cycle arrest which is specific to the skeletal muscle lineage.

5.3.5. Rbm10v2 may be an important regulator of alternative splicing during cardiac differentiation

The protein expression profile for Rbm10v2 throughout cardiac differentiation shows that its expression fell very soon following induction of differentiation, increased near D3, and then dropped until D7. This is a different pattern than that seen throughout skeletal muscle differentiation, and suggests a different function for this Rbm10 variant in both lineages. At D3 of cardiac differentiation, when Rbm10v2 expression was shown to be increased, cell cycle arrest and apoptosis have already occurred in differentiating cells (Figure 2). However, the expression of specific metabolic proteins required for the establishment of the target muscle cell type begins (Andrés & Walsh, 1996). Therefore, Rbm10v2 may be involved in regulating the expression and/or the alternative splicing of such metabolic factors. Such a function has not yet been reported for Rbm10v2. However, in transformed cells, knockdown of Rbm10 has been shown to affect the expression and alternative splicing of many different genes (manuscript in preparation). Hence, although its role may be different, Rbm10v2 appears to be important to both skeletal and cardiac muscle cell differentiation.

5.4. Rbm5, Rbm10v1 and Rbm10v2 may be post-transcriptionally regulated

The mRNA and protein expression profiles rarely correlated in this study, with the most significant variations in expression usually only seen at the protein level. This held true, at least to a certain extent, for *Rbm5*, *Rbm10v1* and *Rbm10v2* expression throughout both skeletal and cardiac myoblast differentiation. The lack of correlation between mRNA and protein expression levels suggests that *Rbm5*, *Rbm10v1* and *Rbm10v2* may be the targets of post-transcriptional or translational regulation throughout differentiation.

One reason why these variants may be regulated in such a way during differentiation is that the effects of post-transcriptional and translational regulation are experienced much faster in the cell than the modulation brought about by transcriptional regulation. Thus the cell can more rapidly respond to environmental variations (i.e. exposure to differentiation medium) (Holcik & Sonenberg, 2005). During differentiation there are many cellular events occurring at once and in tandem, with each being strictly regulated by specific mechanisms. Therefore, immediate changes in the expression levels of particular proteins (perhaps including Rbm5, Rbm10v1 and Rbm10v2) could be necessary, and thus accomplished via post-transcriptional or translational modifications (Yahi et al., 2006).

An example of a protein which undergoes post-translational regulation during differentiation is the transcription factor Myocyte enhancer factor 2 (MEF2). During differentiation, MEF2 is acetylated, allowing it to bind better to DNA and thus increasing the transcription of its target genes (Angelelli et al., 2008). Another example of post-translational regulation in muscle is that of FoxO3, a member of the Forkhead Box O (FoxO) family of transcription factors. FoxO3 regulates the expression of various muscle atrophy related genes (Bertaggia et al., 2012; Mammucari et al., 2007; Sandri et al., 2004), and can also be acetylated. FoxO3 acetylation leads to a decrease in its activity, and consequent relocation to the cytoplasm. Once in the cytoplasm, FoxO3 is ubiquitylated by a ubiquitin ligase and consequently degraded (Bertaggia et al., 2012; Brault et al., 2010). This mechanism is extremely important in the prevention of excessive muscle mass loss, for example (Bertaggia et al., 2012). Therefore, the post-transcriptional and/or translational regulation of Rbm5, Rbm10v1 and Rbm10v2 suggested in the current study hint to the importance of their controlled expression in development. Based on their

amino acid sequences, such modifications could include phosphorylation and/or acetylation.

5.5. Absence of expression change does not necessarily indicate absence of function

One important point to remember when interpreting the results of this study is that samples were collected only once every 24 hours throughout the first seven days of myoblast differentiation. Therefore, a dramatic peak or drop in the expression of an Rbm5 or Rbm10 variant could have been missed. For example, TNF-alpha was shown to have an important peak in expression *within* the first 24 hours of C2C12 skeletal myoblast differentiation (Li & Schwartz, 2001). Such a rapid change in expression would not have been detected in our study. Thus, future work could include taking more samples, especially throughout the first 48 to 72 hours of differentiation, when apoptosis and cell cycle arrest occur, to see if such dramatic and rapid shifts in Rbm5 or Rbm10 splice variant expression occur.

Furthermore, when interpreting these results it is important to remember that if a variant does not undergo significant changes in expression throughout differentiation, this does not necessarily mean that the variant is not playing a role. For example, the expression of RBM4 was shown not to change significantly during differentiation. However, it was suggested that Rbm4 may still play an important role in differentiation, by strategically down-regulating polypyrimidine tract-binding (PTB) protein. PTB is a very important regulator of alternative splicing and other aspects of mRNA metabolism in mammalian cells (Lin & Tarn, 2011; Sawicka et al., 2008). Therefore, this work is only a first step in determining if Rbm5 and Rbm10 play a role in myoblast differentiation, and what that role may be.

5.6. Conclusion

RBM5 and RBM10 play an important role in transformed cells, in part by affecting the alternative splicing and/or expression of factors involved in apoptosis and cell cycle arrest, two processes that, if gone array, can lead to the development of cancer (Reed, 1999). Little is known, however, about the function of RBM5 and RBM10 splice variants in non-transformed cells, and whether their observed role in transformed cells is a cause or a consequence of the transformed state. The present study provides initial evidence as to the role of Rbm5 and Rbm10 in a non-transformed system. First, it shows, for the first time, that *Rbm5* splice variants *Rbm5+5+6* and *Lust* are in fact expressed in rat, and throughout rat skeletal and cardiac myoblast differentiation. Secondly, this investigation demonstrates that *Rbm5*, *Rbm10v1* and *Rbm10v2* are expressed at both the mRNA and protein level in rat muscle cells and throughout rat skeletal and cardiac myoblast differentiation. Similarities between *Rbm5+5+6* and *Lust* mRNA expression profiles during skeletal muscle differentiation suggest that both variants are involved in similar processes throughout differentiation, and/or work to regulate each other. In cardiac differentiation, however, only *Lust* was shown to have a potentially important role, with its expression levels remaining unchanged throughout differentiation, while those of *Rbm5+5+6* declined. Significant changes in expression were observed for Rbm5 and Rbm10v1 protein only during skeletal muscle differentiation, whereas changes in Rbm10v2 protein were observed during both skeletal and cardiac muscle differentiation. However, these variations in Rbm5, Rbm10v1 and Rbm10v2 protein expression did not correlate with their mRNA expression results. This suggests that *Rbm5, Rbm10v1* and

Rbm10v2 undergo important post-transcriptional or translational regulation during differentiation, suggesting in turn that they may play an important role in lineage determination.

In all, temporal changes in Rbm5 and Rbm10 splice variant expression throughout both skeletal and cardiac myoblast differentiation hint that these variants may be playing a similar role in differentiation as in transformed cells, including influencing alternative splicing, apoptosis and/or cell cycle arrest; however, it is important to note that these expression changes could be indicative of the involvement of Rbm5 and Rbm10 in completely different, potentially differentiation-specific, cellular processes. Based on the expression data alone, it is not yet possible to link a function to Rbm5 and Rbm10 during myoblast differentiation. Nonetheless, this work did lay the groundwork for future functional studies.

To more thoroughly assess the function of Rbm5 and Rbm10 during myoblast differentiation, future studies could include a systematic analysis of the effects of Rbm5 and Rbm10 inhibition on the physiology of both skeletal and cardiac myoblast differentiation, and the expression of cell cycle and apoptosis regulatory factors. Protein: RNA binding studies, particularly focusing on a comparison between the days of differentiation where the Rbm protein of interest is significantly differentially expressed, would also help to give a more precise understanding of the exact mechanism of action of the protein. All in all, uncovering the role of Rbm5 and Rbm10 in non-transformed systems will help to acquire a wider range of knowledge regarding the function of these proteins and, consequently, a better understanding of their importance in transformed cells. This information could potentially guide future therapeutic endeavours to ensure maximum efficacy in cancer cells and minimal effects in normal tissue.

References

Ahuja, P., Sdek, P., & MacLellhan, W. R. (2007). Cardiac myocyte cell cy cle control in development, disease, and regeneration. *Physiological Reviews*, *87*(2), 521–44.

Amanchy, R., Zhong, J., Molina, H., Chaerkady, R., Iwahori, A., Kalume, D. E., Grønborg, M., et al. (2008). Identification of c-Src tyrosine kinase substrates using mass spectrometry and peptide microarrays. *Journal of Proteome Research*, *7*(9), 3900–10.

Andrés, V., & Walsh, K. (1996). Myogenin expression, cell cycle withdrawal, and phenotypic differentiation are temporally separable events that precede cell fusion upon myogenesis. *The Journal of Cell Biology*, *132*(4), 657–66.

Angelelli, C., Magli, A., Ferrari, D., Ganassi, M., Matafora, V., Parise, F., Razzini, G., et al. (2008). Differentiation-dependent lysine 4 acetylation enhances MEF2C binding to DNA in skeletal muscle cells. *Nucleic Acids Research*, *36*(3), 915–28.

Applied Biosystems. (2008). Guide to Performing Relative Quantitation of Gene Expression Using Real-Time Quantitative PCR. *General Support Documents, P/N 437109*, 70.

Aravind, L., & Koonin, E. V. (1999). G-patch: a new conserved domain in eukaryotic RNA-processing proteins and type D retroviral polyproteins. *Trends in Biochemical Sciences1*, *24*(9), 342–4.

Baśkiewicz-Masiuk, M., & Machaliński, B. (2004). The role of the STAT5 proteins in the proliferation and apoptosis of the CML and AML cells. *European Journal of Haematology*, *72*(6), 420–9.

Behzadnia, N., Golas, M. M., Hartmuth, K., Sander, B., Kastner, B., Deckert, J., Dube, P., et al. (2007). Composition and three-dimensional EM structure of double affinity-purified, human prespliceosomal A complexes. *The EMBO Journal*, *26*(6), 1737–48.

Bertaggia, E., Coletto, L., & Sandri, M. (2012). Posttranslational modifications control FoxO3 activity during denervation. *American Journal of Physiology. Cell Physiology*, *302*(3), C587–96.

Bettiol, E., Sartiani, L., Chicha, L., Krause, K. H., Cerbai, E., & Jaconi, M. E. (2007). Fetal bovine serum enables cardiac differentiation of human embryonic stem cells. *Differentiation; Research in Biological Diversity*, *75*(8), 669–81.

Birney, E., Kumar, S., & Krainer, A. R. (1993). Analysis of the RNA-recognition motif and RS and RGG domains: conservation in metazoan pre-mRNA splicing factors. *Nucleic Acids Research*, *21*(25), 5803–16.

Black, D. L. (2003). Mechanisms of alternative pre-messenger RNA splicing. *Annual Review of Biochemistry*, *72*, 291–336.

Bland, C. S., Wang, E. T., Vu, A., David, M. P., Castle, J. C., Johnson, J. M., Burge, C. B., et al. (2010). Global regulation of alternative splicing during myogenic differentiation. *Nucleic Acids Research*, *38*(21), 7651–64.

Blau, H. M., Chiu, C. P., & Webster, C. (1983). Cytoplasmic activation of human nuclear genes in stable heterocaryons. *Cell*, *32*(4), 1171–80.

Bonnal, S., Martínez, C., Förch, P., Bachi, A., Wilm, M., & Valcárcel, J. (2008). RBM5/Luca-15/H37 regulates Fas alternative splice site pairing after exon definition. *Molecular Cell*, *32*(1), 81–95.

Brault, J. J., Jespersen, J. G., & Goldberg, A. L. (2010). Peroxisome proliferator-activated receptor gamma coactivator 1alpha or 1beta overexpression inhibits muscle protein degradation, induction of ubiquitin ligases, and disuse atrophy. *The Journal of Biological Chemistry*, *285*(25), 19460–71.

Brostrom, M. A., Reilly, B. A., Wilson, F. J., & Brostrom, C. O. (2000). Vasopressin-induced hypertrophy in H9c2 heart-derived myocytes. *The International Journal of Biochemistry & Cell Biology*, *32*(9), 993–1006.

Burattini, S., Ferri, P., Battistelli, M., Curci, R., Luchetti, F., & Falcieri, E. (2004). C2C12 murine myoblasts as a model of skeletal muscle development: morpho-functional characterization. *European Journal of Histochemistry : EJH*, *48*(3), 223–33.

Burd, C. G., & Dreyfuss, G. (1994). Conserved structures and diversity of functions of RNA-binding proteins. *Science*, *265*(5172), 615–21.

Bustin, S. A., & Nolan, T. (2004). Template handling, preparation, and quantification. In S. A. Bustin (Ed.), *The Real-Time PCR Encyclopaedia A-Z of Quantitative PCR* (pp. 87–120). La Jolla, CA: International University Line.

Callebaut, I., & Mornon, J.-P. (2005). OCRE: a novel domain made of imperfect, aromatic-rich octamer repeats. *Bioinformatics*, *21*(6), 699–702.

Chang, D. W., Xing, Z., Pan, Y., Algeciras-Schimnich, A., Barnhart, B. C., Yaish-Ohad, S., Peter, M. E., et al. (2002). c-FLIP(L) is a dual function regulator for caspase-8 activation and CD95-mediated apoptosis. *The EMBO Journal*, *21*(14), 3704–14.

Chen, M., & Manley, J. L. (2009). Mechanisms of alternative splicing regulation: insights from molecular and genomics approaches. *Nature reviews. Molecular Cell Biology*, *10*(11), 741–54.

Coleman, M. P., Ambrose, H. J., Carrel, L., Németh, A. H., Willard, H. F., & Davies, K. E. (1996). A novel gene, DXS8237E, lies within 20 kb upstream of UBE1 in Xp11.23 and has a different X inactivation status. *Genomics*, *31*(1), 135–8.

Comelli, M., Domenis, R., Bisetto, E., Contin, M., Marchini, M., Ortolani, F., Tomasetig, L., et al. (2011). Cardiac differentiation promotes mitochondria development and ameliorates oxidative capacity in H9c2 cardiomyoblasts. *Mitochondrion*, *11*(2), 315–26.

Deckert, J., Hartmuth, K., Boehringer, D., Behzadnia, N., Will, C. L., Kastner, B., Stark, H., et al. (2006). Protein composition and electron microscopy structure of affinity-purified human spliceosomal B complexes isolated under physiological conditions. *Molecular and Cellular Biology*, *26*(14), 5528–43.

Dee, K., Freer, M., Mei, Y., & Weyman, C. M. (2002). Apoptosis coincident with the differentiation of skeletal myoblasts is delayed by caspase 3 inhibition and abrogated by MEK-independent constitutive Ras signaling. *Cell Death and Differentiation*, *9*(2), 209–18.

di Giacomo, V., Rapino, M., Sancilio, S., Patruno, A., Zara, S., Di Pietro, R., & Cataldi, A. (2010). PKC-δ signalling pathway is involved in H9c2 cells differentiation. *Differentiation; Research in Biological Diversity*, *80*(4-5), 204–12.

Drabkin, H. A., West, J. D., Hotfilder, M., Heng, Y. M., Erickson, P., Calvo, R., Dalmau, J., et al. (1999). DEF-3(g16/NY-LU-12), an RNA binding protein from the 3p21.3 homozygous deletion region in SCLC. *Oncogene*, *18*(16), 2589–97.

Dreyfuss, G., Matunis, M. J., Piñol-Roma, S., & Burd, C. G. (1993). hnRNP proteins and the biogenesis of mRNA. *Annual Review of Biochemistry*, *62*, 289–321.

Edamatsu, H., Kaziro, Y., & Itoh, H. (2000). LUCA15, a putative tumour suppressor gene encoding an RNA-binding nuclear protein, is down-regulated in ras-transformed Rat-1 cells. *Genes to Cells : Devoted to Molecular & Cellular Mechanisms*, *5*(10), 849–58.

Edmondson, D. G., & Olson, E. N. (1989). A gene with homology to the myc similarity region of MyoD1 is expressed during myogenesis and is sufficient to activate the muscle differentiation program. *Genes & Development*, *3*(5), 628–40.

Ellis, R. E., Yuan, J. Y., & Horvitz, H. R. (1991). Mechanisms and functions of cell death. *Annual Review of Cell Biology*, *7*, 663–98.

Fidziańska, A., & Goebel, H. H. (1991). Human ontogenesis. 3. Cell death in fetal muscle. *Acta Neuropathologica*, *81*(5), 572–7.

Florea, L., Di Francesco, V., Miller, J., Turner, R., Yao, A., Harris, M., Walenz, B., et al. (2005). Gene and alternative splicing annotation with AIR. *Genome Research*, *15*(1), 54–66.

Fujio, Y., Guo, K., Mano, T., Mitsuuchi, Y., Testa, J. R., & Walsh, K. (1999). Cell cycle withdrawal promotes myogenic induction of Akt, a positive modulator of myocyte survival. *Molecular and Cellular Biology*, *19*(7), 5073–82.

Furukawa, T., Kuboki, Y., Tanji, E., Yoshida, S., Hatori, T., Yamamoto, M., Shibata, N., et al. (2011). Whole-exome sequencing uncovers frequent GNAS mutations in intraductal papillary mucinous neoplasms of the pancreas. *Scientific Reports*, *1*, 161-8.

Fushimi, K., Ray, P., Kar, A., Wang, L., Sutherland, L. C., & Wu, J. Y. (2008). Up-regulation of the proapoptotic caspase 2 splicing isoform by a candidate tumor suppressor, RBM5. *Proceedings of the National Academy of Sciences of the United States of America*, *105*(41), 15708–13.

Gazdar, A. F., Ihde, D. C., Saijo, N., Shimoyama, M., & Yokota, J. (1994). Report of the Seventh International Symposium of the Foundation for Promotion of Cancer Research: Fundamental and Clinical Research in Lung Cancer. *Japanese Journal of Clinical Oncology*, *24*(4), 233–239.

Geigl, J. B., Langer, S., Barwisch, S., Pfleghaar, K., Lederer, G., & Speicher, M. R. (2004). Analysis of gene expression patterns and chromosomal changes associated with aging. *Cancer Research*, *64*(23), 8550–7.

Germain, P., Chambon, P., Eichele, G., Evans, R. M., Lazar, M. A., Leid, M., De Lera, A. R., et al. (2006). International Union of Pharmacology. LX. Retinoic acid receptors. *Pharmacological Reviews*, *58*(4), 712–25.

Golden, J. A., Bracilovic, A., McFadden, K. A., Beesley, J. S., Rubenstein, J. L., & Grinspan, J. B. (1999). Ectopic bone morphogenetic proteins 5 and 4 in the chicken forebrain lead to cyclopia and holoprosencephaly. *Proceedings of the National Academy of Sciences of the United States of America*, *96*(5), 2439–44.

Guo, W., Schafer, S., Greaser, M. L., Radke, M. H., Liss, M., Govindarajan, T., Maatz, H., et al. (2012). RBM20, a gene for hereditary cardiomyopathy, regulates titin splicing. *Nature Medicine*, *18*(5), 766–73.

Hanahan, D., & Weinberg, R. A. (2000). The Hallmarks of Cancer. *Cell*, *100*(1), 57–70.

Hayashi, S., & Inoue, A. (2007). Cardiomyocytes re-enter the cell cycle and contribute to heart development after differentiation from cardiac progenitors expressing Isl1 in chick embryo. *Development, Growth & Differentiation*, *49*(3), 229–39.

Hescheler, J., Meyer, R., Plant, S., Krautwurst, D., Rosenthal, W., & Schultz, G. (1991). Morphological, biochemical, and electrophysiological characterization of a clonal cell (H9c2) line from rat heart. *Circulation Research*, *69*(6), 1476–86.

Holcik, M., & Sonenberg, N. (2005). Translational control in stress and apoptosis. *Nature Reviews. Molecular Cell Biology*, *6*(4), 318–27.

Imielinski, M., Berger, A. H., Hammerman, P. S., Hernandez, B., Pugh, T. J., Hodis, E., Cho, J., et al. (2012). Mapping the hallmarks of lung adenocarcinoma with massively parallel sequencing. *Cell*, *150*(6), 1107–20.

Inoue, A., Takahashi, K. P., Kimura, M., Watanabe, T., & Morisawa, S. (1996). Molecular cloning of a RNA binding protein, S1-1. *Nucleic Acids Research*, *24*(15), 2990–7.

James, C. G., Ulici, V., Tuckermann, J., Underhill, T. M., & Beier, F. (2007). Expression profiling of Dexamethasone-treated primary chondrocytes identifies targets of glucocorticoid signalling in endochondral bone development. *BMC Genomics*, *8*(1), 205.

Jin, W., Niu, Z., Xu, D., & Li, X. (2012). RBM5 promotes exon 4 skipping of AID pre-mRNA by competing with the binding of U2AF65 to the polypyrimidine tract. *FEBS Letters*, *586*(21), 3852–7.

Johnston, J. J., Teer, J. K., Cherukuri, P. F., Hansen, N. F., Loftus, S. K., Chong, K., Mullikin, J. C., et al. (2010). Massively parallel sequencing of exons on the X chromosome identifies RBM10 as the gene that causes a syndromic form of cleft palate. *American Journal of Human Genetics*, *86*(5), 743–8.

Kageyama, K., Ihara, Y., Goto, S., Urata, Y., Toda, G., Yano, K., & Kondo, T. (2002). Overexpression of calreticulin modulates protein kinase B/Akt signaling to promote apoptosis during cardiac differentiation of cardiomyoblast H9c2 cells. *The Journal of Biological Chemistry*, *277*(22), 19255–64.

Kalsotra, A., Xiao, X., Ward, A. J., Castle, J. C., Johnson, J. M., Burge, C. B., & Cooper, T. A. (2008). A postnatal switch of CELF and MBNL proteins reprograms alternative splicing in the developing heart. *Proceedings of the National Academy of Sciences of the United States of America*, *105*(51), 20333–8.

Karagiannis, T. C., Lin, A. J. E., Ververis, K., Chang, L., Tang, M. M., Okabe, J., & El-Osta, A. (2010). Trichostatin A accentuates doxorubicin-induced hypertrophy in cardiac myocytes. *Aging*, *2*(10), 659–68.

Karlen, Y., McNair, A., Perseguers, S., Mazza, C., & Mermod, N. (2007). Statistical significance of quantitative PCR. *BMC Bioinformatics*, *8*(1), 131.

Kee, H. J., Kim, J.-R., Nam, K.-I., Park, H. Y., Shin, S., Kim, J. C., Shimono, Y., et al. (2007). Enhancer of polycomb1, a novel homeodomain only protein-binding partner, induces skeletal muscle differentiation. *The Journal of Biological Chemistry*, *282*(10), 7700–9.

Keene, J. D., & Query, C. C. (1991). Nuclear RNA-binding Proteins. *Progress in Nucleic Acid Research and Molecular Biology*, *41*, 179–202.

Kenan, D. J., Query, C. C., & Keene, J. D. (1991). RNA recognition: towards identifying determinants of specificity. *Trends in Biochemical Sciences*, *16*, 214–20.

Kim, M. Y., Hur, J., & Jeong, S. (2009). Emerging roles of RNA and RNA-binding protein network in cancer cells. *BMB Reports*, *42*(3), 125–30.

Kim, Y.-S., Hwan, J. D., Bae, S., Bae, D.-H., & Shick, W. A. (2010). Identification of differentially expressed genes using an annealing control primer system in stage III serous ovarian carcinoma. *BMC Cancer*, *10*, 576.

Kimes, B., & Brandt, B. (1976). Properties of a clonal muscle cell line from rat heart. *Experimental Cell Research*, *98*(2), 367–81.

Kobayashi, T., Ishida, J., Musashi, M., Ota, S., Yoshida, T., Shimizu, Y., Chuma, M., et al. (2011). p53 transactivation is involved in the antiproliferative activity of the putative tumor suppressor RBM5. *International Journal of Cancer. 128*(2), 304–18.

Koenig, M., Hoffman, E. P., Bertelson, C. J., Monaco, A. P., Feener, C., & Kunkel, L. M. (1987). Complete cloning of the duchenne muscular dystrophy (DMD) cDNA and preliminary genomic organization of the DMD gene in normal and affected individuals. *Cell*, *50*(3), 509–17.

Koh, K. N., Kang, M. J., Frith-Terhune, A., Park, S. K., Kim, I., Lee, C. O., & Koh, G. Y. (1998). Persistent and heterogenous expression of the cyclin-dependent kinase inhibitor, p27KIP1, in rat hearts during development. *Journal of Molecular and Cellular Cardiology*, *30*(3), 463–74.

Krecic, A. M., & Swanson, M. S. (1999). hnRNP complexes: composition, structure, and function. *Current Opinion in Cell Biology*, *11*(3), 363–71.

Lai, M.-C., Kuo, H.-W., Chang, W.-C., & Tarn, W.-Y. (2003). A novel splicing regulator shares a nuclear import pathway with SR proteins. *The EMBO Journal*, *22*(6), 1359–69.

Li, F., Wang, X., Bunger, P. C., & Gerdes, A. M. (1997). Formation of binucleated cardiac myocytes in rat heart: I. Role of actin-myosin contractile ring. *Journal of Molecular and Cellular Cardiology*, *29*(6), 1541–51.

Li, H., & Bingham, P. M. (1991). Arginine/serine-rich domains of the su(wa) and tra RNA processing regulators target proteins to a subnuclear compartment implicated in splicing. *Cell*, *67*(2), 335–42.

Li, P., Wang, K., Zhang, J., Zhao, L., Liang, H., Shao, C., & Sutherland, L. C. (2012). The 3p21.3 tumor suppressor RBM5 resensitizes cisplatin-resistant human non-small cell lung cancer cells to cisplatin. *Cancer Epidemiology*, *36*(5), 481–9.

Li, Y. P., & Schwartz, R. J. (2001). TNF-alpha regulates early differentiation of C2C12 myoblasts in an autocrine fashion. *FASEB Journal*, *15*(8), 1413–5.

Liang, H., Zhang, J., Shao, C., Zhao, L., Xu, W., Sutherland, L. C., & Wang, K. (2012). Differential expression of RBM5, EGFR and KRAS mRNA and protein in non-small cell lung cancer tissues. *Journal of Experimental & Clinical Cancer Research : CR*, *31*(1), 36.

Lin, J.-C., & Tarn, W.-Y. (2005). Exon selection in alpha-tropomyosin mRNA is regulated by the antagonistic action of RBM4 and PTB. *Molecular and Cellular Biology*, *25*(22), 10111–21.

Lin, J.-C., & Tarn, W.-Y. (2011). RBM4 down-regulates PTB and antagonizes its activity in muscle cell-specific alternative splicing. *The Journal of Cell Biology*, *193*(3), 509–20.

Livak, K. J., & Schmittgen, T. D. (2001). Analysis of relative gene expression data using real-time quantitative PCR and the 2(-Delta Delta C(T)) Method. *Methods (San Diego, Calif.)*, *25*(4), 402–8.

L'Ecuyer, T., Horenstein, M. S., Thomas, R., & Vander Heide, R. (2001). Anthracycline-induced cardiac injury using a cardiac cell line: potential for gene therapy studies. *Molecular Genetics and Metabolism*, *74*(3), 370–9.

Mammucari, C., Milan, G., Romanello, V., Masiero, E., Rudolf, R., Del Piccolo, P., Burden, S. J., et al. (2007). FoxO3 controls autophagy in skeletal muscle in vivo. *Cell Metabolism*, *6*(6), 458–71.

Maquat, L. E., & Carmichael, G. G. (2001). Quality control of mRNA function. *Cell*, *104*(2), 173–6.

Martelli, F., Cenciarelli, C., Santarelli, G., Polikar, B., Felsani, A., & Caruso, M. (1994). MyoD induces retinoblastoma gene expression during myogenic differentiation. *Oncogene*, *9*(12), 3579–90.

Martín-Garabato, E., Martínez-Arribas, F., Pollán, M., Lucas, A. R., Sánchez, J., & Schneider, J. (2008). The small variant of the apoptosis-associated X-chromosome RBM10 gene is co-expressed with caspase-3 in breast cancer. *Cancer Genomics & Proteomics*, *5*(3-4), 169–73.

Martínez-Arribas, F., Agudo, D., Pollán, M., Gómez-Esquer, F., Díaz-Gil, G., Lucas, R., & Schneider, J. (2006). Positive correlation between the expression of X-chromosome RBM genes (RBMX, RBM3, RBM10) and the proapoptotic Bax gene in human breast cancer. *Journal of Cellular Biochemistry*, *97*(6), 1275–82.

Menard, C. (1999). Modulation of L-type Calcium Channel Expression during Retinoic Acid-induced Differentiation of H9C2 Cardiac Cells. *Journal of Biological Chemistry*, *274*(41), 29063–70.

Miller, G., Socci, N. D., Dhall, D., D'Angelica, M., DeMatteo, R. P., Allen, P. J., Singh, B., et al. (2009). Genome wide analysis and clinical correlation of chromosomal and transcriptional mutations in cancers of the biliary tract. *Journal of Experimental & Clinical Cancer Research: CR*, *28*(1), 62.

Miller, J. B., & Stockdale, F. E. (1986). Developmental regulation of the multiple myogenic cell lineages of the avian embryo. *The Journal of Cell Biology*, *103*(6 Pt 1), 2197–208.

Miner, J. H., & Wold, B. (1990). Herculin, a fourth member of the MyoD family of myogenic regulatory genes. *Proceedings of the National Academy of Sciences of the United States of America*, *87*, 1089–93.

Moss, R. L., & Fitzsimons, D. P. (2006). Myosin light chain 2 into the mainstream of cardiac development and contractility. *Circulation Research*, *99*(3), 225–7.

Mourtada-Maarabouni, M., Keen, J., Clark, J., Cooper, C. S., & Williams, G. T. (2006). Candidate tumor suppressor LUCA-15/RBM5/H37 modulates expression of apoptosis and cell cycle genes. *Experimental Cell Research*, *312*(10), 1745–52.

Mourtada-Maarabouni, M., Sutherland, L. C., Clark, J. P., Cooper, C. S., & Williams, G. T. (2001). Regulation of T-cell apoptosis by sequences encoded at the LUCA-15 candidate tumour suppressor Locus. *Nature Biotechnology*, *12*(40).

Mourtada-Maarabouni, M., Sutherland, L. C., Meredith, J. M., & Williams, G. T. (2003). Simultaneous acceleration of the cell cycle and suppression of apoptosis by splice variant delta-6 of the candidate tumour suppressor LUCA-15/RBM5. *Genes to Cells: Devoted to Molecular & Cellular Mechanisms*, *8*(2), 109–19.

Mourtada-Maarabouni, M, Sutherland, L. C., & Williams, G. T. (2002). Candidate tumour suppressor LUCA-15 can regulate multiple apoptotic pathways. *Apoptosis*, *7*(5), 421–32.

Mourtada-Maarabouni, M., & Williams, G. T. (2006). The Antiapoptotic RBM5/LUCA-15/H37 Gene and Its Role in Apoptosis and Human Cancer: Research Update. *The Scientific World Journal*, *6*, 1705–12.

Muntoni, F. (2003). Cardiomyopathy in muscular dystrophies. *Current Opinion in Neurology*, *16*(5), 577–83.

Nagase, T., Seki, N., Tanaka, A., Ishikawa, K., & Nomura, N. (1995). Prediction of the coding sequences of unidentified human genes. IV. The coding sequences of 40 new genes (KIAA0121-KIAA0160) deduced by analysis of cDNA clones from human cell line KG-1. *DNA research*, *2*(4), 167–74, 199–210.

Nakahata, S., & Kawamoto, S. (2005). Tissue-dependent isoforms of mammalian Fox-1 homologs are associated with tissue-specific splicing activities. *Nucleic Acids Research*, *33*(7), 2078–89.

Nambara, E., Keith, K., McCourt, P., & Naito, S. (1995). A regulatory role for the ABI3 gene in the establishment of embryo maturation in Arabidopsis thaliana. *Development*, *121*(3), 629–36.

Ng, K.-M., Lee, Y.-K., Chan, Y.-C., Lai, W.-H., Fung, M.-L., Li, R. A., Siu, C.-W., et al. (2010). Exogenous expression of HIF-1 alpha promotes cardiac differentiation of embryonic stem cells. *Journal of Molecular and Cellular Cardiology*, *48*(6), 1129–37.

Novitch, B. G., Mulligan, G. J., Jacks, T., & Lassar, A. B. (1996). Skeletal muscle cells lacking the retinoblastoma protein display defects in muscle gene expression and accumulate in S and G2 phases of the cell cycle. *The Journal of Cell Biology*, *135*(2), 441–56.

Novitch, Bennett G., Spicer, D. B., Kim, P. S., Cheung, W. L., & Lassar, A. B. (1999). pRb is required for MEF2-dependent gene expression as well as cell-cycle arrest during skeletal muscle differentiation. *Current Biology*, *9*(9), 449–59.

Oh, J. J., Grosshans, D. R., Wong, S. G., & Slamon, D. J. (1999). Identification of differentially expressed genes associated with HER-2/neu overexpression in human breast cancer cells. *Nucleic Acids Research*, *27*(20), 4008–17.

Oh, J. J., Razfar, A., Delgado, I., Reed, R. A., Malkina, A., Boctor, B., & Slamon, D. J. (2006). 3p21.3 tumor suppressor gene H37/Luca15/RBM5 inhibits growth of human lung cancer cells through cell cycle arrest and apoptosis. *Cancer Research*, *66*(7), 3419–27.

Oh, J. J., West, A. R., Fishbein, M. C., & Slamon, D. J. (2002). A candidate tumor suppressor gene, H37, from the human lung cancer tumor suppressor locus 3p21.3. *Cancer Research*, *62*(11), 3207–13.

O'Leary, D. A., Sharif, O., Anderson, P., Tu, B., Welch, G., Zhou, Y., Caldwell, J. S., et al. (2009). Identification of small molecule and genetic modulators of AON-induced dystrophin exon skipping by high-throughput screening. *PloS One*, *4*(12), e8348.

Pan, Q., Shai, O., Lee, L. J., Frey, B. J., & Blencowe, B. J. (2008). Deep surveying of alternative splicing complexity in the human transcriptome by high-throughput sequencing. *Nature Genetics*, *40*(12), 1413–5.

Peng, J., Valeshabad, A. K., Li, Q., & Wang, Y. (2013). Differential expression of RBM5 and KRAS in pancreatic ductal adenocarcinoma and their association with clinicopathological features. *Oncology Letters*, *5*(3), 1000–4.

Pereira, S. L., Ramalho-Santos, J., Branco, A. F., Sardão, V. A., Oliveira, P. J., & Carvalho, R. A. (2011). Metabolic remodeling during H9c2 myoblast differentiation: relevance for in vitro toxicity studies. *Cardiovascular Toxicology*, *11*(2), 180–90.

Pfaffl, M.W. (2005). Nucleic acids: mRNA identification and quantification. In P. J. Worsfold & P. K. Gallagher (Eds.), *Encyclopedia of Analytical Science* (Second., pp. 417–26). Academic Press.

Pfaffl, M. W. (2006). Relative quantification. In M. T. Dorak (Ed.), *Real-time PCR* (pp. 63–82). New York, NY: Taylor & Francis Group.

Poolman, R. A., Gilchrist, R., & Brooks, G. (1998). Cell cycle profiles and expressions of p21CIP1 AND P27KIP1 during myocyte development. *International Journal of Cardiology*, *67*(2), 133–42.

Pownall, M. E., Gustafsson, M. K., & Emerson, C. P. (2002). Myogenic regulatory factors and the specification of muscle progenitors in vertebrate embryos. *Annual Review of Cell and Developmental Biology*, *18*, 747–83.

Ramaswamy, S., Ross, K. N., Lander, E. S., & Golub, T. R. (2003). A molecular signature of metastasis in primary solid tumors. *Nature Genetics*, *33*(1), 49–54.

Reed, J. C. (1999). Dysregulation of Apoptosis in Cancer. *Journal of Clinical Oncology*, *17*(9), 2941–53.

Revil, T., Gaffney, D., Dias, C., Majewski, J., & Jerome-Majewska, L. A. (2010). Alternative splicing is frequent during early embryonic development in mouse. *BMC Genomics*, *11*(1), 399.

Rintala-Maki, N. D., & Sutherland, L. C. (2004). LUCA-15/RBM5, a putative tumour suppressor, enhances multiple receptor-initiated death signals. *Apoptosis*, *9*(4), 475–84.

Rintala-Maki, N. D, Abrasonis, V., Burd, M., & Sutherland, L. C. (2004). Genetic instability of RBM5/LUCA-15/H37 in MCF-7 breast carcinoma sublines may affect susceptibility to apoptosis. *Cell Biochemistry and Function*, *22*(5), 307–13.

Rintala-Maki, N. D., Goard, C. A., Langdon, C. E., Wall, V. E., Traulsen, K. E. A., Morin, C. D., Bonin, M., et al. (2007). Expression of RBM5-related factors in primary breast tissue. *Journal of Cellular Biochemistry*, *100*(6), 1440–58.

Rintala-Maki, N. D., & Sutherland, L. C. (2009). Identification and characterisation of a novel antisense non-coding RNA from the RBM5 gene locus. *Gene*, *445*(1-2), 7–16.

Rottbauer, W., Wessels, G., Dahme, T., Just, S., Trano, N., Hassel, D., Burns, C. G., et al. (2006). Cardiac myosin light chain-2: a novel essential component of thick-myofilament assembly and contractility of the heart. *Circulation Research*, *99*(3), 323–31.

Sabourin, L A, & Rudnicki, M. A. (2000). The molecular regulation of myogenesis. *Clinical Genetics*, *57*(1), 16–25.

Sandri, M., Cantini, M., Massimino, M. L., Geromel, V., & Arslan, P. (1996). Myoblasts and Myotubes in Primary Cultures Deprived of Growth Factors undergo to Apoptosis. *Basic and Applied Myology*, *6*(4), 257–60.

Sandri, M., Sandri, C., Gilbert, A., Skurk, C., Calabria, E., Picard, A., Walsh, K., et al. (2004). Foxo transcription factors induce the atrophy-related ubiquitin ligase atrogin-1 and cause skeletal muscle atrophy. *Cell*, *117*(3), 399–412.

Sawicka, K., Bushell, M., Spriggs, K. A., & Willis, A. E. (2008). Polypyrimidine-tract-binding protein: a multifunctional RNA-binding protein. *Biochemical Society Transactions*, *36*(Pt 4), 641–7.

Schmittgen, T D, & Zakrajsek, B. A. (2000). Effect of experimental treatment on housekeeping gene expression: validation by real-time, quantitative RT-PCR. *Journal of Biochemical and Biophysical Methods*, *46*(1-2), 69–81.

Schmittgen, Thomas D, & Livak, K. J. (2008). Analyzing real-time PCR data by the comparative CT method. *Nature Protocols*, *3*(6), 1101–8.

Shao, C., Zhao, L., Wang, K., Xu, W., Zhang, J., & Yang, B. (2012). The tumor suppressor gene RBM5 inhibits lung adenocarcinoma cell growth and induces apoptosis. *World Journal of Surgical Oncology*, *10*, 160.

Shu, Y., Rintala-Maki, N. D., Wall, V. E., Wang, K., Goard, C. A., Langdon, C. E., & Sutherland, L. C. (2007). The apoptosis modulator and tumour suppressor protein RBM5 is a phosphoprotein. *Cell Biochemistry and Function*, *25*(6), 643–53.

Souazé, F., Ntodou-Thomé, A., Tran, C. Y., Rostène, W., & Forgez, P. (1996). Quantitative RT-PCR: limits and accuracy. *BioTechniques*, *21*(2), 280–5.

Strausberg, R. L., Feingold, E. A., Grouse, L. H., Derge, J. G., Klausner, R. D., Collins, F. S., Wagner, L., et al. (2002). Generation and initial analysis of more than 15,000 full-length human and mouse cDNA sequences. *Proceedings of the National Academy of Sciences of the United States of America*, *99*(26), 16899–903.

Sugliani, M., Brambilla, V., Clerkx, E. J. M., Koornneef, M., & Soppe, W. J. J. (2010). The conserved splicing factor SUA controls alternative splicing of the developmental regulator ABI3 in Arabidopsis. *The Plant Cell*, *22*(6), 1936–46.

Sutherland, L C, Edwards, S. E., Cable, H. C., Poirier, G. G., Miller, B. A., Cooper, C. S., & Williams, G. T. (2000). LUCA-15-encoded sequence variants regulate CD95-mediated apoptosis. *Oncogene*, *19*(33), 3774–81.

Sutherland, L. C., Lerman, M., Williams, G. T., & Miller, B. A. (2001). LUCA-15 suppresses CD95-mediated apoptosis in Jurkat T cells. *Oncogene*, *20*(21), 2713–9.

Sutherland, L. C., Rintala-Maki, N. D., White, R. D., & Morin, C. D. (2005). RNA binding motif (RBM) proteins: a novel family of apoptosis modulators? *Journal of Cellular Biochemistry*, *94*(1), 5–24.

Swiderski, R. E., & Solursh, M. (1990). Precocious appearance of cardiac troponin T pre-mRNAs during early avian embryonic skeletal muscle development in ovo. *Developmental Biology*, *140*(1), 73–82.

Thiselton, D. L., McDowall, J., Brandau, O., Ramser, J., D'Esposito, F., Bhattacharya, S. S., Ross, M. T., et al. (2002). An integrated, functionally annotated gene map of the DXS8026-ELK1 interval on human Xp11.3-Xp11.23: potential hotspot for neurogenetic disorders. *Genomics*, *79*(4), 560–72.

Timmer, T., Terpstra, P., van den Berg, A., Veldhuis, P. M., Ter Elst, A., Voutsinas, G., Hulsbeek, M. M., et al. (1999). A comparison of genomic structures and expression patterns of two closely related flanking genes in a critical lung cancer region at 3p21.3. *European Journal of Human Genetics*, *7*(4), 478–86.

van Deutekom, J. C., Janson, A. A., Ginjaar, I. B., Frankhuizen, W. S., Aartsma-Rus, A., Bremmer-Bout, M., den Dunnen, J. T., et al. (2007). Local dystrophin restoration with antisense oligonucleotide PRO051. *The New England Journal of Medicine*, *357*(26), 2677–86.

Vandromme, M., Gauthieu-Rouvière, C., Carnac, G., Lamb, N., & Fernandez, A. (1992). Serum Response Factor p67 SRF Is Expressed and Required during Myogenic Differentiation of Both Mouse C2 and Rat L6 Muscle Cell Lines. *The Journal of Cell Biology*, *118*(6), 1489–1500.

Walsh, K., & Perlman, H. (1997). Cell cycle exit upon myogenic differentiation. *Current Opinion in Genetics & Development*, *7*(5), 597–602.

Wang, E. T., Sandberg, R., Luo, S., Khrebtukova, I., Zhang, L., Mayr, C., Kingsmore, S. F., et al. (2008). Alternative isoform regulation in human tissue transcriptomes. *Nature*, *456*(7221), 470–6.

Wang, J., Guo, K., Wills, K. N., & Walsh, K. (1997). Rb functions to inhibit apoptosis during myocyte differentiation. *Cancer Research*, *57*(3), 351–4.

Wang, J., & Walsh, K. (1996). Resistance to apoptosis conferred by Cdk inhibitors during myocyte differentiation. *Science*, *273*(5273), 359–61.

Wang, K., Bacon, M. L., Tessier, J. J., Rintala-Maki, N. D., Tang, V., & Sutherland, L. C. (2012). RBM10 Modulates Apoptosis and Influences TNF-α Gene Expression. *Journal of Cell Death*, *5*, 1–19.

Wei, M. H., Latif, F., Bader, S., Kashuba, V., Chen, J. Y., Duh, F. M., Sekido, Y., et al. (1996). Construction of a 600-kilobase cosmid clone contig and generation of a transcriptional map surrounding the lung cancer tumor suppressor gene (TSG) locus on human chromosome 3p21.3: progress toward the isolation of a lung cancer TSG. *Cancer Research*, *56*(7), 1487–92.

Welling, D. B., Lasak, J. M., Akhmametyeva, E., Ghaheri, B., & Chang, L.-S. (2002). cDNA microarray analysis of vestibular schwannomas. *Otology & neurotology*, *23*(5), 736–48.

Yaffe, D. (1968). Retention of differentiation potentialities during prolonged cultivation of myogenic cells. *Proceedings of the National Academy of Sciences of the United States of America*, *61*, 477–83.

Yahi, H., Philipot, O., Guasconi, V., Fritsch, L., & Ait-Si-Ali, S. (2006). Chromatin modification and muscle differentiation. *Expert Opinion on Therapeutic Targets*, *10*(6), 923–34.

Zacksenhaus, E., Jiang, Z., Chung, D., Marth, J. D., Phillips, R. A., & Gallie, B. L. (1996). pRb controls proliferation, differentiation, and death of skeletal muscle cells and other lineages during embryogenesis. *Genes & Development*, *10*(23), 3051–64.

Zhao, L., Li, R., Shao, C., Li, P., Liu, J., & Wang, K. (2012). 3p21.3 tumor suppressor gene RBM5 inhibits growth of human prostate cancer PC-3 cells through apoptosis. *World Journal of Surgical Oncology*, *10*(1), 247.

Zieve, G. W., & Sauterer, R. A. (1990). Cell biology of the snRNP particles. *Critical Reviews in Biochemistry and Molecular Biology*, *25*(1), 1–46.

Appendix. Post-transcriptional regulation of Rbm5 expression in H9c2 cells

Leslie C. Sutherland, Julie J. Loiselle and Sarah J. Tessier

Summary

Having examined the expression of Rbm5 during myoblast differentiation and found sustained protein levels throughout cardiac myocyte development, we decided to determine if full-length Rbm5 expression was a cause or a consequence of differentiation. Our hypothesis was that if Rbm5 protein expression was necessary for cardiac myocyte development, then inhibition of expression would prevent myoblast differentiation into at least the cardiac lineage. Our objective was therefore to inhibit Rbm5 expression and examine the effect on H9c2 differentiation. Towards this end, stable knockdown myoblast clones and a transient knockdown population were generated. Expression analyses demonstrated a significant decrease in *Rbm5* mRNA levels but, surprisingly, no effect on Rbm5 protein levels. When expression of the Rbm5 paralogue Rbm10 was examined, to ensure no off-target knockdown effect and investigate any possible compensatory effects, Rbm10 protein levels were found to be significantly elevated, in both the clones and the transiently transfected population. These results suggest that Rbm5 expression is regulated by a process that includes RNA sequestration and/or controlled translation, and that (a) Rbm5 function is compensated for by Rbm10, and/or (b) Rbm10 expression is regulated by Rbm5. We have developed a model to describe our findings, and suggest further experiments for testing its validity. Since upregulation of Rbm10 might compensate for downregulated Rbm5, and consequently might mask any potential

knockdown effect on cardiac differentiation, it could lead to incorrect conclusions regarding the importance of Rbm5 for this process. It is therefore imperative to determine how both Rbm5 and Rbm10 protein expression is regulated.

Chapter A1. Introduction

In general, the expression of RBM5 is highest in cells that have reduced proliferation such as aging cells (Geigl et al., 2004), dormant seeds (Sugliani et al., 2010) and in adult thymus compared to fetal liver (Drabkin et al., 1999), and lowest in highly proliferating cells, e.g., most cancers such as non-small cell lung cancers (Oh et al., 2002), vestibular schwannomas (Welling et al., 2002), prostate cancers (Zhao et al., 2012), stage III serious ovarian carcinomas (Kim et al., 2010), pancreatic cancers (Peng et al., 2013) and biliary tract cancers (Miller et al., 2009). In fact, *RBM5* was shown to one of nine genes down regulated in metastasis and part of the 17 common gene signatures associated with metastasis in various solid tumour types (Ramaswamy et al., 2003). The triggers for these expression fluctuations are unknown; however, using cancer cell lines, some of the mechanisms by which RBM5 expression can be regulated have been identified. For instance, RBM5 can be downregulated at the transcriptional level by a process that involves the read-through of polymerase from the upstream *RBM6* gene and the consequent generation of “transcription-induced chimeras” (Wang et al., 2007). Changes in RBM5 expression also occur via the regulation of alternative splicing, a role played by HER2 (Rintala-Maki et al., 2007) and potentially the antisense non-coding *RBM5*-related factor, *LUST* (Rintala-Maki & Sutherland, 2009). Post-transcriptionally, RBM5 can be differentially phosphorylated (Shu et al., 2007).

Changes in RBM5 expression levels are associated with changes in both the expression level and the alternative splicing of downstream transcripts. For example, overexpression of RBM5 in the human leukemic cell line CEM-C7 was associated with altered expression of 35 genes, including cyclin-dependant kinase 2 (*CDK2*) and signal transducer and activator of transcription 5B (*Stat5b*), which are involved in processes such as G1/S transition and apoptosis, respectively (Mourtada-Maarabouni et al., 2006). Knockdown of RBM5 was associated with altered expression of many genes in a number of different cell lines (a normal lung epithelial cell line (BEAS-2B), a normal breast epithelial cell line (MCF-10A) and three different lung cancer cell lines with varying RBM5 expression levels (A549, Calu-6 and NCI-H1299)), notably increasing the expression of genes involved in cell adhesion, migration and motility, processes important to metastasis (Oh et al., 2010). In addition, in the MCF-7 breast adenocarcinoma cell line, RBM5 and TNF-α expression were shown to be positively correlated, TNF-α being an important apoptosis regulatory factor (Wang et al., 2012). RBM5 also regulates alternative splicing of pre-mRNAs involved in apoptosis (exclusion of caspase-2 exon 9 (Fushimi et al., 2008), *FasR* exon 6 (Bonnal et al., 2008) and *c-FLIP* exon 7 (Bonnal et al., 2008)), seed maturation (the inclusion of an *ABIα/β* exon (Sugliani et al., 2010)), muscular dystrophy (exclusion of Dytrophin exons 40 and 72 (O'Leary et al., 2009)) and immunoglobulin diversification (exclusion of *AID* exon 4 (Jin et al., 2012)).

Is it important to note that RBM5 shares highest homology with another RBM protein, RBM10 (Sutherland et al., 2005). In fact, RBM5 and RBM10 are approximately 50% homologous at the protein level in both human and rat. Also, endogenous RBM5 and

RBM10v1 protein expression levels have been shown to be significantly positively correlated in primary breast cancer samples (Rintala-Maki et al., 2007).

In this mini-study we set out to determine the importance of Rbm5 to myoblast differentiation by manipulating Rbm5 expression levels. *Rbm10* mRNA and protein expression levels were examined, to rule out off-target knockdown effects. The interesting observations that were made have been incorporated into a model that will be tested in future experiments. Based on our findings, we determined that any study involving a manipulation of Rbm5 expression levels to determine its importance during myoblast differentiation will first require a more thorough understanding of the relationship between Rbm5 and Rbm10. The results reported here constitute our initial attempts to gain this understanding, prior to future functional/physiological studies.

Chapter A2. Materials and methods

A2.1. Stable knockdown. Culture of H9c2 cells prior to transfection was performed as described in Chapter 2. At 24 hours prior to transfection, cells were passed in 100 mm plates (Sarstedt, Montreal, QC) to be approximately 35% confluent at the time of transfection. Twenty four hours following the appropriate plating, 12 μL of Lipofectamine 2000 (Life Technologies, Burlington, ON) was mixed with 1.5 mL of Opti-MEM reduced serum medium with GlutaMAX, and incubated at room temperature for five minutes. The appropriate shRNA construct (12 μg) was also mixed with 1.5 mL of Opti-MEM reduced serum medium with GlutaMAX, and incubated at room temperature for five minutes. Control samples were transfected with CSHCTR001-nU6 shRNA scrambled control (GeneCopoeia, Rockville, MD, USA). Rbm5 knockdown

samples were transfected with both MSH039757-1 and MSH039757-6 *Rbm5*-specific shRNAs (6 μg of each) (GeneCopoeia) (Table 1). The Rbm5-specific shRNAs were 100% homologous to both rat and mouse *Rbm5* sequence. Following, the Lipofectamine 2000+Opti-MEM and shRNA+Opti-MEM solutions were mixed together and incubated at room temperature for 35 minutes. The transfection solution was then added to the normal, serum-containing medium on the cells. Selection began 24 hours post-transfection by treating cells with 1 μg/mL of puromycin. Cells were then cultured in antibiotic-containing medium to select for successful transfectants for at least 28 days following transfection and until they filled a 100 mm plate (Sarstedt).

Table 1. Small interfering RNA *Rbm5* knockdown oligonucleotides.

Type of oligonucleotide	Oligonucleotide name	Sense oligonucleotide sequence	Location	Homology to RBM10	Homology
shRNA	CSHCTR001-nU6		Scrambled	N/A	N/A
	MSH039757-1	5' GUAGUGGAAGAUAUGGUUC 3'	Exon 3	(12/19) 63%	R M
	MSH039757-6	5' GAGCGAUAUUCGAGAAAUG 3'	Exon 4/5	(12/19) 63%	R M H
siRNA	Trilencer-27mer universal scrambled negative control		Scrambled	N/A	N/A
	ON-TARGET RBM5 duplex siRNA	5' GAGCGAUAUUCGAGAAAUG 3'	Exon 4/5	(12/19) 63%	R M H

H, R, M indicate homology to human, rat and mouse sequences, respectively.
Sense sequence indicated for siRNA

A2.2. Transient knockdown. Culture of H9c2 cells prior to transfection was performed as described in Chapter 2. Twenty four hours prior to transfection, cells were passed to 6-well plates (Sarstedt) so as to be 40% confluent at the time of transfection. Twenty four hours after appropriately plating cells, 5 µL of Lipofectamine 2000 Reagent (Life Technologies) was added to 245 µL of Opti-MEM reduced serum medium with GlutaMAX (Life Technologies), and incubated at room temperature for five minutes. The appropriate siRNA was also added to 245 µL of Opti-MEM reduced serum medium with GlutaMAX, and incubated at room temperature for five minutes. The siRNA used for the control samples was Trilencer-27mer universal scrambled negative control siRNA duplex (OriGene, Rockville, MD, USA). For Rbm5 knockdown samples, custom ON-TARGET RBM5 duplex siRNA (Dharmacon, ThermoFisher Scientific, Ottawa, ON) was used: sense sequence was 5'-GAGCGAUAUUCGAGAAAUG-3' and antisense sequence was 5'-CAUUUCUCGAAUAUCGCUC-3' (Figure 1 and Table 1). siRNAs were administered to cells as such, to a final concentration of 10 nM. Following their 5 minute incubation, the Lipofectamine 2000+Opti-MEM and siRNA+Opti-MEM solutions were mixed together and incubated at room temperature for 20 minutes. Next, the transfection solution was added to the normal, serum-containing medium on the cells. Medium was not changed after addition of transfection solution, and cell pellets were collected at 72 hours post-transfection.

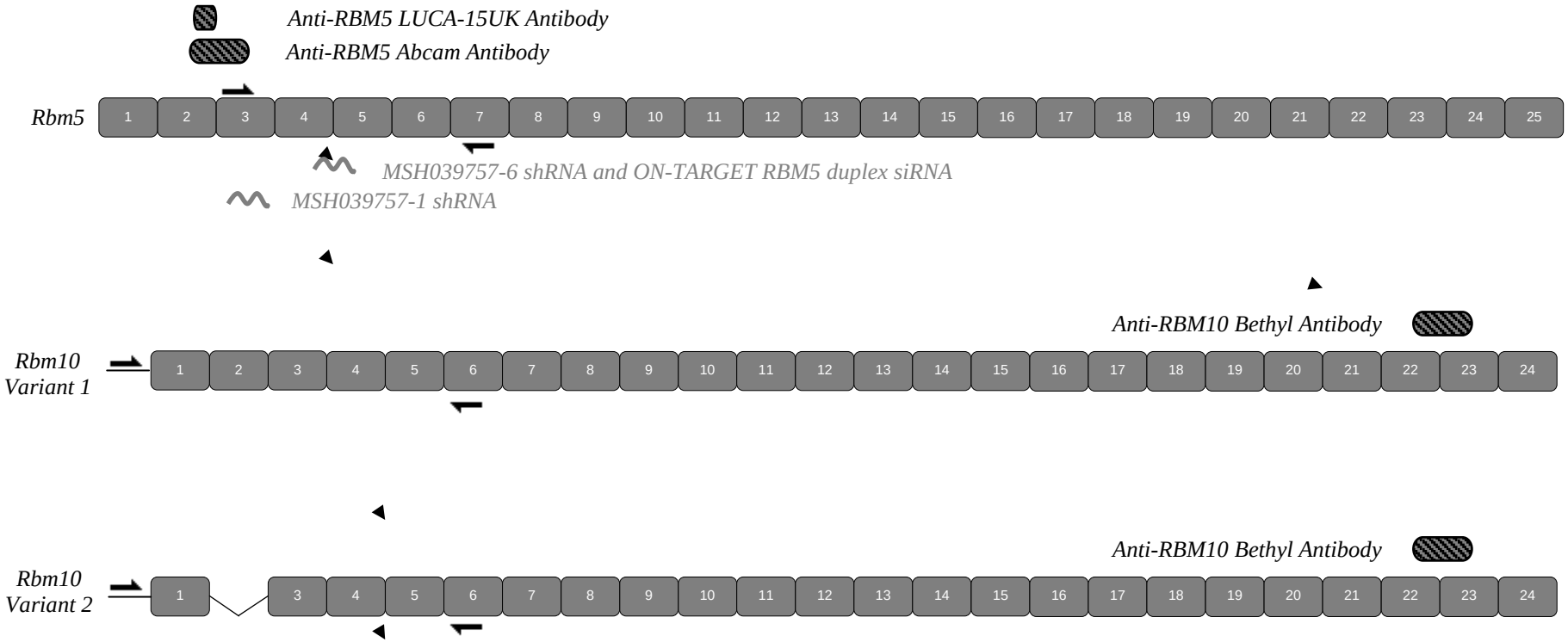

Figure 1. Position of shRNAs, siRNA, PCR primers and antibodies used in this study on the corresponding rat Rbm transcript. Exons are represented by correspondingly numbered dark grey blocks. Exon and intron sizes are not to scale. Approximate location of forward and reverse primers used for PCR are indicated by right and left facing arrows on the transcript in question. Size of arrow does not correspond to primer length in relation to exon or intron length, but gives the approximate position of the primer within the given exon or intron. Rat-specific sequences were used for primer design. Approximate antibody binding sites are indicated by black ovals with grey slanted lines, and the corresponding antibody's name is indicated. Grey zig-zags represent approximate location of indicated siRNA or shRNA on indicated variant.

A2.3. Transient overexpression. Procedure followed is the same as that described in Chapter 2, using human *RBM5* in a pcDNA3 vector.

A2.4. RNA expression analysis. RNA extraction and reverse transcription (RT) were performed as described in Chapter 2. End-point semi-quantitative PCR was used to analyze *Rbm5*, *Rbm10v1* and *Rbm10v2* mRNA expression in all samples, instead of the more sensitive real-time quantitative PCR, since only dramatic changes in expression were of interest to us. *Gapdh* expression was also examined in all samples, via RT-PCR, to normalize results. No strand-specific RT reactions were performed in this study since only the expression of full-length *Rbm5* was analyzed, not that of its sense-specific splice variants. PCR was performed using 1 µL of cDNA, 1 µL of the corresponding forward and reverse primers (10 µM) (AlphaDNA, Montreal, QC) (Table 2), 1 µL of dNTP (10 µM) (Life Technologies), 2 µL of 10X Buffer (New England Biolabs, Whitby, ON), 1 µL of Taq DNA Polymerase (500 U/mL) (New England Biolabs), and sterile distilled water for a total volume of 15 µL per reaction. PCR cycles were as follows: (1) one cycle of 95ºC for 5 minutes, (2) gene specific number of cycles of 95ºC for 30 seconds, primer-specific annealing temperature (Table 1) for 30 seconds, and 72ºC for 45 seconds, and (3) one final extension cycle of 72ºC for 10 minutes. Step 2 of the PCR program was repeated 24 times for *Gapdh* amplification, and 38 times for *Rbm5* and *Rbm10* amplification. PCR products were separated by electrophoresis through a 2% Tris-acetate EDTA (TAE) agarose gel and stained with SYBR Safe DNA gel stain (Life Technologies). Densitometric analysis was performed using AlphaEase FC software (Alpha Innotec). *Rbm5* and *Rbm10* mRNA expression values were first normalized to the expression of *Gapdh*, the reference gene used. Next, the average of the normalized expression value obtained for all technical replicates of a same biological replicate was determined. This average normalized expression

Table 2. Primers for RT-PCR.

Gene name	Primers		Homology
Gapdh	Forward	5’ ACCACAGTCCATGCCATCAC 3’	R M H
	Reverse	5’ TCCACCACCCTGTTGCTGTA 3’	R M H
	Product size in rat	452 bp	
	Annealing Temperature	58˚C	
	Accession No.	Rat: BC059110, Mouse: BC082592, Human: BC004109	
Rbm5	Forward	5’ ATGGGTTCAGACAAAAGAG 3’	R M H
	Reverse	5’ GCATTGCAATGTGCTTTCCTTGA 3’	R M H
	Product size	520 bp	
	Annealing Temperature	55˚C	
	Accession No.	Rat: BC166477, Mouse: BC023854, Human: AF091263	
Rbm10	Forward	5’ ATTGGCTCCCGTCGAACTAACAGT 3’	R
	Reverse	5’ ACTTCTCTCGGCGCTTGAAGTTCT 3’	R M
	Product size in rat	Rbm10v1: 916 bp, Rbm10v2: 682 bp	
	Annealing Temperature	63˚C	
	Accession No.	Rat: NM_152861, Mouse: NM_001167776, Human: NM_152856	

H, R, M indicate homology to human, rat and mouse sequences, respectively

value was then expressed as fold-change from the control sample of that biological replicate, and averaged for the various biological replicates. This gave the final expression value that was graphed.

A2.5. Protein expression analysis. Protein extraction and quantification were performed as described in Chapter 2. Western blot analysis for protein expression was also performed as described in Chapter 2, with only the described Abcam and LUCA-15UK anti-rat-RBM5 primary antibodies used to analyze Rbm5 protein expression. Densitometric analysis was performed on the resulting blots using AlphaEase FC software to quantify expression. The resulting Rbm5 and Rbm10 protein expression values were first normalized to the expression of α-tubulin, the reference gene used. Following, the average of the normalized expression value for all technical replicates of the same biological replicate was determined. Next, the normalized expression values were expressed as fold-change from the control sample of the corresponding biological replicate. Finally, the normalized fold-change in expression obtained for the various biological replicates was averaged and graphed.

Chapter A3. Results

A3.1. *Rbm5* mRNA knockdown has no effect on Rbm5 protein levels

One hundred and seventeen *Rbm5* shRNA transfected H9c2 clones were obtained following 28 or 29 days of selection in puromycin. All 117 clones were screened for *Rbm5* mRNA expression. Three clones (Clones 87, 9 and 100) with significant decrease of *Rbm5* mRNA expression (>80%), compared to the scrambled control, were chosen for further analysis, along with one clone (Clone 104) with partial knockdown (~10%) and one clone (Clone 12) with no visible knockdown (Figure 2A). Surprisingly, Rbm5 protein levels were not significantly decreased in any of the Rbm5 knockdown clones (Figure 2B). To rule out any possible clonal effect that could account for abnormal regulation of protein expression, a transient transfection using siRNA-specific to *Rbm5* sequence (but different from one of the shRNA sequences used) was carried out. Knockdown was only ~ 40% but, once again, there was no decrease in Rbm5 protein levels (Figure 3). To ensure that antibody affinity was not an issue, two different anti-RBM5 antibodies were used (Figure 3).

A3.2. Rbm5 knockdown correlates with increased Rbm10 protein levels

Since rat Rbm10 has 57% homology at the DNA level with Rbm5, to ensure no off-target effect of the theoretically Rbm5-specific sh/siRNAs on Rbm10 expression, Rbm10 expression was also examined in the knockdowns. Since stable and transient knockdown of Rbm5 could have resulted from different shRNA and siRNA sequences (Table 1), both stable and transient knockdowns were tested for off-target effects on Rbm10. *Rbm5* shRNA and siRNA sequences were 19-mers with 7 mismatches to rat *Rbm10,* meaning they had 63% similarity. In the clones, at the RNA level (Figure 4A), *Rbm10v1* expression did not change

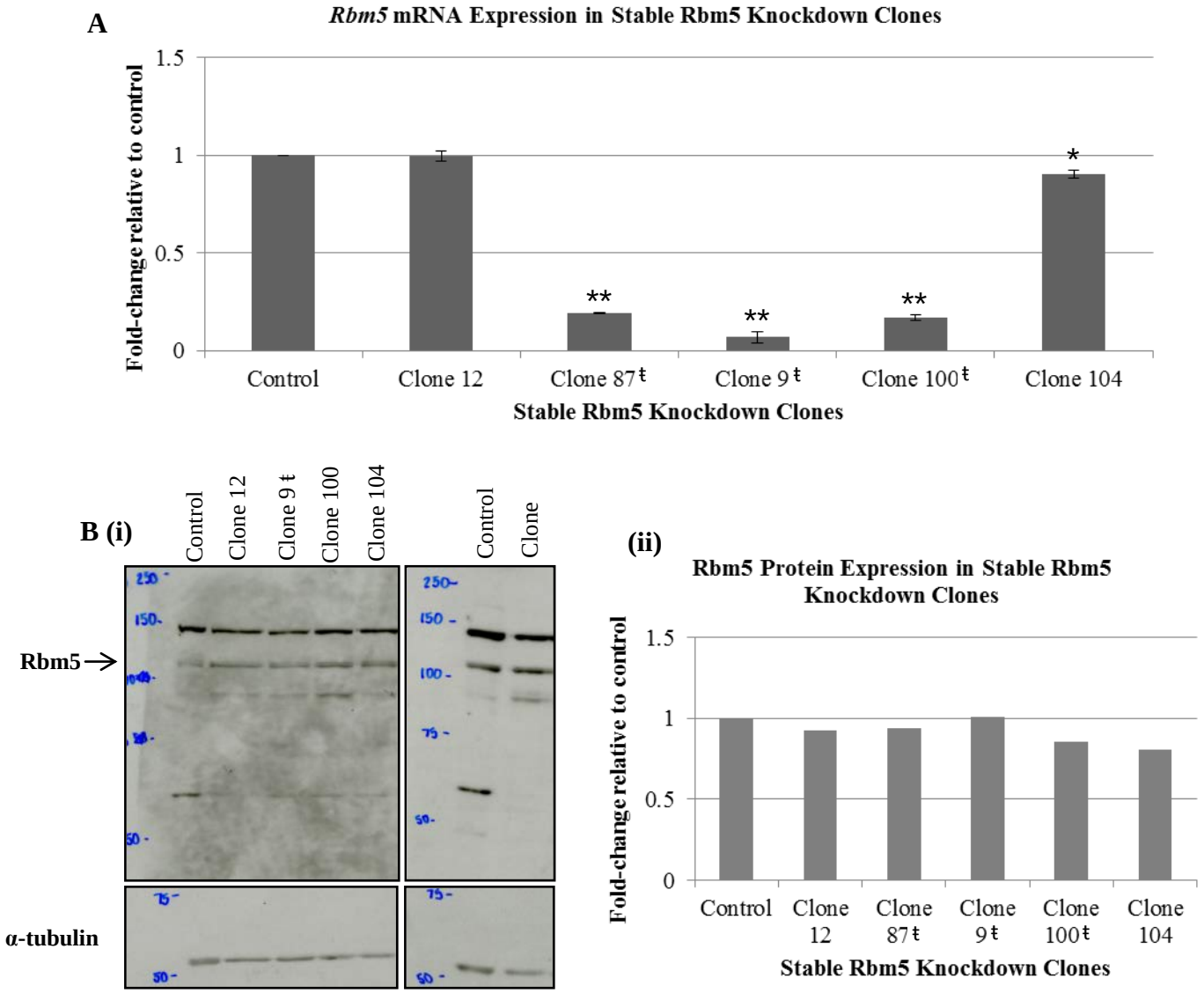

Figure 2. Rbm5 expression in shRNA stably transfected H9c2 clones. Control refers to sample transfected with scrambled control shRNA. (ŧ) beside a clone's name indicates that Rbm5 mRNA expression in that clone showed a decrease of 50% or more compared to the scrambled control. **A.** Quantification of RT-PCR results for *Rbm5* expression in H9c2 control, and stable RBM5 knockdown clones. *Rbm5* expression values were first normalized to *Gapdh* and then expressed as fold-change from the control sample (scrambled siRNA transfectant). Data represents results from technical duplicates of one biological replicate. Error bars indicate standard error. Statistical significance was evaluated in comparison with the control sample with a Student's unpaired *t*-test (* indicates $p < 0.05$, and ** indicates $p < 0.01$). **B (i).** Western blots of protein samples from H9c2 control and stable RBM5 knockdown clones. Blots were probed with Abcam anti-RBM5 primary antibody, stripped and probed for α-tubulin (used as a reference gene). Precision Plus ladder was used, and ladder values refer to weight in kDa. **B (ii).** Quantification of Western blot results for Rbm5 protein expression in H9c2 control and stable RBM5 knockdown samples. Expression was normalized to α-tubulin and expressed as fold-change from the control sample. Values represent results from B(i) blot.

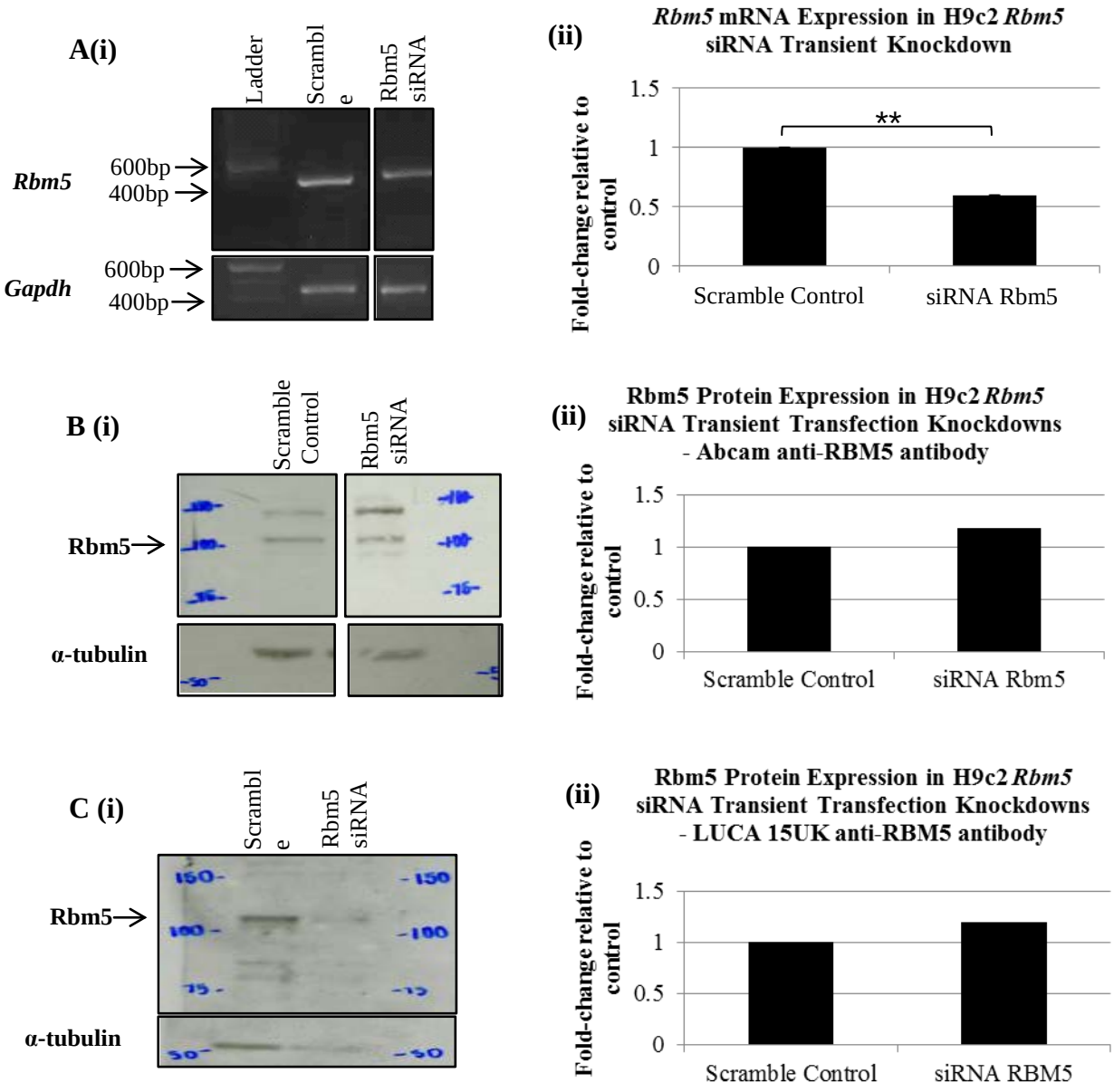

Figure 3. Rbm5 expression in siRNA transiently transfected H9c2 cells. H9c2 transient scramble and Rbm5 siRNA transfected cells (collected at 72 hours post-transfection). **A (i).** RT-PCR results for *Rbm5* and *Gapdh* amplification. Results are representative of technical duplicates performed from one biological replicate. **(ii).** Quantification of RT-PCR results from (i). Values normalized to *Gapdh*. Data represent results from technical duplicates, and error bars indicate standard error. Statistical significance was evaluated with a Student's unpaired *t*-test (** indicates $p < 0.01$). **B** and **C.** Western blots of protein samples. Blots were probed with Abcam (**B (i)**) and LUCA-15UK (**C (i)**) anti-RBM5 primary antibodies, respectively. Blots were then stripped and probed for α–tubulin (used as reference gene). Ladder values refer to weight in kDa. **B (ii)** and **C(ii).** Quantification of Western blot results for Rbm5 protein expression as determined with Abcam (**B (ii)**) and LUCA-15UK (**B(ii)**) anti-RBM5 primary antibodies, respectively. Expression normalized to α-tubulin and expressed as fold-change from the control sample. Values represent results from B(i) and C(i), respectively.

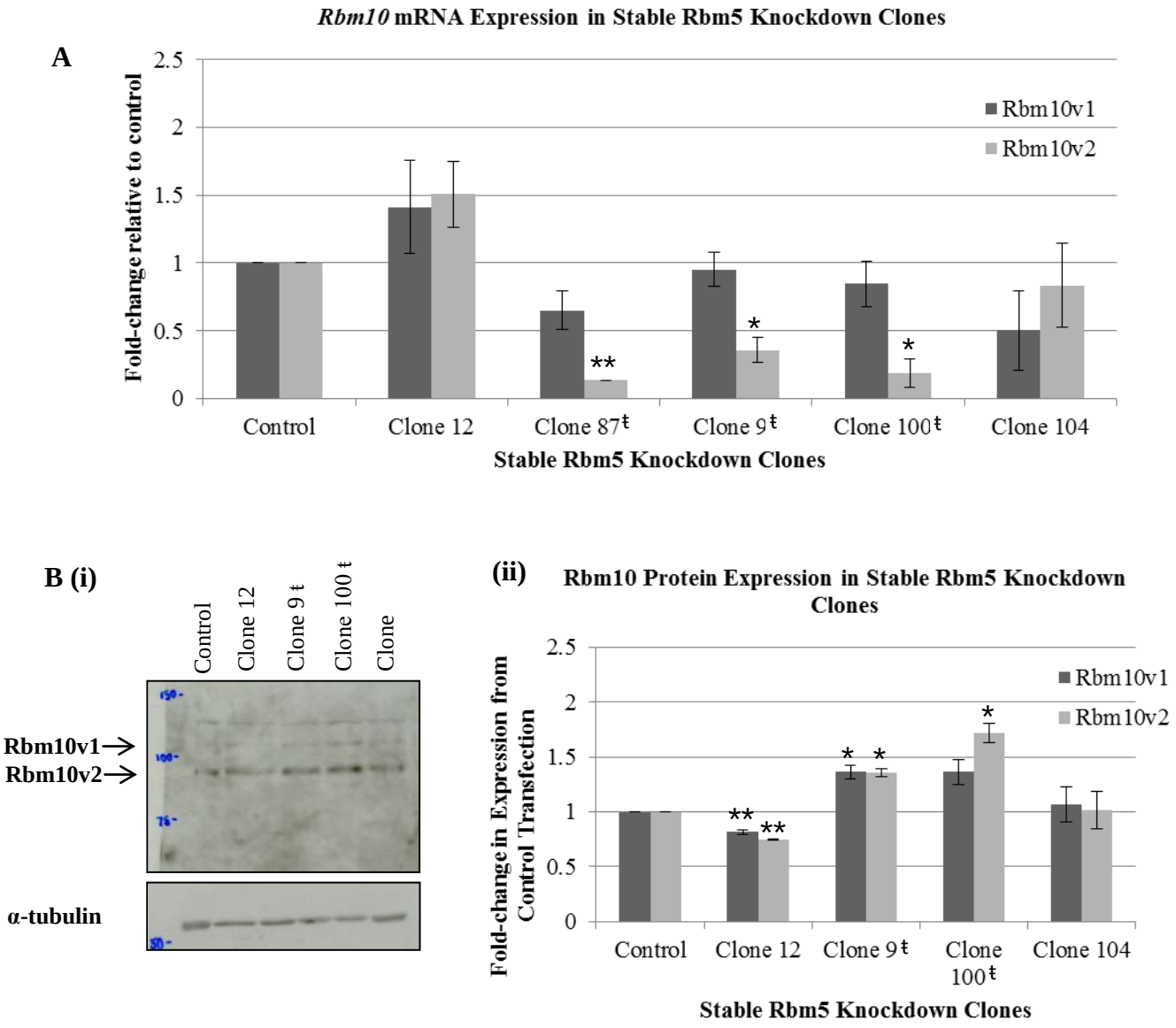

Figure 4. Rbm10 expression in stable H9c2 Rbm5 knockdown clones.
Control refers to scrambled control transfection. (t) beside a clone's name indicates that it showed a decrease in *Rbm5* mRNA expression of 50% or more (successful *Rbm5* knockdown at the mRNA level). **A.** Quantification of RT-PCR results for *Rbm10* expression in H9c2 control, and stable *RBM5* shRNA transfected clones. Values were first normalized to *Gapdh* and then expressed as fold-change from the control sample (scrambled siRNA transfectant). Data represents results from technical duplicates from one biological replicate, and error bars indicate standard error. **B. (i)** Western blot of protein samples from H9c2 control and stable RBM5 knockdown clones. Blots were probed with Bethyl anti-RBM10 primary antibody, stripped and probed for α-tubulin (used as a reference gene). Precision Plus ladder was used, and ladder values refer to weight in kDa. **(ii)** Quantification of Western blot results for Rbm10 protein expression in stable RBM5 knockdown clones. Expression was normalized to α-tubulin and expressed as fold-change from the control sample. Values represent results from technical duplicates performed on one biological replicate. Statistical significance was evaluated in comparison with the control sample using a Student's unpaired *t*-test (* indicates $p < 0.05$, and ** indicates $p < 0.01$).

significantly amongst any of the clones or from the control. *Rbm10v2* expression, on the other hand, significantly decreased in all of the clones with the most significant *Rbm5* RNA knockdown (Clones 87, 9 and 100). At the protein level (Figure 4B), Rbm10v1 and Rbm10v2 expression was surprising increased, but only in the Rbm5 clones with the most significant *Rbm5* RNA knockdown. Additionally, Rbm10v1 and Rbm10v2 protein expression was unexpectedly decreased in Clone 12, which had showed no change in *Rbm5* mRNA expression levels as a result of knockdown. Contrary to the results in the stable Rbm5 knockdowns, in the transient Rbm5 knockdown, *Rbm10v2* mRNA expression was significantly increased, compared to the scrambled control (Figure 5A). Similar to the stable knockdowns, both Rbm10v1 and Rbm10v2 protein expression increased (2-fold) compared to the scrambled control (Figure 5B). Knockdown data are summarized in Table 3. It is important to note that all experiments should be performed in biological triplicates before any conclusions can be made.

A.3.3. Rbm5 overexpression does not correlate with decreased Rbm10 protein levels

Since inhibition of *Rbm5* RNA correlated with increased expression of RBM10v1 and RBM10v2 protein in both stable and transient knockdowns, we sought to determine if the reverse were true, and overexpression of Rbm5 correlated with decreased Rbm10 expression. Transient overexpression of *RBM5* mRNA and protein from the human cDNA sequence (which has approximately 80% homology with rat) was confirmed (Figure 6), but *Rbm10v1* and *Rbm10v2* mRNA and protein expression levels remained unchanged, compared to the scrambled control transfectants (Figure 7).

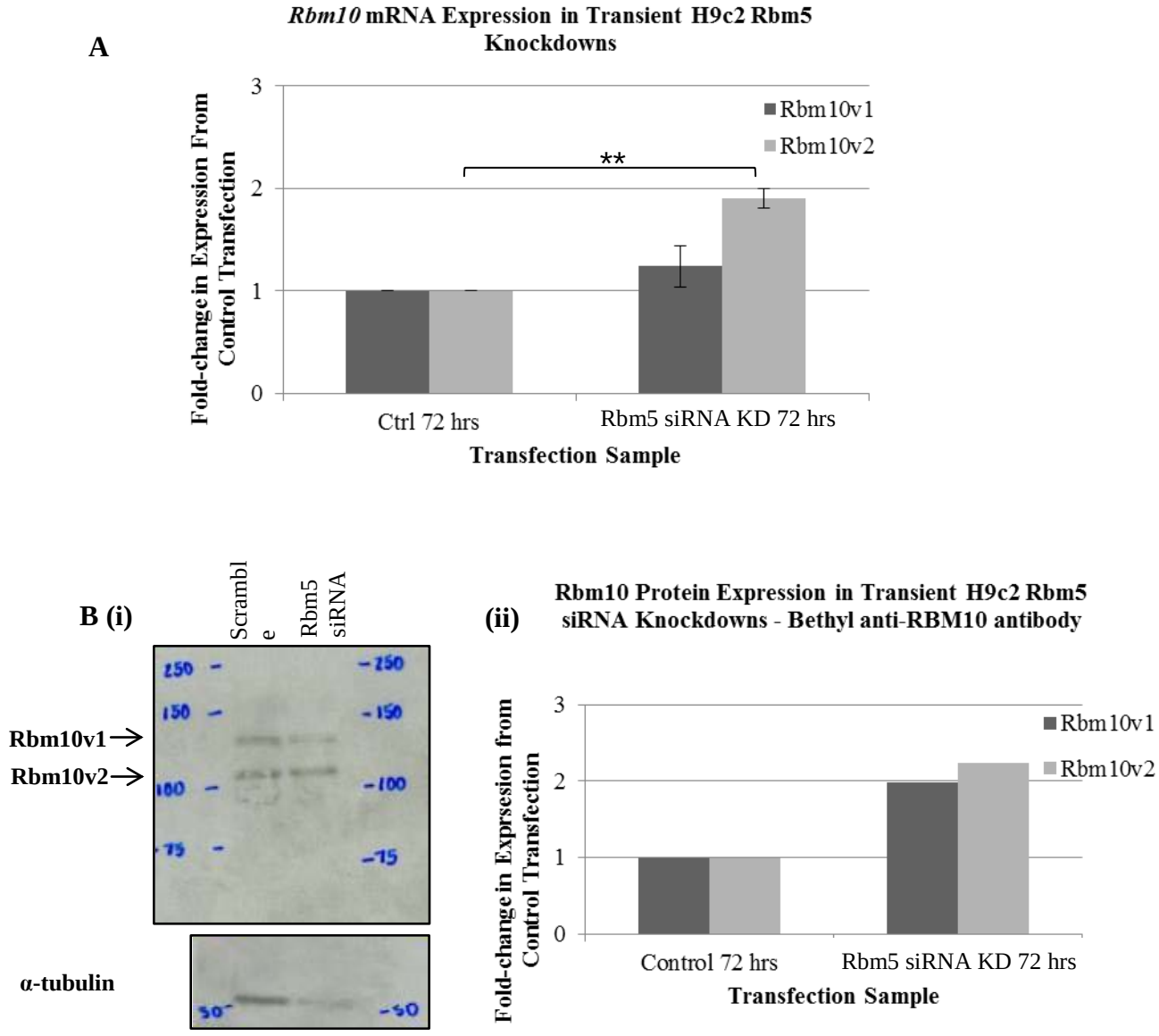

Figure 5. Rbm10 expression in siRNA transiently transfected H9c2 cells.
A. Quantification of RT-PCR results for *Rbm10* mRNA expression in H9c2 control, and Rbm5 transient knockdown (KD) samples. Values normalized to *Gapdh* and expressed as fold-change from the control sample (scramble siRNA transfectant). Data represent results from technical duplicates, and error bars indicate standard error. Statistical significance was evaluated with a Student's unpaired *t*-test (** indicates $p < 0.01$). **B. (i)** Western blot of protein samples from H9c2 cells transiently transfected with a scrambled control, or Rbm5 siRNA (samples collected at 72 hours post-transfection). Blots were probed with Bethyl anti-RBM10 primary antibody, stripped and probed for α-tubulin (used as reference gene). Precision Plus ladder was used, and ladder values refer to weight in kDa. **(ii).** Rbm10 protein expression in H9c2 control, and Rbm5 transient KD samples. Results obtained from quantification of Western blot results from **(i)**. Expression normalized to α-tubulin and expressed as fold- change from the control sample. Values represent results from one technical replicate.

Table 3. Summary of H9c2 knockdown expression level data, expressed as a percentage of the scrambled control

	Stables †					Transient ‡
	Clone 87	**Clone 9**	**Clone 100**	**Clone 104**	**Clone 12**	
Rbm5						
RNA	19	7	17	90	100	59
protein	94	101	86	81	93	118
Rbm10v1						
RNA	65	95	85	50	141	124
protein	not analysed	137	136	106	81	198
Rbm10v2						
RNA	14	36	19	83	151	190
protein	not analysed	135	171	102	75	224

† One sample, analysed in duplicate for RNA.

‡ One transient transfection, analysed in duplicate for RNA.

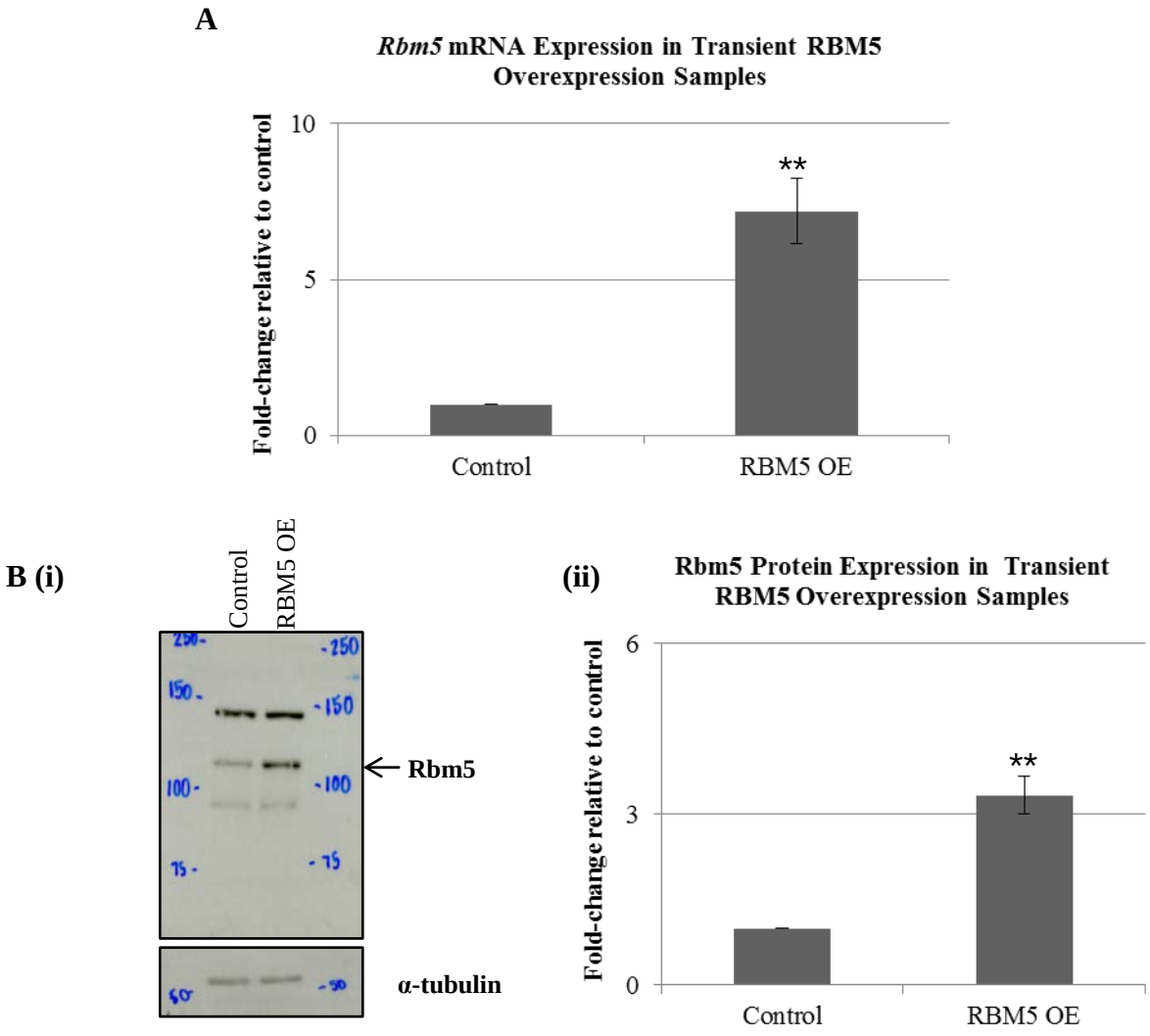

Figure 6. Rbm5 expression in transient RBM5 overexpression samples.
Control refers to samples transiently transfected with scrambled control pcDNA3, and RBM5OE refers to samples transiently transfected with pcDNA3.RBM5 (RBM5 overexpression (OE) samples). Samples were collected at 48 hours post-transfection. (**A**) Quantification of RT-PCR results for *Rbm5* expression in H9c2 control, and transient Rbm5 OE samples. Values were normalized to *Gapdh* and expressed as fold-change from the control sample. Data represent results from technical duplicates performed on biological triplicates. Error bars indicate standard error. **B (i)** Western blot of protein from H9c2 control and RBM5 transient OE samples. Blots were probed with Abcam anti-RBM5 primary antibody, stripped and probed for α-tubulin (used as reference gene). Precision Plus ladder was used, and ladder values refer to weight in kDa. Results shown are representative of results obtained from technical duplicates performed on biological triplicates. **(ii)** Quantification of Western blot results for Rbm5 protein expression in H9c2 control and transient RBM5 OE samples. Expression normalized to α-tubulin and expressed as fold-change from the control sample. Values represent results from biological triplicates, performed in technical duplicate. Statistical significance was evaluated in comparison with the control sample with a Student's unpaired *t*-test (** indicates $p < 0.01$).

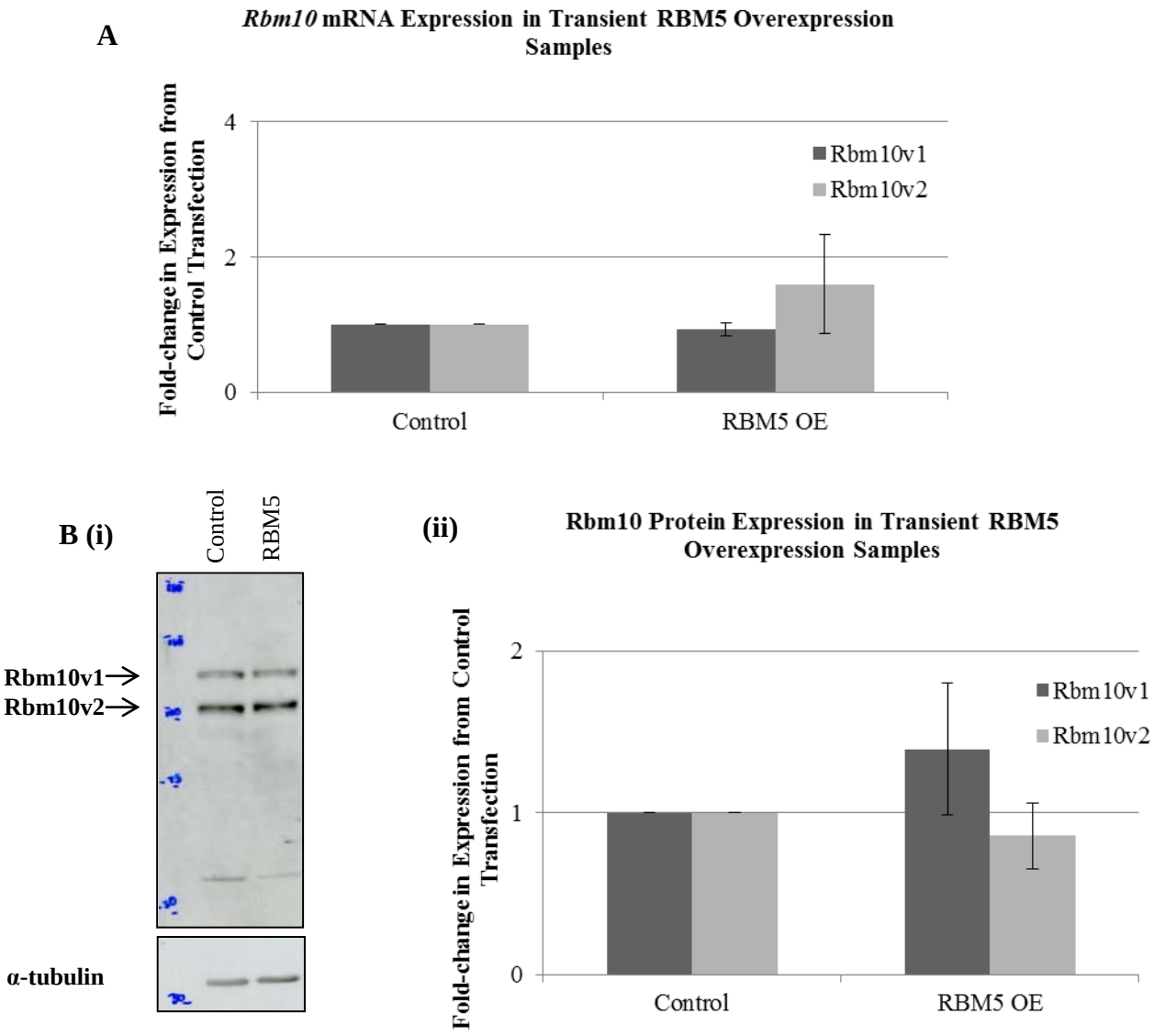

Figure 7. Rbm10 expression in H9c2 transient RBM5 overexpression samples.
Control refers to samples transiently transfected with scrambled control pcDNA3, and RBM5OE to samples transiently transfected with pcDNA3.RBM5 (RBM5 overexpression (OE) samples). Transfection samples were collected at 48 hours post-transfection. **A.** Quantification of RT-PCR results for *Rbm10v1* and *Rbm10v2* mRNA expression in H9c2 control, and transient RBM5 OE samples. Values were normalized to *Gapdh* and expressed as fold-change from the control sample. Data represent results from biological triplicates, performed technical duplicates. Error bars indicate standard error. **B**. **(ii)** Western blot for Rbm5 protein expression in H9c2 control and transient RBM5 OE samples. Blots were probed with Bethyl anti-RBM10 primary antibody, stripped and probed for α-tubulin (used to as a reference gene). Precision Plus ladder was used, and ladder values refer to weight in kDa. Results shown are representative of results obtained for biological triplicates performed in technical duplicate. **(ii)** Quantification of Western blot results for Rbm10 protein expression in H9c2 control and transient Rbm5 OE samples. Expression normalized to α-tubulin and expressed as fold-change from the control sample. Values represent results from biological triplicates, performed in technical duplicate. Statistical significance was evaluated in comparison with the control sample with a Student's unpaired *t*-test. No statistical significances of $p < 0.05$ were observed.

Chapter 4A. Discussion

Our results suggest the following:

A4.1. Only a small quantity of *Rbm5* mRNA is translated

Knockdown of *Rbm5* mRNA is not reflected at the protein level. Lack of a positive correlation between *Rbm5* RNA and protein expression in the transient transfections could possibly relate to the fact that (a) Rbm5 protein is very stable, or (b) the mRNA was only inhibited by 40%. When combined with the lack of a correlation in the stable clone observations (where mRNA was inhibited by 80-93%), the data suggest that unchanged Rbm5 protein expression levels in the stable clones was not due to any possible clonal effect but to a more general phenomenon. One possible explanation for this lack of correlation between *Rbm5* mRNA and protein expression levels in the knockdown experiments is that only a fraction of endogenous *Rbm5* mRNA is actually translated into protein. Transfection of shRNA complementary to a sequence of *Rbm5* mRNA lead to degradation of up to 90% of the *Rbm5* mRNA (Figure 8), but the ~ 10% that was left might be all that is normally translated in the wild-type myoblasts. One possible reason to account for the fact that only a small portion of *Rbm5* mRNA may be translated is that messenger ribonucleoproteins (mRNPs) may be involved in sequestering the majority of *Rbm5* mRNA in H9c2 cells. Precedent for this occurs in *Xenopus* oogenesis, where 80% of maternal mRNAs are sequestered in mRNP storage particles, and translation is inhibited until specific time-points during early embryogenesis when the mRNAs are recruited to ribosomes and finally translated (Spirin, 1966; Tafuri & Wolffe, 1993). A

second precedent occurs in P19 murine embryonic carcinoma cell differentiation, where the composition of mRNP-sequestered mRNAs changes following exposure to differentiation-inducing stimuli (Tenenbaum et al., 2000). Furthermore, in satellite cells, transcripts of *Myf5*, an important regulator of myogenesis, have been shown to be sequestered in mRNP granules. Upon activation of the satellite cells these granules dissociate, leading to liberation of *Myf5* transcripts and consequently higher levels of Myf5 (Crist et al., 2012). This regulatory mechanism thus allows quiescent satellite cells to transcribe *Myf5* without activating differentiation. A similar mechanism could be occurring in the H9c2 cells, which would explain not only why 90% knockdown of *Rbm5* mRNA is not reflected at the protein level, but why the changes in Rbm5 protein levels during cardiac differentiation were not positively correlated with changes in *Rbm5* mRNA levels (i.e., during differentiation, it is not the total amount of *Rbm5* mRNA in the cell that is important but the amount that is not sequestered, and thus available for translation).

In the overexpression experiments exogenous human *RBM5* mRNA was translated. If our sequestering hypothesis is correct, this result suggests that either (a) the cell could distinguish between exogenous *RBM5* and endogenous *Rbm5* transcript, or (b) there was a finite quantity of *Rbm5* message that could be sequestered, a quantity that might be regulated by levels of endogenous Rbm5 protein or *Rbm10* mRNA/protein levels.

A4.2. Regulation of Rbm5 protein expression in H9c2/myoblasts has unique characteristics

Correlations between *RBM5* expression at both the mRNA and protein levels have been examined in breast (Oh et al., 2002; Rintala-Maki et al., 2007), lung (Liang et al., 2012)

and pancreatic (Peng et al., 2013) non-tumour and tumour tissue, and various cell lines including A549 (lung adenocarcinoma) (Li et al., 2012; Oh et al., 2010), Calu-6 (possibly lung carcinoma) (Oh et al., 2010), NCI-H1299 (non-small cell lung carcinoma) (Oh et al., 2010), U2OS (osteosarcoma) (Kobayashi et al., 2011), PC-3 (prostate adenocarcinoma) (Zhao et al., 2012), BEAS-2B (immortalized human bronchial epithelial cells) (Oh et al., 2010), HEK293 (human embryonic kidney cells) (Fushimi et al., 2008), MCF-10A (immortalized epithelial cells derived from human fibrocystic mammary tissue) (Oh et al., 2010) and those of various mantle cell and follicular lymphomas (Weinkauf et al., 2007): a positive correlation between mRNA and protein expression levels was consistently observed. Only in non-tumour breast tissue was a positive correlation between *RBM5* mRNA and protein expression not observed (Rintala-Maki et al., 2007). Therefore, the mechanism suggested above in which only a percentage of *Rbm5* mRNA is translated, and the rest is sequestered (perhaps in mRNPs) may be a restricted phenomenon that occurs in, for example, particular cell types or in cells with certain growth characteristics, including rat myoblasts.

A.4.3. Decreased *Rbm5* mRNA levels regulate Rbm10 protein expression

It was interesting to note that, despite unchanged levels of Rbm5 protein, Rbm10 protein levels went up. This observation was particularly interesting in view of the fact that *Rbm10v2* mRNA levels significantly decreased in the stable KDs. Any potential off-target effect of *Rbm5* shRNA on *Rbm10* was considered highly unlikely once the elevated levels of Rbm10 protein were observed. The results suggest a complex regulatory mechanism linking degradation of *Rbm5* mRNA with Rbm10 protein expression.

We could postulate that depletion of *Rbm5* mRNA "reserves" triggered an increase in Rbm10v2 protein stability (Figure 8). Even though there was no decrease in Rbm5 protein, the cell anticipated this might be the case, and stabilized Rbm10. The difference in *Rbm10v2* mRNA expression in the transient versus the stable Rbm5 knockdowns could have resulted from decreases in reserve *Rbm5* mRNA that initially triggered increases in both transcription and translation of *Rbm10* but, over time (i.e., in stables), a decrease in *Rbm10* mRNA in order to avoid increasing Rbm10 protein levels too much. In this scenario, higher reserves of Rbm10 protein would have been generated, potentially to more rapidly respond if *Rbm5* mRNA levels decreased further.

A4.4. Model

Based on the results of the Rbm5 knockdown and overexpression experiments, we hypothesize that the majority of *Rbm5* transcripts are sequestered in the nucleus, possibly in mRNPs, and unavailable for translation. Release of sequestered transcripts would occur at certain points during differentiation, as required. Therefore, this could be the post-transcriptional mechanism regulating Rbm5 expression throughout H9c2 skeletal and cardiac myoblast differentiation suggested by results in the corresponding thesis.

Furthermore, since Rbm10 protein expression is increased upon reduction of *Rbm5* mRNA, we hypothesize a mechanism tasked with regulating *Rbm5* mRNA levels, in order to ensure sufficient quantities of reserve material. Upon depletion, or at least partial depletion, of this stock, the mechanism rapidly increases *Rbm10* mRNA and protein levels, in order to ensure the cell cycle, apoptosis and alternative splicing are

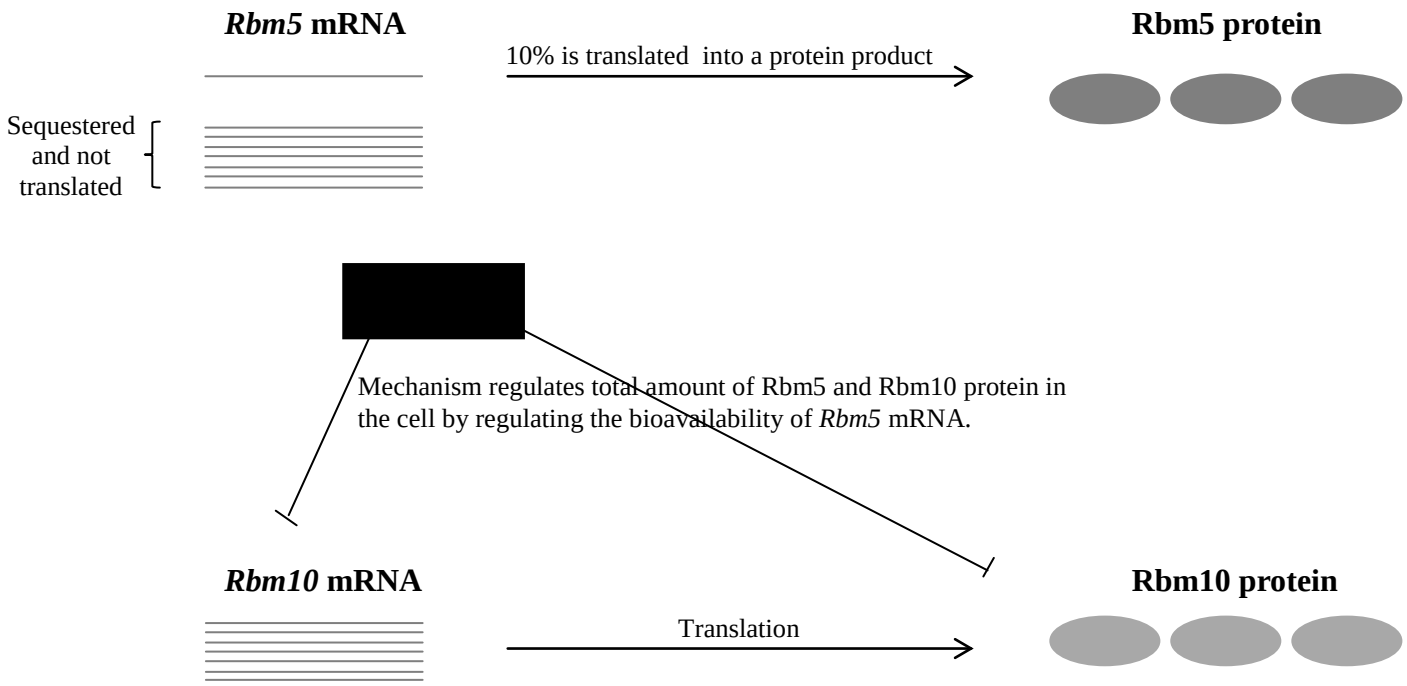

Figure 8. Model for regulation of Rbm5 and Rbm10 protein expression in H9c2 cells.
In growing H9c2 cells, only 10% of *Rbm5* mRNA transcripts are translated, with the remaining transcripts remaining sequestered in the cell, preventing their translation. A regulatory mechanism (represented by the black box) surveys *Rbm5* mRNA levels in the cell to ensure that adequate stocks are maintained. Upon depletion of *Rbm5* stocks, the mechanism increases levels of *Rbm10* to compensate.

adequately regulated. This assumes that Rbm10 can, at least partially, compensate for Rbm5 functions in myoblasts (Figure 8).

To test the validity of this model, the following experiments could be carried out. First, additional Rbm5 transient knockdowns should be generated (current model is based only on results from one biological replicate) in order verify that the differences observed regarding Rbm10 expression in the Rbm5 transient vs. stable knockdown samples are reproducible. Additional Rbm5 knockdown experiments could also be performed, using different siRNA and shRNA sequences, to further confirm our results. Other experiments could include knockdown and overexpression of Rbm10 in H9c2 cells and evaluation of *Rbm10* and *Rbm5* mRNA and protein expression levels in these samples. This would give us more information concerning the potential compensatory mechanism/functional overlaps of Rbm5 and Rbm10. Also, overexpression using rat Rbm5 instead of human, to begin to determine if there might possibly be a finite amount of Rbm5 that can be sequestered, and if perhaps only rat *Rbm5* transcripts are able to be sequestered in rat myoblasts.

Furthermore, mRNPs could be isolated from rat myoblasts to determine if *Rbm5* is indeed sequestered in such particles. mRNPs could also be isolated from samples taken throughout rat skeletal and cardiac myoblast differentiation to see if sequestered levels of *Rbm5* change throughout differentiation (i.e., when Rbm5 protein levels change). Finally, mRNPs could be isolated from various cancer cell lines in order to determine if *Rbm5* is also sequestered in such particles in transformed cells; *Rbm5* mRNA and protein expression have been previously shown to coordinate in a number of transformed cell lines, therefore *Rbm5* may not be sequestered in such particles in cancer cells.

Chapter 5A. Conclusion

The results from this work suggest that *Rbm5* is post-transcriptionally regulated in rat myoblasts. More specifically, the results suggest that the majority of *Rbm5* RNA is somehow sequestered (but available for knockdown by siRNA), as that only a small portion is ever translated. Results from *Rbm10* mRNA and protein expression in Rbm5 knockdown and overexpression samples also suggest that there is a mechanism that tightly monitors *Rbm5* mRNA levels, and increases *Rbm10* levels to compensate for a reduction in *Rbm5* mRNA. Therefore, as in transformed cells, Rbm5 and Rbm10 may influence similar cellular processes in myoblasts. Furthermore, this role may be of utmost importance, explaining the suggested strict regulation of Rbm5 expression in myoblasts.

References

Bonnal, S., Martínez, C., Förch, P., Bachi, A., Wilm, M., & Valcárcel, J. (2008). RBM5/Luca-15/H37 regulates Fas alternative splice site pairing after exon definition. *Molecular Cell*, *32*(1), 81–95.

Crist, C. G., Montarras, D., Buckingham, M. (2012). Muscle satellite cells are primed for myogenesis but maintain quiescence with sequestration of Myf5 mRNA targeted by microRNA-31 in mRNP granules. *Cell Stem Cell*, *11*(1), 118-26.

Drabkin, H. A., West, J. D., Hotfilder, M., Heng, Y. M., Erickson, P., Calvo, R., Dalmau, J., et al. (1999). DEF-3(g16/NY-LU-12), an RNA binding protein from the 3p21.3 homozygous deletion region in SCLC. *Oncogene*, *18*(16), 2589–97.

Fushimi, K., Ray, P., Kar, A., Wang, L., Sutherland, L. C., & Wu, J. Y. (2008). Up-regulation of the proapoptotic caspase 2 splicing isoform by a candidate tumor suppressor, RBM5. *Proceedings of the National Academy of Sciences of the United States of America*, *105*(41), 15708–13.

Geigl, J. B., Langer, S., Barwisch, S., Pfleghaar, K., Lederer, G., & Speicher, M. R. (2004). Analysis of gene expression patterns and chromosomal changes associated with aging. *Cancer Research*, *64*(23), 8550–7.

Jin, W., Niu, Z., Xu, D., & Li, X. (2012). RBM5 promotes exon 4 skipping of AID pre-mRNA by competing with the binding of U2AF65 to the polypyrimidine tract. *FEBS Letters*, *586*(21), 3852–7.

Kim, Y.-S., Hwan, J. D., Bae, S., Bae, D.-H., & Shick, W. A. (2010). Identification of differentially expressed genes using an annealing control primer system in stage III serous ovarian carcinoma. *BMC Cancer*, *10*, 576.

Kobayashi, T., Ishida, J., Musashi, M., Ota, S., Yoshida, T., Shimizu, Y., Chuma, M., et al. (2011). p53 transactivation is involved in the antiproliferative activity of the putative tumor suppressor RBM5. *International Journal of Cancer*, *128*(2), 304–18.

Li, P., Wang, K., Zhang, J., Zhao, L., Liang, H., Shao, C., & Sutherland, L. C. (2012). The 3p21.3 tumor suppressor RBM5 resensitizes cisplatin-resistant human non-small cell lung cancer cells to cisplatin. *Cancer Epidemiology*, *36*(5), 481–9.

Liang, H., Zhang, J., Shao, C., Zhao, L., Xu, W., Sutherland, L. C., & Wang, K. (2012). Differential expression of RBM5, EGFR and KRAS mRNA and protein in non-small cell lung cancer tissues. *Journal of Experimental & Clinical Cancer Research : CR*, *31*(1), 36.

Miller, G., Socci, N. D., Dhall, D., D'Angelica, M., DeMatteo, R. P., Allen, P. J., Singh, B., et al. (2009). Genome wide analysis and clinical correlation of chromosomal and transcriptional mutations in cancers of the biliary tract. *Journal of Experimental & Clinical Cancer Research: CR*, *28*(1), 62.

Mourtada-Maarabouni, M., Keen, J., Clark, J., Cooper, C. S., & Williams, G. T. (2006). Candidate tumor suppressor LUCA-15/RBM5/H37 modulates expression of apoptosis and cell cycle genes. *Experimental Cell Research*, *312*(10), 1745–52.

Oh, J. J., Taschereau, E. O., Koegel, A. K., Ginther, C. L., Rotow, J. K., Isfahani, K. Z., & Slamon, D. J. (2010). RBM5/H37 tumor suppressor, located at the lung cancer hot spot 3p21.3, alters expression of genes involved in metastasis. *Lung Cancer*, *70*(3), 253–62.

Oh, J. J., West, A. R., Fishbein, M. C., & Slamon, D. J. (2002). A candidate tumor suppressor gene, H37, from the human lung cancer tumor suppressor locus 3p21.3. *Cancer Research*, *62*(11), 3207–13.

O'Leary, D. A., Sharif, O., Anderson, P., Tu, B., Welch, G., Zhou, Y., Caldwell, J. S., et al. (2009). Identification of small molecule and genetic modulators of AON-induced dystrophin exon skipping by high-throughput screening. *PloS One*, *4*(12), e8348.

Peng, J., Valeshabad, A. K., Li, Q., & Wang, Y. (2013). Differential expression of RBM5 and KRAS in pancreatic ductal adenocarcinoma and their association with clinicopathological features. *Oncology Letters*, *5*(3), 1000–4.

Ramaswamy, S., Ross, K. N., Lander, E. S., & Golub, T. R. (2003). A molecular signature of metastasis in primary solid tumors. *Nature Genetics*, *33*(1), 49–54.

Rintala-Maki, N. D., Goard, C. A., Langdon, C. E., Wall, V. E., Traulsen, K. E. A., Morin, C. D., Bonin, M., et al. (2007). Expression of RBM5-related factors in primary breast tissue. *Journal of Cellular Biochemistry*, *100*(6), 1440–58.

Rintala-Maki, N. D., & Sutherland, L. C. (2009). Identification and characterisation of a novel antisense non-coding RNA from the RBM5 gene locus. *Gene*, *445*(1-2), 7–16.

Shu, Y., Rintala-Maki, N. D., Wall, V. E., Wang, K., Goard, C. A., Langdon, C. E., & Sutherland, L. C. (2007). The apoptosis modulator and tumour suppressor protein RBM5 is a phosphoprotein. *Cell Biochemistry and Function*, *25*(6), 643–53.

Spirin, A. S. (1966). Chapter 1 On "Masked" Forms of Messenger Rna in Early Embryogenesis and in Other Differentiating Systems. In A. A. Moscona & A. Monroy (Eds.), *Current Topics in Developmental Biology* (Volume 1., Vol. 1, pp. 1–38). New York, NY: Elsevier.

Sugliani, M., Brambilla, V., Clerkx, E. J. M., Koornneef, M., & Soppe, W. J. J. (2010). The conserved splicing factor SUA controls alternative splicing of the developmental regulator ABI3 in Arabidopsis. *The Plant Cell*, *22*(6), 1936–46.

Sutherland, L. C., Rintala-Maki, N. D., White, R. D., & Morin, C. D. (2005). RNA binding motif (RBM) proteins: a novel family of apoptosis modulators? *Journal of Cellular Biochemistry*, *94*(1), 5–24.

Tafuri, S. R., & Wolffe, A. P. (1993). Selective Recruitment of Masked Maternal mRNA from Messenger Ribonucleoprotein Particles ContainingF RGYZ (mRNP4). *The Journal of Biological Chemistry*, *268*(32), 24255–61.

Tenenbaum, S. A., Carson, C. C., Lager, P. J., & Keene, J. D. (2000). Identifying mRNA subsets in messenger ribonucleoprotein complexes by using cDNA arrays. *Proceedings of the National Academy of Sciences of the United States of America*, *97*(26), 14085–90.

Wang, K., Bacon, M. L., Tessier, J. J., Rintala-Maki, N. D., Tang, V., & Sutherland, L. C. (2012). RBM10 Modulates Apoptosis and Influences TNF-α Gene Expression. *Journal of Cell Death*, *5*, 1–19.

Wang, K., Ubriaco, G., & Sutherland, L. C. (2007). RBM6-RBM5 transcription-induced chimeras are differentially expressed in tumours. *BMC Genomics*, *8*(1), 348.

Weinkauf, M., Christopeit, M., Hiddemann, W., & Dreyling, M. (2007). Proteome- and microarray-based expression analysis of lymphoma cell lines identifies a p53-centered cluster of differentially expressed proteins in mantle cell and follicular lymphoma. *Electrophoresis*, *28*, 4416–26.

Welling, D. B., Lasak, J. M., Akhmametyeva, E., Ghaheri, B., & Chang, L.-S. (2002). cDNA microarray analysis of vestibular schwannomas. *Otology & neurotology : official publication of the American Otological Society, American Neurotology Society [and] European Academy of Otology and Neurotology*, *23*(5), 736–48.

Zhao, L., Li, R., Shao, C., Li, P., Liu, J., & Wang, K. (2012). 3p21.3 tumor suppressor gene RBM5 inhibits growth of human prostate cancer PC-3 cells through apoptosis. *World Journal of Surgical Oncology*, *10*(1), 247.